Pneumatic Pellet Injector for JET*)

C.Andelfinger, K.Büchl, D.Jacobi,
W.Sandmann, J.Schiedeck,
H.B.Schilling, G.Weber

IPP 1/219 July 1983

MAX-PLANCK-INSTITUT FÜR PLASMAPHYSIK
8046 GARCHING BEI MÜNCHEN

MAX-PLANCK-INSTITUT FÜR PLASMAPHYSIK
GARCHING BEI MÜNCHEN

Pneumatic Pellet Injector for JET*)

C.Andelfinger, K.Büchl, D.Jacobi,
W.Sandmann, J.Schiedeck,
H.B.Schilling, G.Weber

IPP 1/219 July 1983

*) This work was done under contract number JE 2/9016 Scientific and Engineering Design of Pellet Injectors for JET.

Die nachstehende Arbeit wurde im Rahmen des Vertrages zwischen dem Max-Planck-Institut für Plasmaphysik und der Europäischen Atomgemeinschaft über die Zusammenarbeit auf dem Gebiete der Plasmaphysik durchgeführt.

IPP 1/219

C. Andelfinger, K. Büchl,
D. Jacobi, W. Sandmann,
J. Schiedeck, H.B. Schilling,
G. Weber

Pneumatic Pellet Injector for JET

Abstract

Pellet injection is a useful tool for plasma diagnostics of tokamaks. Pellets can be applied for investigation of particle, energy and impurity transport, fueling efficiency and magnetic surfaces. Design, operation and control of a single shot pneumatic pellet gun is described in detail including all supplies, the vacuum system and the diagnostics of the pellet. The arrangement of this injector in the torus hall and the interfaces to the JET system and CODAS are considered. A guide tube system for pellet injection is discussed but it will not be recommended for JET.

Content

Page

1. Introduction

In the past few years pellet injectors have been installed in several experiments /1/. Investigations have mainly been concentrated on ablation and penetration depths of pellets. Fuelling experiments with pellets have only been conducted in a few devices. Another successful application was found in Wendelstein WVIIA. By pellet injection during the current-free phase a target plasma was created for more efficient energy absorption of neutral beam heating. However, in ASDEX the experiments with a pneumatic pellet gun showed that pellets are an excellent tool for plasma diagnostics. For instance, by small perturbation of the plasma it became possible to study the transport locally in the plasma. It should be useful to apply this technique to the JET plasma as well. However, owing to the changed plasma parameters of JET compared with ASDEX an extended version of the pellet gas gun had to be developed. The improvements concern the pellet size and the pellet velocity. Pellets of a size of 2.6 mm in diameter and length were accelerated to velocities of up to 1600 m/s. The design and operation of the gun have also been improved. Special attention was paid to remote handling, control by computer and radiation hardening for the extended phase of JET. In the following sections some remarks are made on plasma diagnostics, which will be possible with pellets, and a detailed description of a gas gun pellet injector for JET is given.

2. Active diagnostics with pellets

First pellet injectors were developed for refuelling of plasma devices. It has been found, however, that present-day plasma machines can be refilled by gas puffing and recycling alone. Otherwise it is not yet known if future larger tokamaks, e.g. JET, TFTR, JT-60 and T-15, can be refuelled only from the edge. Refuelling experiments with pellets would therefore also be conducted in the next step of plasma machines.

In the last few years it has been shown in some tokamak experiments, e.g. ASDEX and PDX, that pellet injection may be a powerful tool for plasma diagnostics. Most of the investigations concern transport of particles and energy. They are based on the assumption of small distortions in density or temperature of the plasma by pellets. Other investigations take advantage of the dependence of pellet ablation on local plasma properties.

Apart from the usual plasma diagnostics in tokamaks, photography of the ablation trace and measurement of the H_α emission are important methods of investigating plasma-pellet interaction. The penetration depth of the pellet, which is required for many investigations and time -dependent ablation, should also be determined during pellet injection in JET. All these experiments can be done by single-pellet injection using pneumatic pellet guns.

2.1 Fuelling efficiency

The fuelling efficiency γ is the portion of the injected pellet or gas material which enters the bulk plasma. Owing to the deep deposition it is assumed that pellet refuelling is more efficient than gas puffing. But this is not obvious. As a result of the sudden changes of density and temperature profiles instabilities can be induced which transport the injected material out of the plasma in a very short time. Constant gas puffing and pellet injection cannot be compared directly. Averaging for the pellets should be done, but this depends on confinement times and pellet frequencies. However, for a single-gas pulse and a pellet direct comparison is possible. In the case of a limiter plasma a rough estimate can be made, starting with the global equation for refuelling of the bulk plasma:

$$\frac{dN_e}{dt} = -\frac{N_e}{\tau_p} + \gamma_g \phi_g + r\left[\frac{N_e}{\tau_p} + (1-\gamma_g)\phi_g\right] + r\begin{bmatrix}(1-\gamma_g)\hat{\phi}_g \\ (1-\gamma_p)\hat{\phi}_p\end{bmatrix} + \begin{matrix}\gamma_g \hat{\phi}_g \\ \gamma_p \hat{\phi}_p\end{matrix}$$

Change in electrons = loss + constant gas puffing + constant recycling + recycling by gas pulse / pellet + gas pulse / pellet

τ_p = particle confinement time
γ_g = fuelling efficiency for gas puffing
γ_p = fuelling efficiency for pellets
ϕ_g = constant gas flux
$\hat{\phi}_g$ = gas pulse flux
$\hat{\phi}_p$ = pellet flux

If we assume that the change of the total number of particles is small and τ_p, γ_g and r are unchanged, the condition for the steady state is valid in approximation:

$$0 = -\frac{N_e}{\tau_p} + \gamma_g \phi_g + r\left[\frac{N_e}{\tau_p} + (1-\gamma_g)\phi_g\right] \qquad (2)$$

If we only consider the time when recycling has not yet become effective

$$\left.\frac{dN_e}{dt}\right|_g \approx \gamma_g \hat{\phi}_g \quad (3) \qquad N_{gas} = \int_{\text{gas pulse}} \hat{\phi}_g \, dt \quad (4)$$

$$\left.\frac{dN_e}{dt}\right|_{pel} \approx \gamma_p \hat{\phi}_p \quad (5) \qquad N_{pel} = \int_{\text{ablation}} \hat{\phi}_p \, dt \quad (6)$$

the density profile is not changed, it follows that

$$\frac{\gamma_p}{\gamma_g} \approx \frac{\Delta_{\text{pellet}}\int n_e \, dl}{N_{pel}} \cdot \frac{N_{gas}}{\Delta_{\text{gas pulse}}\int n_e \, dl} \qquad (7)$$

A good impression of different refuelling methods is obtained in a divertor experiment if the gas pressure in the divertor chamber is measured. In Fig. 1 the line density in the bulk plasma is increased for the same amount by a gas pulse or a pellet. In the case of the gas pulse a large portion of gas streams along the scrape-off layer into the divertor. Refuelling by pellets is much more efficient, only a small part of the pellet being observed in the divertor chamber.

2.2 Particle transport

The density profile will be disturbed by pellet injection. This is shown in Fig. 2. This disturbance will be balanced by particle transport. It is assumed that the perturbation is small compared with the steady-state value of the plasma density, and the toroidal transport is fast compared with the radial transport. The density profiles at different times after pellet injection will be measured by Thomson scattering and interferometry. An example is given for ASDEX where the density profiles are determined by HCN interferometry (Fig. 3). These profiles can be calculated with the continuity equation for the density perturbation n_e:

$$\frac{\partial \tilde{n}_e}{\partial t} = \text{div}\, \tilde{\Gamma} \qquad (8)$$

where $\tilde{\Gamma}$ is the particle flux disturbance perpendicular to the magnetic surfaces. We assume that other source terms such as recycling are not changed during the time considered. Using

$$\tilde{\Gamma} = -D\left(\frac{\partial \tilde{n}_e}{\partial r} + \frac{2r}{a^2}\tilde{n}_e\right) \qquad (9)$$

and

$$D = 0.4\ m^2/s \qquad (10)$$

we get the density profiles also shown in Fig. 3 (dashed curves). They are in a fairly good agreement with the measured curves. This confirms the anomalously high diffusion coefficient D already measured in earlier experiments. Owing to the low number of interferometer channels the profiles are relatively uncertain. We therefore cannot decide on the inward term and on the radial dependence of the diffusion coefficient. But if the density profiles can be measured with high accuracy, it should be possible to determine the radial dependence of D and to decide if an inward drift term exists.

2.3 Energy transport

Injected pellet ablate typically in between 0.2 and 1.0 ms, depending on the size and velocity of the pellet and on the plasma parameters. The ablation of the pellet is an adiabatic process. The energy used for vaporization, ionization and heating of the pellet material mostly originates from the thermal energy of the plasma. Nonthermal electrons and ions only have to be considered in special cases. The pellet therefore produces a sudden rise in density and a sudden drop in temperature up to its penetration radius.

The temperature profile of the plasma is perturbed. In the outer zones the temperature decreases. Inside the radius of penetration the profile should not be influenced. The variation of density and temperature profiles can be calculated by means of the neutral gas shielding model /2/. In Fig. 4 the dashed curve is the temperature profile before and the solid curve is the profile after pellet injection, calculated for ASDEX. The perturbed temperature and density profiles can be used for transport calculations. This affords the possibility of obtaining information on the thermal conductivity and energy confinement time.

Very fast energy transport in the bulk plasma has been observed in ASDEX. The injected 1 mm pellets penetrate to a radius of about 20 cm.

The drop of temperature measured by electron cyclotron emission for $r > 20$ cm is in rather good agreement with the calculations of Fig. 4, which shows the temperature profile immediately after pellet injection. But for $r < 20$ cm no temperature variation should occur if we neglect transport by charge exchange. However, at the same time when the temperature drops in the outer shells, the temperature also drops in the core of the plasma. The time is of the order of the ablation time of the pellet. In Fig. 5 the temperature variation is shown for four radii for pellet injection at 4.3 ms. The energy transport in the plasma seems to be much faster than expected from the known global energy confinement times of the order of a few ten milliseconds.

2.4 Impurity transport

The injection of small neon-doped pellets is an excellent method of studying the transport of impurity ions. The pellets contain about 1% neon and 99% deuterium. They are produced from a gas mixture of neon and deuterium. The transport will be calculated in the same way as the particle transport for the bulk plasma. With an inward drift term neglected, the diffusive radial flow Γ_i for the ions of kind i is given by

$$\Gamma_i = -D \frac{\partial n_i}{\partial r} \tag{11}$$

Using the diffusion model and the known plasma parameters, Behringer /3/ calculated the temporal evolution of several ionization states of neon. The parameter for this calculation was the diffusion coefficient D. The pellet was described by the deposition curve along the penetration depth. In Fig. 6 for NeX the results are compared with measurements made in an ASDEX discharge with $n_e = 4.4 \times 10^{13}$ cm^{-3} and $T_e(0) = 620$ eV. Very good agreement is obtained for $D = 4000$ cm^2/s, which was also measured for deuterium of the bulk plasma. The applied pellets had a diameter of 1.0 mm and a velocity of 900 m/s. The calculations neglect recycling, which should give only small errors within the confinement time. The deviation after 300 ms can be caused by recycling.

2.5 Magnetic surfaces

Besides the transport phenomena several other observations are made together with pellet injection. Most of them are not well understood up to now. For instance, an observed radial structure in ablation will be discussed here. If a pellet is injected radially into a tokamak, the deposition profile along the radius can be calculated by means of the neutral gas shielding model /2/. In Fig. 7 a deposition profile for a pellet 1 mm in diameter with a velocity of 800 m/s is shown. If we assume that D_α emission is proportional to the particle deposition, the D_α emission signal measured with a PIN diode should have the same shape as the deposition profile. But in the emission profile we observe a series of maxima (Fig. 7). When the pellet trace from a tangential port in the torus (Fig. 8) is photographed, slight intensity variations are noticeable. A very different picture is seen, however, if the camera looks from the top or, because this is not possible at ASDEX, if it looks obliquely from the top (Fig. 9). Then luminous stripes in the toroidal direction starting in both directions at the pellet trace can be seen (Fig. 10). Presumably, this effect is connected with the magnetic flux tubes and the energy content in the magnetic surfaces. The expansion of neutral particles is spherical and only neutral deuterium can be observed by D_α emission. Two possible hypotheses will be briefly considered. If we assume a sphere of neutral particles expanding from the pellet, then at the different energy contents available in the magnetic surfaces the excitation and ionization of the gas differ in the radial direction and produce luminous stripes. If we assume production of a dense, partially ionized plasma at the pellet surface, which flows along the field lines then the available energy in a magnetic surface determines the ablated number of particles. A stripe structure again results from the different energy contents available in the magnetic surfaces. Different availability of energy can originate from total energy content in the surface but also from closed field lines in rational surfaces, which allow to take away only a part of the stored energy.

Accidental variations of ablation caused by, for instance, non-spherical pellet shape or hot spots on the pellet can be excluded since two adjacent pellets were observed at the same time. In such case the luminous stripes of one pellet correspond with the stripes of the second pellet. This is a strong indication of the importance of the magnetic field for this effect.

Experiments were only conducted with pellets which cross the axis of the plasma owing to their bigger mass (Fig. 11). The ablation changes abruptly at the axis of the plasma because the pellet enters magnetic surfaces which it had already crossed once. Behind the plasma axis the pellet therefore sees cooled plasma sheaths and the ablation is strongly reduced. We thus have a method of visualizing the plasma axis.

3. Pellet requirements

With the pellet as a diagnostic tool, the pellets have to meet some conditions. The first condition is that the perturbation of the plasma is small, i.e. profiles should not change appreciably. Our experience and that of other experiments shows that an increase of particles of 10 to 40% is acceptable. This means the pellet mass for the diagnostics in JET should not exceed 10^{21} particles or a diameter of 3 mm. Another condition should be fulfilled for the penetration depth of the pellet. For refuelling it could be sufficient for the pellet to cross the scrape-off layer, but for diagnostics the penetration depth has to be of the order of the minor radius of the plasma. The length of pellet path depends on the plasma particles, which are mainly responsible for ablation. These can be thermal electrons, fast ions, runaway electrons, etc. The neutral gas shielding model /2/, which is based on ablation by thermal electrons, calls for pellet velocities of 500 to 2000 m/s for the different phases of JET. This is shown in Fig. 12. Desirable properties of pellet injection are good reproducibility for the mass and velocity of the pellet as well as the trajectory of the pellet. The mass and velocity change from shot to shot between $\pm$ 10 and 2o%, but they have to be measured for each shot. The stray angle for the trajectories are smaller than $\pm 0.5^{o}$, which is equivalent to a distance of $\pm$ 5.8 cm at the plasma axis.

It is also desirable to have different materials available for the injection. There are the hydrogen isotopes. But neon-doped pellets are also available.

In addition, a good reliability of the pellet injection is an important condition for the experiments. The pellet gas guns used in ASDEX and WVIIA have a reliability of more than 90%.

The pellet gas gun which is described in this report was built for JET-sized pellets. It was found in the test to have a reliability also better than 90%.

The pellets produced by gas guns are able to meet the requirements for diagnostics in JET for a wide range of operation.

4. Engineering design

In the following sections a description of the mechanical design, operation and control of the gas gun pellet injector will be given. The arrangement of the pellet injection system is shown in Fig. 13. First we consider the cryostat and the gun lock which is fixed to the heat exchanger of the cryostat. Then the vacuum system will be described. The pellet diagnostics is discussed insofar as it concerns us. The microwave system will be delivered by Risø Laboratory and will be separately reported in detail.

Particular attention is paid to interfaces with JET and to the supplies which have to be made available by JET.

Finally, we give reasons for not recommending the guide tube system as an alternative injection system for application in JET.

4.1 Pellet cryostat

A cryostat cooled by flowing liquid helium is used for solidifying hydrogen isotopes. Apart from being cooled down, the flow of liquid helium is kept constant. The flow cycle is described in Sec. 4.1.2. The pellet gas supply (Sec. 4.1.3) feeds the gas to be solidified into the cryostat. The temperature of the cryostat is controlled by ohmic heating. For freezing the temperature is set to 6 - 8 K. The gas flows into the storage volume of the cryostat. To avoid condensation in the feedline, the temperature should not be too cold. After freezing the solid hydrogen is pressurized by a piston. The pressure is about 30 to 40 MPa. When the temperature is increased the solid will be plastically deformed and slowly starts to flow through a nozzle into the gun lock, where the pellet will be shaped. After that the cryostat is set to its lowest temperature, switching off the ohmic heating. This is to avoid an increase of the temperature to a value which is above the freezing point of the solidified gas. For pellet acceleration the propellent gas enters the gun. Because it is at room temperature, it heats the cryostat and gun by heat conduction for a short time. The heat capacity of the cryostat and the gun has to be large enough to get just a small temperature rise. The processing for pellet production is described in detail in Sec. 4.21.

4.11 Extrusion cryostat /4/

The cryostat was developed in co-operation between IPP and Leybold-Heraeus. The design is shown in Fig. 14. The central part of the cryostat is the copper heat exchanger, which contains the storage volume for the solidified gas, the electric heater, the resistor for temperature measurement and a small cell for the vapour pressure thermometer. The radiation shield is cooled by the outflowing cold helium gas. The cryostat is built on a vacuum flange CF 100. Through a small nozzle in the bottom of the storage volume the solid pellet material can be extruded into the gun part of the pellet injector, which is described in Sec. 4.21. The extrusion is forced by a piston driven by a pneumatic actuator outside the vacuum. The piston rod is sealed by a membrane bellows. The position of the piston is recorded by a position indicator. The quantity of the solidified material can thus be determined.

The lowest temperatures achieved with this device are below 3 K. Control of temperature in the range of 3 K to 40 K is feasible by helium flow control and ohmic heating. For extrusion the temperature will be raised to 8 - 10 K and the piston exerts a pressure of up to 40 MPa into the solid hydrogen. The vapour pressure thermometer is filled with helium of 1500 mbar at room temperature. The cryostat described is very flexible. It is an excellent tool for pellet production.

4.12 Liquid helium supply

For cryostat cooling a liquid helium supply system (Fig. 15) will be required. In the non-active phase of JET the liquid helium can be stored in a 100 l cryogenic tank. In the active phase a liquid helium transfer line from the JET cryogenic area to the gas gun will be necessary and the tank acts as a buffer. In the early phases of JET we shall use a superinsulated tank which can be replaced by a liquid-nitrogen-cooled tank in the extended phase. The mean liquid helium consumption of the cryostat is about 3 l/h. If helium is not to be wasted, a recycling line to the JET cryogenic area for gaseous helium has to be installed. The liquid helium flow is regulated by valves which can be controlled by CODAS. The pressure difference for the flow is produced by a helium-tight vacuum pump. The pressure in the tank is about 1 bar.

The helium flow is measured by a flowmeter in the exhaust line of the pump. The cold helium gas leaving the cryostat is warmed up in electric heaters automatically controlled by Simatic. The liquid helium flow is kept constant by setting also the valves in the liquid helium transfer line.

4.13 Pellet gas supply

The pellet gas supply (Fig. 16) delivers pure gas or gas mixtures for pellet production. Beside the main pellet materials deuterium and hydrogen, other gases are available to produce doped pellets, e.g. with neon.

The gas mixture system is located in the basement below the torus hall. The gas, which is contained in a gas bottle, is sufficient to produce several thousand pellets. Exchange of the gas bottle should not be required during the active phase of JET. In the early phases of JET fast exchange is possible without ventilation of the gas supply system. The mixing of the gases in the volume V5 is CODAS-controlled. Depending on the desired mixture, the ratio of the gas pressure in the volumes V1 to V4 is adjusted by the motor-controlled pressure regulators. The interface to CODAS will be handled with Camac modules.

The mixture system in the basement is only connected by one gas feed line with the pellet cryostat in the torus hall. A very clean gas is needed for operating the gun. Already small admixtures of air, water or oil will prevent correct operation of the cryogenic gas gun. To remove all undesired impurities, the approx. 15 m long transfer line can be evacuated at both the basement side and the gun side of the tube and will be flushed with hydrogen gas. Typical pressures in the transfer line are of the order of several hundred millibars. By means of an additional vacuum line the storage volume of the cryostat can be connected with the high vacuum system of the pellet gun to clean the cryostat before filling.

4.2 Pellet gun

The gun lock is connected directly with the bottom of the heat exchanger of the pellet cryostat (Fig. 17). In the gun lock the pellets will be produced from the extruded solid hydrogen. They will be positioned at the entrance of the barrel for acceleration and the pipe line to the propellent gas supply will be opened. Hydrogen also means, besides hydrogen itself, deuterium or a mixture of these two, or a mixture of hydrogen isotopes doped with an impurity for diagnostic purposes. Good experience was gained with neon-doped pellets.

The pellet size is an important parameter for the penetration depth of the pellet. To produce pellets of different sizes, the gun lock and barrel have to be exchanged, which can be done in 2 to 3 days. Another possibility is the development of multiple-shot guns with several barrels /5/. A three-shot gun is under construction in our laboratory. It will be built in such a way that it can easily be exchanged with the one-shot gun. But this is not part of this contract.

4.21 Gun design and operation

The gun lock has to be manufactured with extremely high precision. Its operation temperature is around 5 to 10 K, but it will be constructed at room temperature. Also if we use materials with nearly the same thermal expansion coefficients, a certain procedure for assembling should be followed. This is noted in the drawings. The principle of the gun lock (Fig. 18) can be described as follows. The extruded solid hydrogen flows through a small channel into a hole with pellet dimensions which is drilled in a cylindrical shell. The thickness of the shell is equal to the pellet length. By turning the cylinder shell 90 degrees the pellet is cut from the extruded rod and positioned at the entrance of the barrel. By the same movement the gun lock opens like a stopcock the pipeline to the fast high-pressure propellent gas valve. This operation is controlled by Simatic. The process starts by increasing the temperature of the cryostat to extrusion temperature, depending on the pressure applied by the piston (Fig. 14) on the stored solid hydrogen. A constant pressure of 30 to 40 MPa is used. The viscous flow starts at a temperature between 5 K and 10 K, which has to be determined every day before the beginning of pellet production. The extrusion is recorded with a position detector which is sensitive to the piston position. When the material fills the pellet mould, the extrusion will be stopped by decreasing the temperature of the cryostat. This is done by lowering the ohmic heating. The gun lock has good heat contact to the cryostat and both temperatures are all the time nearly the same. If the extrusion is not stopped, solid hydrogen will flow into the very fine slits between the gun lock housing and the cylindrical rotor and finally overflow into the insulation vacuum. It then evaporates and the vacuum pressure increases, deteriorating the thermal insulation. On the other hand, the slits should be filled with hydrogen because the gun lock is like a stopcock and the plastic hydrogen acts as a lubricant. After extrusion is stopped, the temperature should not be lowered too much, otherwise the hydrogen becomes brittle and cannot be cut smoothly. A pneumatic drive (Sec. 4.22) turns the rotor by 90 degrees cutting the pellet from the hydrogen rod. The pellet is now in its starting position for acceleration. The temperature will be decreased further to compensate the heat pulse of the propellent gas during the shot by heat capacity. This is done simply by switching off the ohmic heater in the cryostat. For shooting, the fast solenoid valve for the propellent gas is excited, and the gas streams into the gun lock. Usually we use hydrogen gas at room temperature as a propellent. Owing to the gun temperature the gas is cooled down and part of it may condense to the wall. On the other hand, the gun itself increases its temperature. The temperature rise thus has to be limited in order not to vaporize the stored solid hydrogen. Otherwise the gas has to be solidified again and the gas which leaks into the insulation vacuum will load the cryostat. After the shot, when the heat pulse is transferred to the coolant cycle, the temperature of the gun is increased by electric heating to the so-called basic temperature. At basic temperature we freeze further hydrogen gas into the storage volume so that we have the storage level about constant. The piston has to be lifted up for this process. When the vacuum pressure of the insulation system is below 10^{-5} mbar the gun is ready to start the next extrusion. The complete cycle is able to run automatically controlled by Simatic S5-150 and CODAS.

The design of the gun lock is such that it can be used for several pellet sizes. For this purpose the rotary cylindrical shell containing the pellet mould and the barrel have to be replaced by pieces with other mould and barrel diameter. These pieces also have to be manufactured together with the housing of the gun lock. This replacement can take place in a few days because the cryostat has to be at room temperature and the vacuum has to be broken.

4.22 Gun lock drive

For extrusion and for firing, the cylindrical rotor of the gun lock has to be placed in two different positions at an angle of 90 degrees to each other. These positions have to be aligned very exactly. In the position where the pellet is in front of the barrel the alignment should be better than a few hundredths of a millimetre. If this is not fulfilled, there is a high risk that the pellet will already be damaged in the initial phase of acceleration. An adjustable and substantial stop for the rotor therefore has to be installed directly at the gun. The rotor drive (Fig. 19) will be situated outside the vacuum chamber. The angular momentum will be transmitted by a tube with thin wall to keep the heat conduction low. Because the stop is directly at the gun, we have not to take torque of the transmitting tube into account. The vacuum feed-through will be done by bellows. Externally a pneumatic drive will be used.

4.23 Propellent gas system

The propellent gas system (Fig. 20) is developed to supply the pellet gas gun with helium or hydrogen gas up to a pressure of 4 MPa to accelerate the pellet.

Most of the parts of the system are located in the basement below the torus hall. The usual propellent is hydrogen. Only for backup is a helium system also envisaged. The porpellent gas, which is contained in an ordinary gas bottle, is sufficient for several thousand shots. Exchange of the gas cylinder is therefore not required during the active phase of JET. During the early phase of JET empty gas bottles can be exchanged fast by using quick connections and avoiding ventilation of the propellent gas system by valves. The motor-operated pressure regulators have to be controlled by the CODAS system because the gas pressure governs the pellet velocity. The gas pressure of about 20 MPa in the gas bottle has to be reduced to less than 4 MPa, which is permissible for the gun.

The gas supply system in the basement is connected by one gas feedline to the pellet gun. At the gun the propellent gas inlet has a by-pass to a separate storage volume. This is to reduce the propellent flow into the pellet transfer system. After firing of the main fast solenoid valve the pellet leaves the barrel within a few milliseconds. The by-pass solenoid valve is then activated and the propellent pressure in the gun and hence the propellent flow through the barrel is reduced. The closure time of the solenoid valves is of the order of 5 to 10 milliseconds.

The propellent gas system will be evacuated by a separate forepump into the JET hydrogen exhaust line. This is for cleaning the system. It also has to be operated, however, if a high propellent pressure in the system has to be lowered between two shots to alter the pellet velocity required. Then a large amount of gas has to be removed. Because this would overload the backing system, we propose using a separate pump which works into a hydrogen exhaust line. The fast solenoid valves (Fig. 21) which we use to switch the high-pressure propellent gas for shooting are improved commercial high-pressure valves. The improvements concern the solenoid to obtain fast opening and closing of the valve in a few milliseconds and the sealing of the valve to get the valve vacuum tight. The valves have been improved in our laboratory.

4.3 Vacuum system

The vacuum system consists of three sections (Fig. 22) clearly distinguishable in function. Beginning at the cryostat, the first section is for supporting the thermal insulation of the cryostat. During operation pellet material and propellent gas leaks through the gun lock. It has to be pumped off because,if it condenses to the outside of the cryostat, it impairs operation of the gun. Each temperature variation causes evaporation or condensation of this leakage material and the cryostat becomes thermally unstable. In ASDEX and WVIIA a combination of a turbomolecular pump and a bath cryopump is used. To avoid the additional cryogenic pump, we decided to dispense with the cryopump and use a large turbomolecular pump with a pumping speed of at least 2800 l/s for hydrogen.

The gun barrel terminates in the second section of the vacuum system. The volume of this vessel has to be chosen so that the pressure of the propellent gas is strongly reduced and the gas flow through the diaphragm into the next section and finally into the JET torus is limited to an acceptable value. Between shots a high and impurity-free (oil, air) vacuum is required to prevent condensation into the barrel, which acts at its gun end as a cryopump. The pellet diagnostics are also installed in this section. This required ports for the microwave resonator system, the light barriers and the pellet television camera.

The third section is the low-pressure part of the differential pumping system and contains an ultrafast vacuum valve stopping the propellent gas flow before entering the torus. The pellet injector is additionally insulated from the torus by a ceramic break. In the event of an accident, where a pump becomes defective for example, the vacuum system has to be ventilated by helium gas to a pressure of below 1 bar. Gases other than helium without hydrogen, which, however, cannot be used for ventilation for safety reasons,are unsuitable because they soil the cryostat. Cleaning of the cryostat by pumping takes several weeks.

4.31 Vacuum vessel

The complete vacuum system is shown in Fig. 22. The pellet injector is built of two vacuum vessel (Fig. 23). A double-cross vessel (Fig. 33) is the housing for the cryostat, which operates in the vertical position. The propellent gas (Fig. 17) and gun lock drive (Fig. 19) are connected with the gun by special feedthroughs. JET remote handling flanges are used for the vacuum gauges included in branch pipe unit I and for a turbomolecular pump TPU 2200.

The vacuum vessel for the differential pumped diaphragm system is constructed of two symmetrical cylindrical stainless-steel vessels, each 400 mm in diameter and 1100 mm long. Near the entrance of the

the pellet several ports for pellet diagnostics are envisaged. In each vessel two vacuum-tight rings are welded to support the diaphragms of the differential pumping system. The first diaphragm is turned up in the direction of the barrel to get a large vacuum volume but a small diameter of the diaphragm. This diameter and the diameter of the following diaphragms corresponding to a stray angle of one degree of the pellet trajectories, although the measured angle is less than 0.25 degree. Calculations for the gas flow through this system are shown in Fig. 24. The gas flowing into JET up to the closure time of the fast valve of 20 ms is about 0.1 mbar·l. This is 0.6% of the pellet mass based on pellet diameters of 3 mm. A pressure rise during the shot of between 10 and 50 mbar is expected for the first vacuum chamber behind the barrel. This is a large amount of gas which cannot be pumped off by the JET backing system in a short time. Other JET diagnostics using the same backing system will be affected. For a time the backing system at pump P2 will therefore be replaced by a Roots pump pumping into the roughing system. After evacuation of the propellent gas the roots pump will be switched off and the usual backing system is connected to the turbomolecular pump.

The cryostat or insulation vacuum vessel and the diaphragm vessel are not connected directly. The gun barrel is fixed vacuum-tight in the flange connecting both vessels. If alignment of the barrel is necessary, then a bellows and micrometer drive have to be built into the flange. But this is not expected by us.

4.32 Vacuum interface to torus vacuum system

The interface line to the JET torus vacuum system will be the main horizontal port flange of octant II. For the pellet injector an all-metal valve from VAT corresponding to JET standard, series 43 DN 150 with JET remote handling flange, will be needed for separation of the pellet system. A double-walled bellows will decouple the pellet injection system from the movements of the main port flange during bakeout or disruptions.

A ceramic break in series with the bellows for electrical separation will be proposed (Fig. 25).

This is followed by a fast valve which will open the gas gun system during operation just for the time interval of pellet injection. The interspace between the JET valve and the fast valve will be pumped down by the gas gun vacuum system to the pressure level of the torus vacuum. The opening of the separation valve will be controlled by CODAS via pressure gauges on both sides of the valve. The fast valve V2 in Fig. 22 can be opened with atmospheric pressure in the interspace. The opening and closing times are about 20 ms. The life of V2 will be 20,000 closures. The pressure control will be done by JET standard branch pipe units I and Edwards controller 2001.

The interface to the JET backing line will be VAT angle valves DN 35 and CN 16, series 40 with JET standard remote handling flanges. An alternative option may be to combine all forevacuum connections of the UHV pumps to one VAT valve followed by bellows, a ceramic break and the backing line.

The ventilation line connected with the main turbomolecular pump via VAT angle valves CN 10, series 40 must be supplied with helium. Heavier gases will be frozen in the deuterium cryostats. Return to service would take long evacuation times.

The surface treatment of all inner surfaces will be carried out in accordance with JET quality, document JET QUA 108.

4.33 List of pumps, valves and gauges

In the following all JET standard vacuum components outlined in Fig. 22 are listed.

4.33 List of pumps, valves and gauges

In the following all JET standard vacuum components outlined in Fig. 22 are listed.

Item number	Type	Manufacturer
P1	TPU 510 A	Pfeiffer
P2	TPU 510 A	Pfeiffer
V1	DN 150, series 43	VAT
V3	DN 35, series 40	VAT
V4	DN 35, series 40	VAT
V5	DN 35, series 40	VAT
V7	DN 10, series 40	VAT
V8	DN 10, series 40	VAT
V9	DN 10, series 40	VAT
BPU I_1	installed on main port flange	
BPU I_{2-4}		Leybold-Heraeus
BPU III		Leybold-Heraeus
Pe1-4	Penning gauge	
Pe1,2,3,5,6,7	Pirani gauge	

Non-standard components

P3	TPU 2200	Pfeiffer
V2	fast closing valve	CETEC AG

4.34 Material list

Vacuum vessel:	stainless steel DIN 1.4311 or 4301
Cryostates:	electrolytic cupper, plated with gold
	stainless steel, DIN 1.4311
Ceramic break:	stainless steel, DIN 1.4301
	Vacon 70, NiCo 2923, DIN 1.3982
	alumina V96, bellows DIN 1.4541
Beam line:	stainless steel, DIN 1.4311
	bellows DIN 1.4541 or 1.4311
Support structure:	AlMgSi 0.5 F 22, DIN 3.3206.71

4.4 Control and data acquisition

The control of the pneumatic pellet injector is done by cooperation of CODAS with the internal Simatic system as shown in Fig. 13. The flow charts are given in tables 4.41 to 4.45. They are discussed in detail in the following sections.

4.41 Vacuum control

The vacuum system (Fig. 22) is controlled by two Edwards 2001 controllers (see Table 4.35,1-4). The first contoller (EA) is used to handle the Pennings Pe1, Pe2, the Piranis Pi1, Pi2, Pi6, Pi7, the valves V1, V2, V6, V7, V8, V9 and the pump P4.

The second (EB) handles Pe3, Pe4, Pe5, Pi3, Pi5, V3, V4, V5 and P1, P2, P3.

The vacuum readings of the gauges are passed to CODAS via analog outputs of the gauge modules and a 16 channel A/D-CAMAC module (Table 4.41,1-3). The A/D module is also used to monitor the baking temperature (Table 4.41,1). The connections of the input and output units are given by the following scheme: connected device (high-level signal/low-level signal). The JET valve V1 is operated by CODAS and CISS. Request signals to operate V1 are provided by EA U1 Ch1-2. A feedback signal of V1 is provided by CODAS via LSD output on EA U2 Ch1. A request by the operator to close V1 (EA U6 Ch2) is always passed to CODAS, a request to open V1 (EA U6 Ch1) only if Pe2 < Pe1. If Pe1 is high, close V1 will be requested without operator interference.

Close V1 by CISS (EA U5 Ch6) will be requested if V2 fails to react to the close command.

The fast valve V2 is controlled by Edwards controller EA U1 Ch3 in all operational phases except when the vacuum system is ready for pellet shots. In this case control of V2 is passed to the Simatic control system by EA U1 Ch4. When under Edwards control, V2 is always opened if V1 is closed and vice versa.

Pump 4 will only be energized when the propellent gas pressure of the pellet gun is high. After the shot V6 is opened by a Pi6 high signal. When V6 is opened a signal to close V4 (EA U5 Ch8) is passed to EB.

The desired mode of operation (vacuum system on/off, manual/automatic operation) is received by EA U4 Ch6-7. In the off-state the power of all units, except V1 or V2 (one of which remains opened) is switched off. If the off-state has been reached by a shut down procedure initiated by failure of certain components elusive fault alarm will be given (EA U3 Ch3-6, EA U5 Ch5, EB U3 Ch1-3). The off-state can only be left if a reset pulse (EA U4 Ch4) is given which also resets the elusive fault alarms. The vacuum system on-state will only be reached if Pi7 is low and all cooling water circuits (EA-U2 Ch8, EA U4 Ch1-3) are operating after the water supply is switched on. A failure of the backing pressure, cooling system or pumps returns the system to the off-state (through different shutdown procedures). The actual operation mode is passed on to the operator (EA U3 Ch7-8, EA U5 Ch4, EA U5 Ch7) and information concerning the operation mode are exchanged between the controllers (EA U4 Ch5, EA U5 Ch1-3, EA U6 Ch3).

After a valid vacuum-on command EB opens V2-V5 and switches on P1-P3 (EB U1 Ch2-7) if Pi3 and 5 are low. When Pe3 - Pe5 are low, EB U2 Ch1 gives a signal to EB. EA reacts by passing control of V2 to Simatic and issuing a ready-for-shot signal (EA U5 Ch4) if V1 is opened. The system returns to the not-ready state as long as either of Pe3 - Pe5 are high (e.g. after each shot).

A shutdown procedure will be initiated by failure of the backing pressure of the cooling water circuits (initiated by EA) or by failure of P1-P3 (initiated by EB). Two different shutdown procedures will be executed, depending upon the state of the cryostat (EB U6 Ch6). If the cryostat is warm, all connected units of EA and EB are immediately de-energized. If the cryostat is cold, V5 remains open and a signal (EB U3 Ch4) is given to EA to inhibit the opening of the gas admit valves V7-V9. The worst case of shutdown with cold cryostat and failure of the backing pressure or power failure is handled by a passive excess-pressure valve.

In the vacuum-on state the system may be switched to manual control of V3-V5 and P1-P3 (especially to investigate minor faults). The state of these elements is maintained during the transition unless EB U4 Ch2-8 or EB U6 Ch1-5 are operated. Control of major failures remains active in the manual mode. Feedback signals of all valves and pumps are passed to the controllers and to LSD ports (Table 4.11,2,4 bottom) for the operator's information.

List of hardware:

2 controllers Edwards 2001

5 Penning modules (total number)

3 Pirani modules (total number)

8 I/O modules (total number)

8 Relais output/opto input units

1 Amplifier for PT 100

1 CAMAC module CAD1

2 LSD input cards ULS1

2 LSD output cards ULD2

CAMAC and LSD components which are shared with other systems are separately listed.

4.42 Cryostat control

The start pulse can be given by the operator in two manners: firstly, by means of CODAS, and, secondly in the diagnostic area. This initiates the following measurements:

1.) The pressure of the pressurized air: to be sure that all valves can operate. It is indicated when pressurization is not available.

2.) The level of liquid helium: to be sure that enough helium for a full experimental day is available. If this is not the case, the operator gets the command to refill the cryogenic tank with liquid helium.

3.) The pressure in the mixing volume V5: If the pressure PM is lower than an internally programmed limit, this is indicated and the operator gets the command to refill the volume V5 as described in the section on control of fuel gas.

4.) The vacuum: measured by the Edwards controller and given as a 1-bit signal to the SIMATIC, which means that the vacuum is better than 1×10^{-5} mbar.

At the beginning the pellet-fuel-gas pipe line usually has to be cleaned. The cryostat should be at room temperature. The fact that the cryostat is at room temperature is passed on to the Edwards controller for vacuum control as well as the fact that it is cold in a later phase.

For flushing valve V_M opens for a certain time, e.g. 30 s, and valve V_{p2} opens. For nearly 3 min the pipeline is evacuated, then V_M opens again for 30 s for flushing and is again evacuated. This can be done up to five times. After flushing valve V_{p2} closes and the signal is given that the operator can commence to refrigerate the cryostat.

The command "REFRIGERATE CRYOSTAT" initiates the measurement of the helium exhaust pressure P_H, the helium exhaust temperature T_H, the helium flow and the cryostat temperature by the vapour pressure thermometer. Simultaneously pump P6 is switched on and valve V_{HR} opens. Valve V_{HN}, V_{HB} and V_{HM} are closed. For 3 min the helium transfer line is evacuated up to valves V_{HN} and V_{HB}. Then valve V_{HN} is completely opened and the next part of the transfer line is evacuated for 10 min. If the helium exhaust pressure after the 10 min is smaller than 10^{-1} bar, the heater R_{H1} is switched on. If this is not the case, it is evacuated 10 min once more.

The heater regulates by itself, but the temperature is measured with a pt-100 sensor and the value is compared with a programmed temperature of about 20^{o} C. If the temperature is not reached, the heater R_{H1} is switched off and a reserve heater R_{H2} is switched on. A warning signal is given to the operator. When the heater works and the temperature is regulated to about room temperature, the motorized valve V_{HM} near the cryogenic tank is fully opened for 90 min. After this the operator receives the signal to set the optimal conditions with regard to helium flow. This is done by opening or closing the valves V_{HN} and V_{HM}. After optimizing the helium flow, the operator has to set the three temperatures with which the gun operates: the basic temperature of about 6 to 8 K, the extrusion temperature of about 8 to 10 K and the shot temperature of about 3 to 4 K.

If all these values are given to the SIMATIC, or to the HR1 (Leybold-Heraeus) via the SIMATIC, and the cryostat is cold, the operator gives the command for filling in fuel gas. (The fact that the cryostat is cold is additionally passed on to the Edwards controller for vacuum control).

The cryostat is then set to the basic temperature and the piston is lifted to the upper end position. The valve V_{p1} now opens for 60 s. After this the piston is pressed down for 3 s. If the level is less than 90%, the operation is repeated (piston in upper end position, valve V_{p1} open for 60 s, etc.). It is also repeated after each shot to operate with a nearly constant level of solid ice. When the storage volume for the solidified gas is filled up, the operator receives this signal, which is also necessary for further operation of the gun itself.

4.43 Gun control

The command "READY FOR EXPERIMENT" initiates the measuring of the propellent gas pressure P_{pp} at the entrance of the solenoid valve V_{S1} and the pressure of the fuel gas P_{ps} at the entrance of the cryostat.

If the pressure P_{ps} exceeds a certain internally programmed level, the valve V_{ps} is opened and acts as a by-pass to reduce the pressure by pumping off with pump P3. The valve V_{ps} can be handled by the operator (ON and OFF).

Some conditions have to be met to extrude the first pellet into the cylinder shell:

1.) The propellent gas supply has to be ready.

2.) The pellet fuel gas supply has to be ready.

3.) The fast valve V2 must be entrusted to the SIMATIC by the Edwards controller.

4.) The cryostat has to be at the basic temperature.

With these conditions met, a first START PULSE from CODAS, nearly 3 minutes before the shot, causes the rotor to turn to the extrusion position. After this the temperature is increased to the extrusion temperature. When the extrusion temperature is reached after a certain time, the piston is actuated for a short time. The translation of the piston is measured and indicated via CODAS to the operator to control the amount of extruded ice. To finish the extrusion the temperature is decreased again to the basic temperature for a time.

When the "BASIC TEMPERATURE"is reached, the rotor turns back to the shot position. The temperature is decreased further to the shot temperature. When this temperature is reached, the pellet in the cylinder is cooled down as much as possible by opening the by-pass valve V_{HB} (greatest possible liquid helium flow) and switching off the ohmic heater R_{H1}.

With the by-pass valve V_{HB} open, the heater off and the high voltage on for the solenoid shot valve and the shot-by-pass-valve, the fast valve V2 to JET is opened. When this is done, the command "READY TO FIRE" is given to the operator and the above-mentioned states are also announced.

JET now has to give the command for the shot. This signal is delayed for a few milliseconds to derive reset pulses, e.g. for the solenoid shot valve and other diagnostics, and trigger pulses. For trigger pulses a timer of the CAMAC system is used because delay times of microseconds are necessary with a small jitter.

The reset procedure is chosen shortly before the shot to avoid false triggering by spikes, probably generated by magnetic and electric fields during the initial phase of a JET shot.

When all supplies are reset and the diagnostics are prepared, the shot command is given and valve V_{S1} opens. The shot is recorded by a counter. Immediately after valve V_{S1} has opened, the shot by-pass valve is opened (the delay time has to be determined experimentally), the fast valve V_2 closes (to prevent propellent gas from penetrating into the JET vessel), the heater R_{H1} is switched on and the by-pass valve for max. helium flow is closed. The last three signals are also given to the operator for monitoring.

At first, when the fast valve V_2 is closed, the valve V_{S3} opens, to pump off the propellent gas, which is expanded in the small volume just before the valve. The time of about three minutes also has to be determined exactly by experiments.

Valve V_{S3} closes again and the temperature is increased from the shot temperature to the basic temperature. After a certain time a command is given to refill fuel gas and freeze it.

A time, not exactly known but corresponding to the JET cycle has to be allowed to pass before beginning a new shot cycle of the pellet gun.

4.44 Pellet fuel gas control

The fuel gas supply can be started by the operator in the control area or in the diagnostic area. When the supply is initiated, the following cylinder pressures are measured: p_{11}-D_2 , p_{21}-H_2, p_{31}-Ne, p_{41} - reserve gas (not yet determined) and p_M-mixed gas. These pressures are compared with internally programmed values which are proportional to the storage volume of the gases. If any value is beneath this value, the operator gets the signal "INSUFFICIENT GAS" for the corresponding gas.

This procedure is intended to indicate when any cylinder has to be exchanged, but the gas contained in one cylinder should be sufficient for several thousands pellets.

At the command "PREPARE CYLINDER REPLACEMENT" the motorized regulator valve closes. When the regulator valve closes, the pump P6 is switched on and the valve V_{E1}, the corresponding valve V_D and V_C open. Pump P6 is switched off and valve V_{E1} closes when the pressure of the mixing volume is lower than 10^{-1} bar and the regulator valve is totally closed. The operator now gets the signal to exchange the corresponding cylinder by hand. The operator has to lower the working pressures of the gases p_{12}, p_{22}, p_{32}, and p_{42} during operation. This is done by giving the command "REDUCE GAS PRESSURE". The procedure is the same as described above, but the regulator must not be in the zero position.

To increase the working pressure, the operator just has to open the regulator valve and observe the monitored pressure p_{x2}. Pumping off is unnecessary in this case.

When the correct pressure, corresponding to the mix ratio required, is set, the operator gives the signal "PRESSURE P_{xo} OK". This closes the valve V_{DX}.

The operator then has to determine the kind and the pressure of the gas which he wants to use or of the gases when mixing. With several gases he should put them in rising sequence with respect to the pressure because the gas with the lowest pressure whould be filled in first in the mixing volume V5.

When the pulse "READY FOR MIXING" is triggered and all gases are determined in kind and pressure, pump P6 switches on and valve V_{E1} opens. When the vacuum in the mixing volume V5 is less than 10^{-2} bar all valves V_C close. After this the valve V_{D1} opens and the first gas determined flows into volume V5 for a certain time, e.g. 60 s and valve V_{DX} closes again. In the next step the second gas determined flows into V5 and so on until all the gases required are in the volume V5. There they remain for, for example 120 s so that they are properly mixed. The operator now gets a signal that the pellet gas supply is ready to fill the gas into the cryostat.

4.45 Propellent gas control

By means of the START PULSE this system can be controlled and monitored on a display.

The START PULSE initiates measurement of the cylinder pressures p_{51}, p_{61} and the pressure of the pipe system. The cylinder pressure has to be compared with an internally programmed value which announces that the supply of one of the selected propellent gases is not sufficient and has to be replaced by a new cylinder. In the case of helium the operator has to give a signal to the system "PREPARE REPLACING He CYLINDER". This command completely closes the pressure regulator, switches on pump P6 and opens the valves V_{C5} and V_{E3} and thus evacuates the system up to the pressure regulator. When the gas pressure is $p_T \leqq 1$ bar, the by-pass valve V_{E2}, which is not throttled, is opened to evacuate to lower valves. When the pressure is lower than 1 bar, the operator gets a signal to replace the corresponding cylinder by hand. This is done by closing the manually-operated valves (designated in the parts list as number 2), replacing the cylinder and opening the manually operated valves again. After the statements that the cylinder has been replaced and the vacuum in the system is good enough, the valves V_{C5}, V_{C6}, V_{E2} and V_{E3} are closed and the pump P6 is switched off. This condition and the fact that the cylinder pressure is sufficient again gives the operator the command to determine the propellent gas and the propellent gas pressure.

Evacuating the system without replacing a cylinder works in the same way with other commands ("EVACUATE PIPE LINE AND VACUUM Pr OK").

The operator has to select the type of propellent gas and the propellent gas pressure required. If the two conditions, sufficient cylinder pressure and available power supplies for the regulator valves, are met, the valve V_C opens and the measurement of the propellent gas pressure (PGP) is initiated and monitored.

The SIMATIC compares the value required with the real value and decides, if the pressure has to be increased or decreased. In the former case the regulator valve opens until the value required is set.

In the latter case the high pressure has to be diminished by pumping off the gas because of the closed system. Firstly, the regulator valve is set to a lower value,pump P6 is switched on and valve V_{E3} opens until the value is attained. Then valve V_{E3} closes and pump P6 is switched off.

A signal is given to the operator that the PGP is ok. At the end of experimentation the operator can set the system to a STAND-BY State. The operation is the same as "DECREASING THE PGP", the only difference being that the pressure is diminished to a fixed programmed value.

The STAND-BY state is announced to the operator.

4.5 Pellet and ablation diagnostics

In Sec. 2 we have described some applications of pellets for plasma diagnostics. These diagnostics utilize the usual tokamak or stellarator diagnostics for measurements of the processes excited by pellets in the plasma. For evaluation of these diagnostics additional information on the pellet itself has to be acquired. These data are the mass and velocity of the pellet, the time of injection, the trajectory of the pellet, its penetration depth into the plasma and its ablation. For doped pellets the percentage of the impurity is of interest, too. The doping will be determined from the gas mixture before pellet production. But all other properties should be measured from the flying pellet. The mass and velocity of the pellet can be determined a short distance after leaving the barrel, The methods applied are light barriers, pellet photography (Fig. 26) and interaction with microwaves. An excellent method of measuring the trajectory of the pellet and its penetration depth is the photography of ablation traces of the pellet in the plasma (Fig. 8). This method depends on the availability of suitable windows in the torus and it cannot be applied in the extended phase of JET. It will therefore not be discussed here although this method was very successful in ASDEX. Ablation of the pellet can be recorded by D_α and H_α-sensitive diodes. An example is shown in Fig. 7. The D_α emission is given versus time for an 1 mm pellet with 800 m/s injected into ASDEX. If the pellet velocity is known, the penetration depth can be roughly estimated. The uncertainty is caused by the slow slope of emission, and so the pellet crossing the separatrix is hard to identify.

4.51 Microwave and light barrier system

The system will be designed to measure the pellet mass and velocity. Determination of the mass utilizes the perturbation of the field in a microwave cavity /6/ by the dielectric properties of the pellet.

The resonance of the cavity is shifted and the variations in phase and amplitude of the reflected wave give information on the total mass of the pellet. In front of the resonator the pellet crosses a light barrier (Fig. 27) /7/. This gives a trigger pulse which resets the microwave system. The pellet velocity is calculated from the delay time between the optical signal and the microwave signal.

The pellet diagnostic system outlined will be constructed by Risø National Laboratory. A detailed description is given in /13/.

4.52 TV system for pellet shape monitoring

In addition to the pellet mass information obtained by the microwave resonator, a TV recording system will be used to monitor the pellet shape. This system is only intended for informing the operator and will not pass results to CODAS. In order to avoid magnetic interference, a solid-state camera will be used. (Either English Electric Valve P 4300 or Fairchild 3000 with European TV standard will be selected when information about the Fairchild camera is available.)

For the D-D phase only moderate shielding of the camera in conjunction with a solid-state laser will be necessary. This may be achieved by locating them behind a transformer limb using image-forming fibre optics for the laser. In the D-T phase periscope systems to the basement will be necessary to achieve adequate shielding. Both the camera and the laser have to be electrically insulated from the experiment with the only ground connection at the local unit cubicle.

The TV system and its connection to CODAS is shown in Fig. 28. The power of the camera will only be switched on for a few seconds for each pellet shot in order to reduce the sensor temperature. In this way the image quality will be improved without active cooling measures. When the pellet has passed the pellet mass diagnostic, the laser is triggered to produce a shadow image of the pellet. Since the readout time of the sensor is 40 ms laser pulses with closer spacing must be avoided. A circuit which suppresses trigger pulses for 40 ms after each valid trigger is used to prevent double exposure. The method of recording the images on video tape will be similar to a concept worked out by W. Hopmann, W. Kohlhaas and D. Rusbuelt of KFA Jülich for a Limiter Surface Temperature Measurements System for JET.

For storage of the video signals a Sony BVU-820 videorecorder with professional image quality will be used. Each single frame of the recording can be coded and identified by a Sony time code generator/ reader. The encoding consists of the time of the day (hours, minutes, seconds), frame numbering within a second and 8 4-bit words to be defined by the user. These may be used to record the JET discharge number and an additional pellet injector number to identify pellet test shots between the JET discharges. The pellet injector number will be generated by a non-volatile counter which is interfaced by 16-bit LSD inputs.

The videorecorder and the time coder are equipped with 32-bit parallel interfaces for remote control. These can be connected to 4 CAMAC I/0 modules (CPR1) which, in turn, are controlled by an auxiliary crate controller (CAC). The auxiliary controller will be programmed to

- start recording at the beginning of the JET pulse
- stop recording and memorize the last recorded frame at the end of the JET pulse
- return to the last recorded frame in the parameter setup phase (new recording will be inhibited if this position cannot be reached in time.)

The same operations must be executed for pellet test shots without JET discharge. In this case the signals for parameter setup and pulse phase are not generated by the central timing system but internally by the Simatic control system.
The timing signals are handled by a CAMAC timer (CTM1).

Between the shots the recording may be reviewed by a TV monitor in the control room (transmitted by the CODAS video network) as a slow-motion or still picture display. The appropriate time codes and shot numbers are displayed on the mobile console screen for search and identification purposes.

List of hardware

1 Laser laser diode LT-139

1 Video camera English Electric valve P 4300 or Fâirchild 3000 (European TV standard)

1 Power switch (Eurocard, to be developed)

1 Double exposure inhibit (Eurocard, to be developed)

1 Non-volatile pulse counter (Eurocard, to be developed)

1 Video-tape recorder Sony BVG-820

1 Time code generator/reader Sony BVG-1000

4 CAMAC I/O modules CPR1

1 CAMAC auxiliary crate controller CAC

1 CAMAC timer CTM1

Basic CAMAC and LSD components are separately listed.

4.53 D_α diagnostic

D_α emission occurs during the ablation of the pellets. The intensities are a relative measure of the particle deposition in the plasma, and the pulse duration delivers together with the known pellet velocity the penetration depth.

In the beam tube a quartz prism will deflect the light through a vertical standard quartz window DN 35. Via a quartz fibre cable the light will be transmitted to a diode installed in the basement for radiation protection.

The maximum ablation time will be of the order of 2 ms. Because a fine structure of the signal is of interest, a sampling rate of 1 MHz will be required.

Most parts of the electronics needed for data acquisition and remote control could be taken from the "provisional soft X-ray diagnostic". Figures 29 to 31 show the electronic scheme and the detailed circuits in part. The required memory needs a capacity of 5 K words for an observation time of 5 ms after the trigger pulse from the pellet mass diagnostic.

The output of the detector diode is amplified by a preamplifier located close to the diode. An existing preamplifier design from the provisional soft X-ray diagnostic (Fig. 30) has to be modified to cover the required 5000 kHz bandwidth. The gain of the preamplifier can be set by two relays which are operated by changing the power supply voltages. The diode and the preamplifier will be placed in an insulating cabinet. The main amplifier (Fig. 31) located in the local unit cubicle will be connected to local ground. The low bandwidth isolation amplifiers of the provisional soft X-ray diagnostic can therefore be omitted. The gain of the amplifier chain is determined by the setting of 6 LSD output bits. The output of the main amplifier is connected via an anti-aliasing filter to a CAMAC ADC module (CAD4) with an associated memory module (CME4). The CAD5 of the provisional soft X-ray diagnostic has to be replaced by CAD4 owing to the 1 MHz sampling rate required. Because of the lower resolution of the CAD4 (10 bit) the bandwidth of the filter may be adjusted close to one half of the sampling frequency. The leak current of the diode is compensated by a digital regulation circuit. A signal from the CAMAC timer (CTM1) is used to freeze in the leak compensation during the JET discharge. A defined leak current can be added to test the amplifier chain. The leak current and the supply voltages are monitored by another CAMAC ADC (CAD1). A second regulation circuit is used for the bias voltage of the diode. The bias voltage is preset with the possibility of changing its value by ramp up and down inputs. Another test facility of the diagnostic is provided by a test light circuit to simulate the light input of the diode.

The data recording is initiated by a trigger pulse from the pellet mass diagnostic. For each trigger pulse the clock-pulse generator generates a burst of 5000 clock pulses of 1 MHz. At the end of the JET pulse further data transfer is inhibited by a stop trigger pulse from the timer. The start signal for the timer is generated by the CTS and, in the case of pellet shots without JET discharge, by the Simatic control system.

List of hardware

1 Detector Diode (to be determined)
1 Preamplifier (to be developed)
1 Main amplifier with power supplies and a test light source (from soft X-ray diagnostic)
1 Clock pulse generator (to be developed)
(CAMAC and LSD components are separately liste.

4.6 Interface to CODAS

Tables 4.61 to 4.63 give an overview of the CAMAC and LSD components and their connections to the associated control and diagnostic devices. More details about the connected circuits are given in the sections noted in the list.

4.7 Support structure

The support structure will be divided in its height for practical reasons. During assembling and testing a height of the order of one metre for the pellet beam tube seems to be reasonable. On the JET site this will be about 6 metres. The essential design can be seen in Fig. 32.

One therefore needs a platform with the dimensions

H = 4950 mm

B = 1000 mm

L = 2 x 2100 mm.

This platform consists of two towers designed as a lattice structure. For the support of the pellet gas gun both towers are placed one after the other in the radial direction.

The platforms support the ground frame with the pellet injectors themselves and a 100 litre storage tank for the liquid helium.

The vacuum vessels and the fast closing valve will be supported by the ground frame at 8 points. The turbomolecular pumps are fixed to the vacuum vessel itself. For mounting of the turbomolecular pumps they can be put down on sliding carriages which are integrated in the ground frame. The TPU 2200 turbomolecular pump needs a separate mounting device.

The Roots pump will be supported by the ground frame with rubber metals between them.

The ground frame has a length of about 3000 mm, a height of 900 mm and a width of 800 mm and has adjusting screws for proper alignment.

The admissible load would be several tons. The arrangement will be oversized for rigidity. The proposed material is aluminium-base alloy AlMgSi 0.5 G 22 corresponding to DIN 3.3206.71.

4.8 JET services

The operation of the pellet injector calls for supplies of liquid helium, helium gas, pressurized air, cooling water, and electric power and connections to the vacuum backing system, vacuum roughing system, hydrogen exhaust line, and helium recycling line. In the torus hall the service lines should go to the support of the pellet gun. In the basement the lines should end near or in the cubicles which contain the gas supply for the pellet injector.

Tables 4.81 and 4.82 separately list the supplies needed for the torus hall and for the basement of the torus hall.

5. Guide tube system

In the arrangement described above the pellet injector is installed in the line of sight of the plasma (Fig. 32). The pellet experiences free flight. An alternative way of injector installation uses a straight or a curved guide tube /6/. Such an arrangement has the advantage of affording the possibility of hiding the pellet injector behind a radiation shield and putting it in any position which is not in the line of sight of the plasma (Fig. 34). But this must be paid for with losses in the velocity and mass of the pellet, with an increase of the stray angles of the pellet trajectories and with limitation of the velocity to a maximum speed governed by the strength of the pellet material. The interaction of pellets with guide tubes was therefore investigated for a wide variety of pellets and guide tubes. These measurements are described in Sec. 5.1, while the conclusions for the application of guide tubes in JET are drawn in Sec. 5.2.

5.1 Pellet transfer through guide tubes

The experiments are done with a pellet gas gun mainly using pellets 2.6 mm in diameter and length, but also with pellets of linear dimensions of 0.6 mm and 1.5 mm. The pellets are fired into a guide tube (Fig. 35). The velocity is measured by light barriers before and after the guide tube. The pellet are also photographed by flash photography at the entrance and exit of the tube. The pellet punches a hole in a target to determine the stray angles of pellet trajectories in a series of shots. In addition, the pressure rises in the vacuum chambers owing to the propellent gas and the evaporation can be measured. A comprehensive report on these experiments is under preparation /8/. The results will therefore just be reviewed briefly.

The stray angle increases from 0.25^{o} at the entrance of the guide tube to between 0.5^{o} and 2.0^{o} at its exit. This depends on the curvature (Fig. 36a), length (Fig. 36b) and diameter of the tube (Fig. 36c). With increasing curvature of the tube the centrifugal forces become more important. The pellet will not undergo collisions with the wall, but will slide along the outside of the inner wall. As a result, the stray angle for small radius of curvature will be small. For large radius of curvature and straight tubes the pellet experiences many collisions with the wall. It is obvious in this case that the stray angle increases linearly with the length of the guide tube.

The loss of velocity was measured for many straight and curved guide tubes (Fig. 37). It was about 10% of the original velocity if only undestroyed pellets were considered.

The determination of the loss of mass assumes that the pellet is not destroyed by collisions. This is correct below velocity limits depending on the guide tube. The pellets are evaporated at their corners, as shown in photographs, and small pieces could be broken off. But all the estimates of the loss of mass are very inaccurate, as also are the measurements of the pressure rise in a test volume. The following approximate result was obtained. Low losses of mass are observed in straight guide tubes with diameters greater than twice the pellet diameters. The losses are of the order of 10%. If curved guide tubes are used, the losses increase with decreasing radius of curvature to 20% for $\rho = 5$ m and 50% for $\rho = 1$ m. For narrow guide tubes with diameters about the pellet diameter nearly 50% of the pellet mass is evaporated.

During their flight through the guide tube collision and centrifugal forces act on the pellet. If these forces exceed the strength of solid hydrogen, the pellet will be fragmented. In our experiments we determined an empirical curve (Fig. 38) for maximum attainable pellet velocities versus radius of curvature of the guide tubes. The range of applied pellet velocities was 300 m/s to 1500 m/s for pellets of 2.6 mm diameter. For straight guide tubes the velocity limit for destruction was not achieved within this range.

5.2 Limitations for guide tubes for JET pellet gun

The application of a guide tube for the JET pellet gun has the advantage that important parts of the gun could be installed behind radiation shielding, e.g. in the basement of the torus hall. Such an arrangement will require a curved guide tube about 15 m in length. The irreproducible loss of velocity and mass are restrictions for pellet injection through guide tubes. The increased stray angle also impairs reproducibility for the injection. Penetration depths for pellets thus vary from shot to shot. But the limitation of the pellet velocity to a maximum velocity is the principal disadvantage of the application of guide tubes. In JET fast pellet velocities in the range between 1000 m/s and 2000 m/s achieving deep penetration of the order of the plasma radius are necessary for diagnostics with pellets. The use of bent guide tubes therefore cannot be recommended. The use of straight guide tubes has no substantial advantage compared with the use of diaphragm systems with differential pumping. We thus propose dispensing with guide tubes for pellet injection in JET.

Acknowledgements

The authors would like to thank E.Buchelt, G.Prausner, E.Oberlander, W.Drechsler, H.Kollotzek, and J.Werber for their assistance throughout the course of this work. Also we like to acknowledge the effort of Mrs. Ch.Röder, Miss M.Heilmair, A.Nicol and S.Ertl for the preparation of this report.

References

/1/ S.L.Milora
Review of Pellet Fueling
J. Fus. Energy 1 (1), 15, 1981
C.T.Chang, L.W.Jørgensen, P.Nielsen, L.L.Lengyel
The Feasibility of Pellet Refuelling of a Fusion Reactor
Nucl. Fus. 20 (7), 1980, 859
K.Büchl, C.Andelfinger, H.Kollotzek, R.Lang, M.Ulrich
D_2-Pellet Injection System
9. Symp. on Eng. Probl. of Fusion Research, Chicago, Proc. Vol. II, 1725, 1983
G.Fußmann et al.
Investigation of Suprathermal Discharges in the ASDEX Tokamak
9 Int. Conf. on Plasma Physics and Controlled Nuclear Fusion Research, Baltimore IAEA-CN-41/W1, 1982
S.L.Milora et al.
Pellet Injection into PDX Diverted Plasmas
Nucl. Fus. 22 (10), 1263, 1982

/2/ S.L.Milora, C.A.Foster
ORNL Neutral Gas Shielding Model for Pellet-Plasma Interactions
ORNL/TM-5776, 1977

/3/ K.Behringer, K.Büchl, G.Fußmann and ASDEX Team
Investigation of Particle Transport in ASDEX using Neon-doped Pellets
Verh. DPG Regensburg, P51, 395, 1983

/4/ H.J.Forth et al.
Kryostat für die Erzeugung und Beschleunigung von Deuterium-Pellets zum Einsatz in Kernfusionsanlagen
Vakuum-Technik 30 (4), 102, 1981

/5/ S.L.Milora et al.
Development of Hydrogen Pellet Injectors and Pellet Fueling Experiments at ORNL
9. Int. Conf. Plasma Phys. and Contr. Therm. Fus. Res. Baltimore IAEA-CN-41/0-3, 1982

/6/ P.B.Jensen and V.Andersen
Handling of Deuterium Pellets for Plasma Refuelling
J. Phys. D: Appl. Phys. 15, 785, 1982

/7/ V.Andersen, V.O.Jensen
Risø National Laboratory, private communication

/8/ K.Büchl, W.Sandmann
Launching of D_2-Pellets through Guide Tubes
12. SOFT Jülich 1982, Paper F27
K.Büchl, W.Sandmann
IPP-Report, in preparation

/9/ G.Haas
IPP, private communication

/10/ S.L.Milora et al.
Pellet Injection into PDX Diverted Plasmas
Nucl. Fusion 22 (10), 1263, 1982

/11/ K.Büchl, W.Engelhardt, G.Vlases and ASDEX Team
Annual Report, IPP Garching 1981, 20 - 22

/12/ A.Eberhagen
IPP, private communication

/13/ V. Andersen, P. Andersen and P. Christensen
Design of Equipment for Measuring Pellet Masses and Velocities,Proposal July 1983 Risø National Lab., Fusion Research Unit

List of Tables

Figure Captions

Fig. 1: Comparison between gas pulse and pellet injection in ASDEX. Electron line density measured with HCN-Laser interferometer. Gas pressure measured in the upper divertor chamber /9/.

Fig. 2a: Electron density profile after pellet injection for three pellet velocities calculated with neutral gas shielding model. The undisturbed density profile (dashed curve) is fitted to the measured profile of fig. 2b. Pellet diameter 1.0 mm. $T_e(0)$ = 800 eV.

Fig. 2b: Measured density profile of PDX /10/ before and after pellet injection. Pellet diameter 1.0 mm. Pellet velocity 825 m/s. Plasma: $n_e(0) \approx 2 \times 10^{13}$ cm^{-3}; $T_e(0) \approx$ 800 eV.

Fig. 3: Measured (full curves) and calculated (dashed curves) perturbation of the density profile for ASDEX /11/. Pellet diameter 1.0 mm. Pellet velocity $\approx$ 600 m/s.

Fig. 4: Calculated temperature profile after pellet injection into ASDEX. Dashed curve is the measured profile before injection. Pellet diameter 1.0 mm. Pellet velocity = 800 m/s; $n_e(0) = 1.7 \times 10^{13}$ cm^{-3}; $T_e(0)$ = 1640 eV.

Fig. 5: Electron temperature measured by ECE at four radii during pellet injection /12/. Penetration radius of the pellet (1.0 mm ϕ, V_{Pel} = 750 m/s) is about $R_{Pel} \approx$ 15 cm. (origin of time scale is arbitrary)

Fig. 6: NeX-Signal after injection of a neon-doped deuterium pellet (1.0 mm ∅, V_{Pel} = 900 m/s) in ASDEX compared with simulations for different diffusion coefficients /3/. Plasma: $\bar{n}_e = 4.4 \times 10^{13}$ cm^{-3}; $T_e(0)$ = 620 eV.

Fig. 7: Measured D_α-emission during pellet ablation in ASDEX (Pellet: 1.0 mm ∅, V_{Pel} = 725 m/s; $T_e(0)$ = 1640 eV; $n_e(0) = 1.7 \times 10^{13}$ cm^{-3}; penetration radius = 17 cm, # 8837). Calculated deposition profile (0.8 mm ∅, V_{Pel} = 700 m/s; $T_e(0)$ = 1640 eV; $n_e(0) = 1.7 \times 10^{13}$ cm^{-3}).

Fig. 8: Photography of the pellet ablation trace through a tangential port in ASDEX. Pellet 1.0 mm ∅, V_{Pel} = 900 m/s; penetration radius R ≈ 10 cm; Plasma: $\bar{n}_e = 4.4 \times 10^{13}$ cm^{-3}; $T_e(0)$ = 620 eV, # 7900.

Fig. 9: Experimental arrangement for photography of the pellet ablation trace through an oblique port in radial direction in ASDEX.

Fig. 10: Photography of the pellet ablation trace in radial direction using set-up of fig. 9. Shot # 7900 of fig. 8.

Fig. 11: Photography of the pellet ablation trace through a tangential port in ASDEX. Pellet: 1.8 mm ∅, V_{Pel} = 625 m/s; Discharge: $\bar{n}_e = 1.1 \times 10^{13}$ cm^{-3}; $T_e(0)$ ≈ 1000 eV; # 5938.

Fig. 12: Calculated penetration depths into JET for 3.0 mm ∅ D_2-Pellets and different plasmas.

Fig. 13: Block diagram of pellet gas gun system including supply and control devices.

Fig. 14: Pellet cryostat (Leybold-Heraeus, Köln).

Fig. 15: Liquid helium supply of pellet cryostat.

Fig. 16: Pellet fuel gas supply for pure and mixed hydrogen isotopes and mixtures with neon.

Fig. 17: Gun lock with barrel and fast solenoid valves for propellent gas.

Fig. 18: Drawing of pellet gun lock.

Fig. 19: Pellet gun lock with pneumatic motion mechanism.

Fig. 20: Propellent gas supply for pellet acceleration.

Fig. 21: Drawing of the fast solenoid valve for propellent gas inlet to the pellet gun.

Fig. 22: Vacuum system of the pneumatic pellet injector.

Fig. 23: Vacuum vessels for diaphram system with diagnostic ports and vacuum pumps.

Fig. 24: Pressure rise in the vacuum system during pellet injection due to propellent gas flow. Vacuum vessel 1 at the barrel end, the others are following. Diameter of diaphragms 3 and 5 mm. Propellent gas pressure 20 bar.

Fig. 25: Pellet beam line with interface to JET including valves, bellows and a ceramic break.

Fig. 26: Photography of a 2.6 mm D_2-pellet in flight (velocity $\approx$ 1200 m/s).

Fig. 27: Light barrier and microwave diagnostics for determination of velocity and mass of the pellet /7/.

Fig. 28: Block diagram of TV pellet observation and recording system.

Fig. 29: Block diagram of electronics for D_α-diagnostics.

Fig. 30: Preamplifier for D_α-diagnostics.

Fig. 31: Main amplifier for D_α-diagnostics.

Fig. 32: Arrangement of pellet injector and support structure in the Torus Hall.

Fig. 33: Vacuum vessel for pellet cryostat with vacuum pump TPU 2200.

Fig. 34: Guide tube system for pellet injection into JET.

Fig. 35: Experimental arrangement for investigation of pellet propagation through guide tubes.

Fig. 36a: Dependence of stray angles of pellets passing through straight and curved guide tubes on guide tube curvatures. Pellet diameter: 2.6 mm; Guide tube diameter: 6 mm; Length: 2 - 4 m.

Fig. 36b: Dependence of stray angles of pellets passing through straight guide tubes on guide tube lengths. Pellet diameter: 1.5 mm; Guide tube diameter: 6 mm.

Fig. 36c: Dependence of stray angles of pellets passing through straight guide tubes on guide tube diameters. Pellet diameter: 2.6 mm; Guide tube length: 2.5 - 4 m.

Fig. 37: Loss of velocity of pellets in straight and curved guide tubes. Pellet diameter: 2.6 mm.

Fig. 38: Dependence of critical pellet velocity on radius of curvature of guide tubes. Pellets exceeding the critical pellet velocity are destroyed at the end of the guide tube. Guide tube length: 3.5 - 4 m; Pellet diameter: 2.6 mm.

<u>List of drawings</u> (handed over to JET)

2L-1EG-1105	Gas Gun System
1C-1EG-1108	Cryostat
3J-1EG-1100	Liquid Helium Supply
3J-1EG-1101	Pellet Gas Supply
1C-1EG-1106	Gun Lock Propellent Supply
2B-1EG-0003	Zusammenstellung Pelletkanonenschloß
3D-1EG-0004	Housing
3D-1EG-0005	Rotor
4D-1EG-0006	Core
4D-1EG-0007	Stop disc
4D-1EG-0008	Stop
3C-1EG-0009	Gunpipe complete
4D-1EG-0010	Gunpipe flange
4D-1EG-0011	Tube
4D-1EG-0012	Sealing 22/19 Ø
4D-1EG-0013	Sealing 10/8 Ø
4D-1EG-0014	Sealing 13/10 Ø
4D-1EG-0015	Stud short
4D-1EG-0016	Stud long
1C-1EG-1107	Pellet Gun Lock Drive
3J-1EG-1102	Propellent Gas System
3B-1EG-1034	Fast Solenoid Valve
2J-1EG-1103	Vacuum System
OC-1EG-1030	Diaphragm System
OC-1EG-1031	Pellet Beam Line
OB-1EG-1033	Support Structure
OC-1EG-1032	Cryostat Vessel

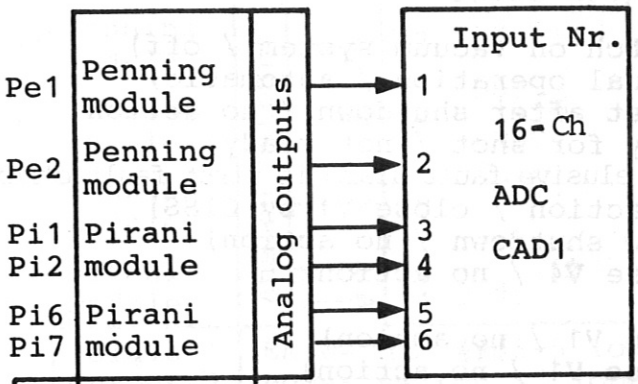

Module	Unit	Ch.Nr.	Function
J/O module	Relais Output EA Unit 1	1	LSD In1 (Open V1 by CODAS / no action)
		2	LSD In2 (Close V1 by CODAS / no action)
		3	Siematic (open/close V2, if control by EA)
		4	Siematic (control of V2 by Siematic /EA)
		5	Power switch V6 (open V6 / close)
		6	Power switch V7 (close V7 /open)
		7	Power switch V8 (close V8 /open)
		8	Power switch V9 (close V9 /open
	Opto Input EA Unit 2	1	LSD out 1 (V1 closed / opened)
		2	Feedback switch V2 (V2 closed / opened)
		3	Feedback switch V6 (V6 closed / opened)
		4	Feedback switch V7 (V7 opened / closed)
		5	Feedback switch V8 (V8 opened / closed)
		6	Feedback switch V9 (V9 opened / closed)
		7	Feedback switch P4 (P4 on / off)
		8	Feedback switch cooling water P1 (P1 on / off)
J/O module	Relais Output EA Unit 3	1	Power switch P4 (P4 on / off)
		2	Power switch cooling water (on / off)
		3	LSD In 3 [cooling water P1 elusive fault alarm if first fault detected / otherwise]
		4	LSD In 4 [cooling water P2 elusive fault alarm if first fault detected / otherwise]
		5	LSD In 5 [cooling water P3 elusive fault alarm if first fault detected / otherwise]
		6	LSD In 6 [cooling water P4 elusive fault alarm if first fault detected / otherwise]
		7	LSD In 7 (vacuum system on / off)
		8	LSD In 8 (manual operation / automatic)
	Opto Input EA Unit 4	1	Feedback switch cooling water P2 (P2 on / off)
		2	Feedback switch cooling water P3 (P3 on / off)
		3	Feedback switch cooling water P4 (P4 on / off)
		4	LSD Out 2 (reset after shutdown / no action) pulsed
		5	EB U1 Ch1 (Pe3-5 low / either of Pe 3-5 high)
		6	LSD Out 3 (switch on vacuum system / off)
		7	LSD Out 4 (manual operation / automatic)
		8	Siematic (propellant gas pressure high / low)

Table 4. 41.1 Vacuum control system

J/O module	Relais Output EA Unit 5 CH.Nr.	1	EB U2 Ch1 (switch on vacuum system / off)
		2	EB U2 Ch2 (manual operation / automatic)
		3	EB U2 Ch3 (reset after shutdown / no action)
		4	LSD In 9 (ready for shot / not ready)
		5	LSD In 10 (Pi7 elusive fault alarm if first fault/otherwise)
		6	LSD In 11 (no action / close V1 by CISS)
		7	LSD In 12 (slow shutdown / no action)
		8	EB U6 Ch7 (close V4 / no action)
	Opto Input EA Unit 6 Ch.Nr.	1	LSD Out 5 (open V1 / no action)
		2	LSD Out 6 (close V1 / no action)
		3	EB U3 Ch4 (slow shutdown / no action)
		4	
		5	
		6	
		7	
		8	
J/O module	Relais Output E Unit Ch.Nr.	1	
		2	
		3	
		4	
		5	
		6	
		7	
		8	
	Opto Input Unit Ch.Nr.	1	
		2	
		3	
		4	
		5	
		6	
		7	
		8	

Feedback switch V2 - LSD In 13 (on/off)
" V6 - LSD In 14 (on/off)
" V7 - LSD In 15 (on/off)
" V8 - LSD In 16 (on/off)
" V9 - LSD In 17 (on/off)
" P4 - LSD In 18 (on/off)
Feedback switch cooling water P1 - LSD In 19 (on/off)
" P2 - LSD In 20 (on/off)
" P3 - LSD In 21 (on/off)
" P4 - LSD In 22 (on/off)

Table 4. 41. 2 Vacuum control system

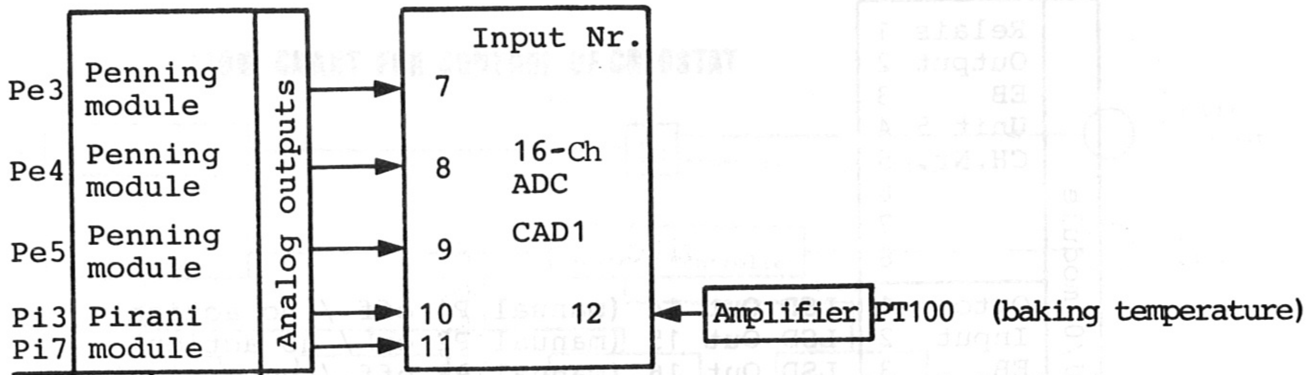

Module	Unit	Ch.Nr.	Signal
J/O module	Relais Output EB Unit 1	1	EA U4 Ch5 (Pe3-5 low / either of P3-5 high)
		2	Power switch V3 (open V3/close)
		3	Power switch V4 (open V4/close)
		4	Power switch V5 (open V5/close)
		5	Power switch P1 (P1 on/off)
		6	Power switch P2 (P2 on/off)
		7	Power switch P3 (P3 on/off)
		8	Siematic (Pi3 high/low)
	Opto Input EB Unit 2	1	EA U5 Ch1 (switch on vacuum system / off)
		2	EA U5 Ch2 (manual operation / automatic)
		3	EA U5 Ch3 (reset after shutdown / no action)
		4	Feedback switch V3 (V3 closed/opened)
		5	Feedback switch V4 (V4 closed/opened)
		6	Feedback switch V5 (V5 closed/opened)
		7	Feedback switch P1 (P1 on/off)
		8	Feedback switch P2 (P2 on/off)
J/O module	Relais Output EB Unit 3	1	LSD In23 (P1 elusive fault alarm
		2	LSD In24 (P2 if first fault detected
		3	LSD In25 (P3 / otherwise)
		4	EA U6 Ch3 (slow shutdown / no action)
		5	
		6	
		7	
		8	
	Opto Input EB Unit 4	1	Feedback switch P3
		2	LSD Out 7 (manual V3 open / no action)
		3	LSD Out 8 (Manual V3 close / no action)
		4	LSD Out 9 (manual V4 open / no action)
		5	LSD Out 10 (manual V4 close / no action)
		6	LSD Out 11 (manual V5 open / no action)
		7	LSD Out 12 (manual V5 close / no action)
		8	LSD Out 13 (manual P1 on / no action)

Table 4. 41. 3 Vacuum control system

J/0 module	Relais Output EB Unit 5 CH.Nr.	1	
		2	
		3	
		4	
		5	
		6	
		7	
		8	
	Opto Input EB Unit 6 CH.Nr.	1	LSD Out 14 (manual P1 off / no action)
		2	LSD Out 15 (manual P2 on / no action)
		3	LSD Out 16 (manual P2 off / no action)
		4	LSD Out 17 (manual P3 on / no action)
		5	LSD Out 18 (manual P3 off / no action)
		6	Siematic (cryostat warm/cold)
		7	EA U5 Ch8 (close V4 / no action)
J/0 module	Relais Output E Unit 6 CH.Nr.	1	
		2	
		3	
		4	
		5	
		6	
		7	
		8	
	Opto Input Unit CH.Nr.	1	
		2	
		3	
		4	
		5	
		6	
		7	
		8	

Feedback switch V3 - LSD In26
" V4 - LSD In27
" V5 - LSD In28
" P1 - LSD In29
" P2 - LSD In30
" P3 - LSD In31

Table 4. 41. 4 Vacuum control system

FLOW CHART FOR CONTROL OF CRYOSTAT

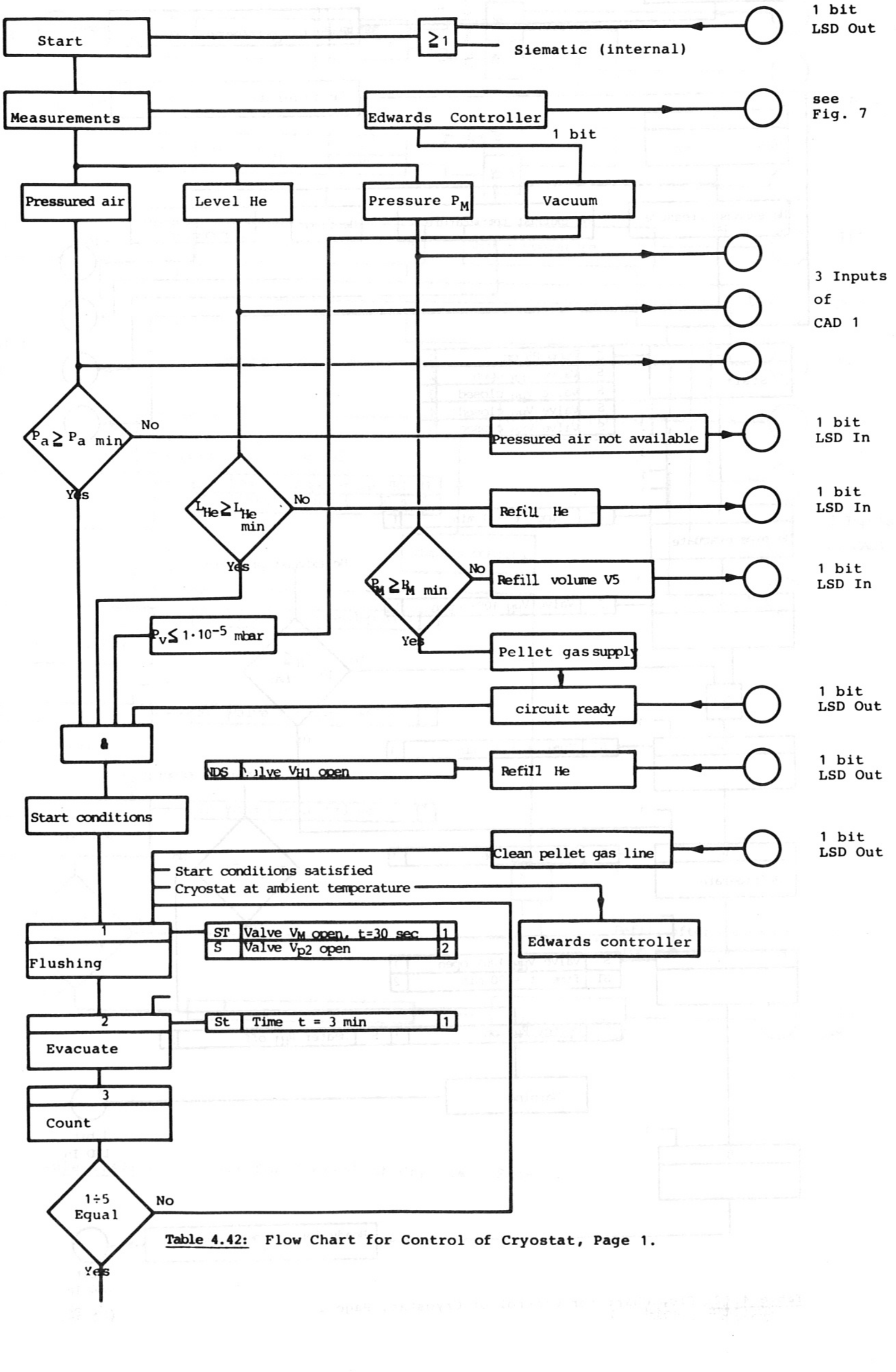

Table 4.42: Flow Chart for Control of Cryostat, Page 1.

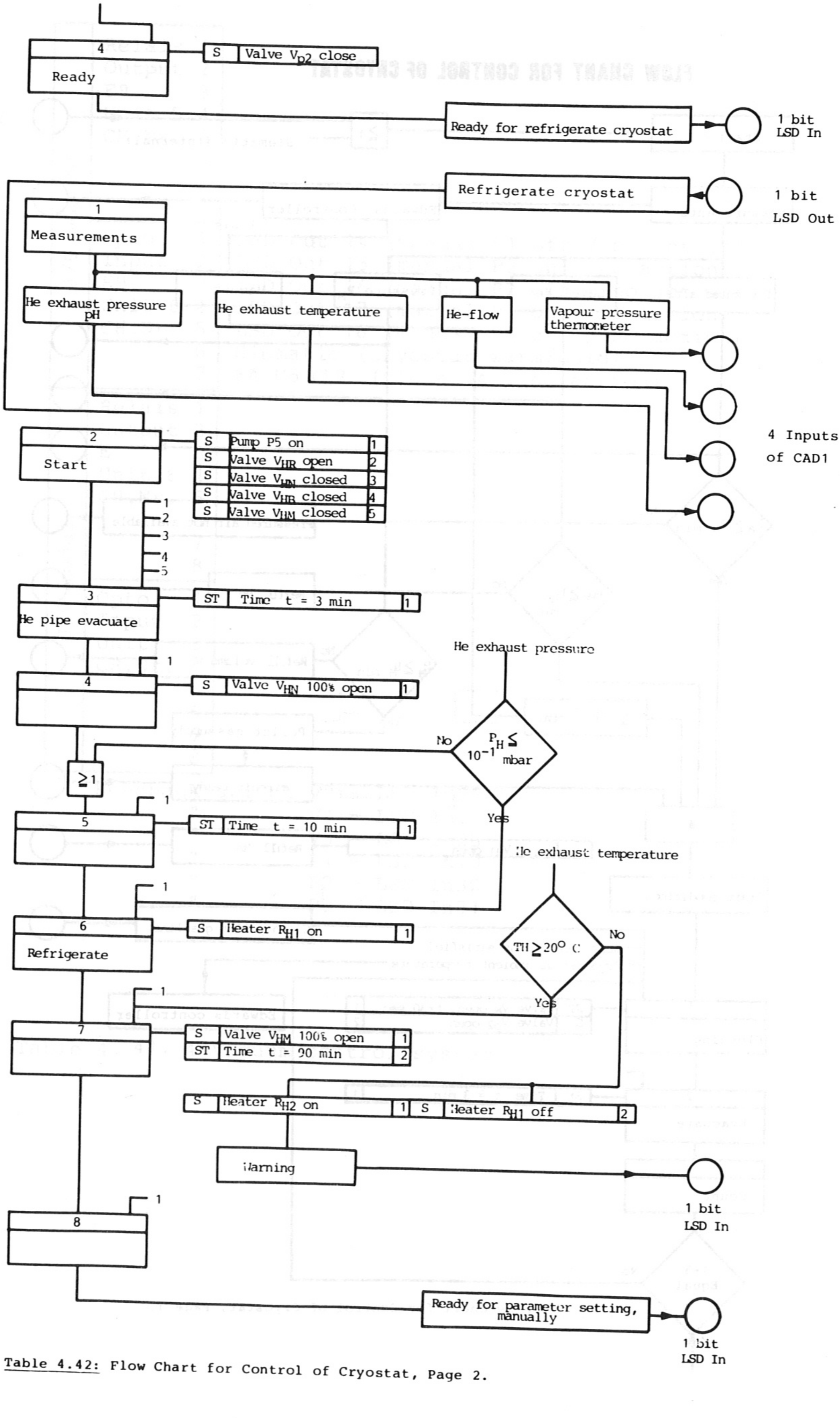

Table 4.42: Flow Chart for Control of Cryostat, Page 2.

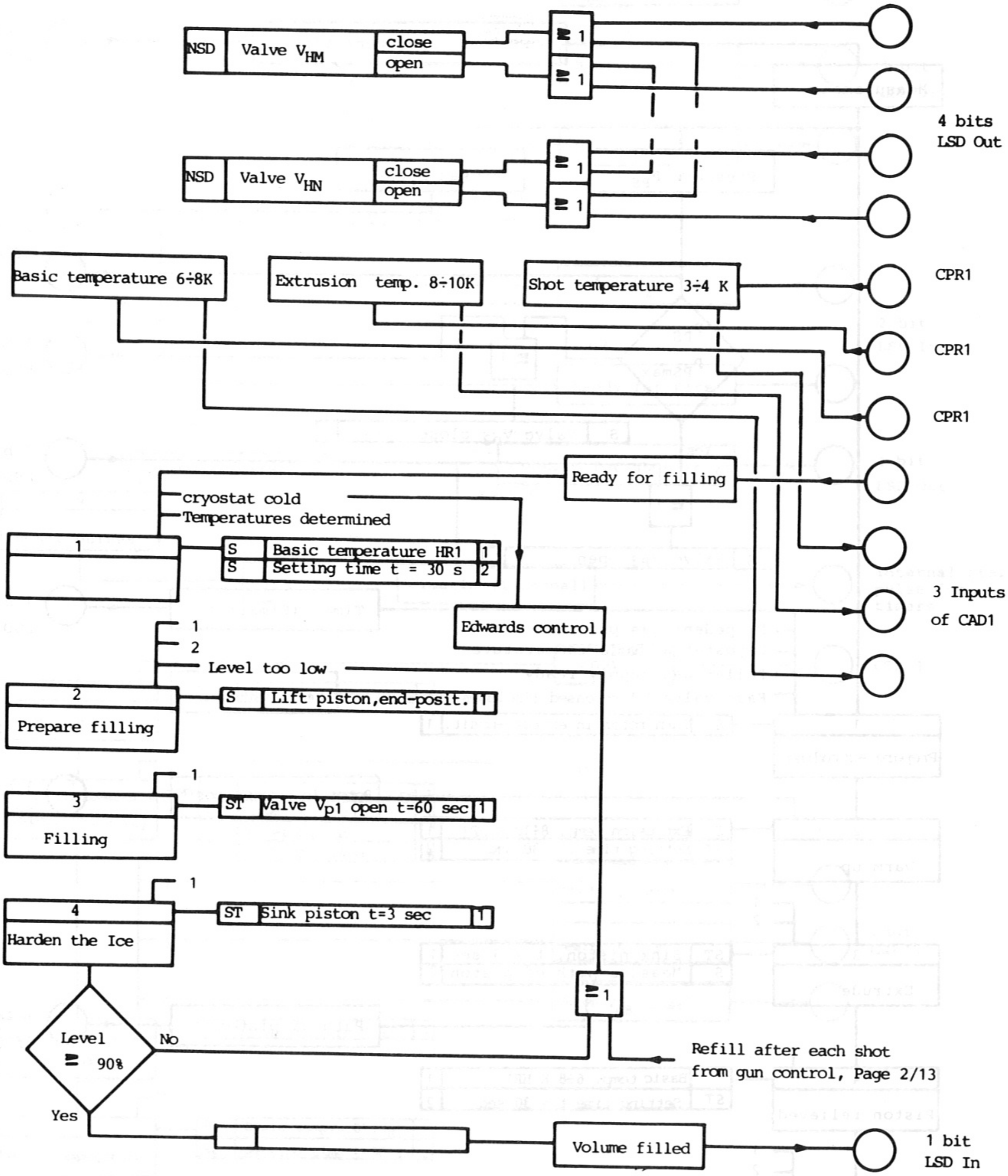

Table 4.42: Flow Chart for Control of Cryostat, Page 3.

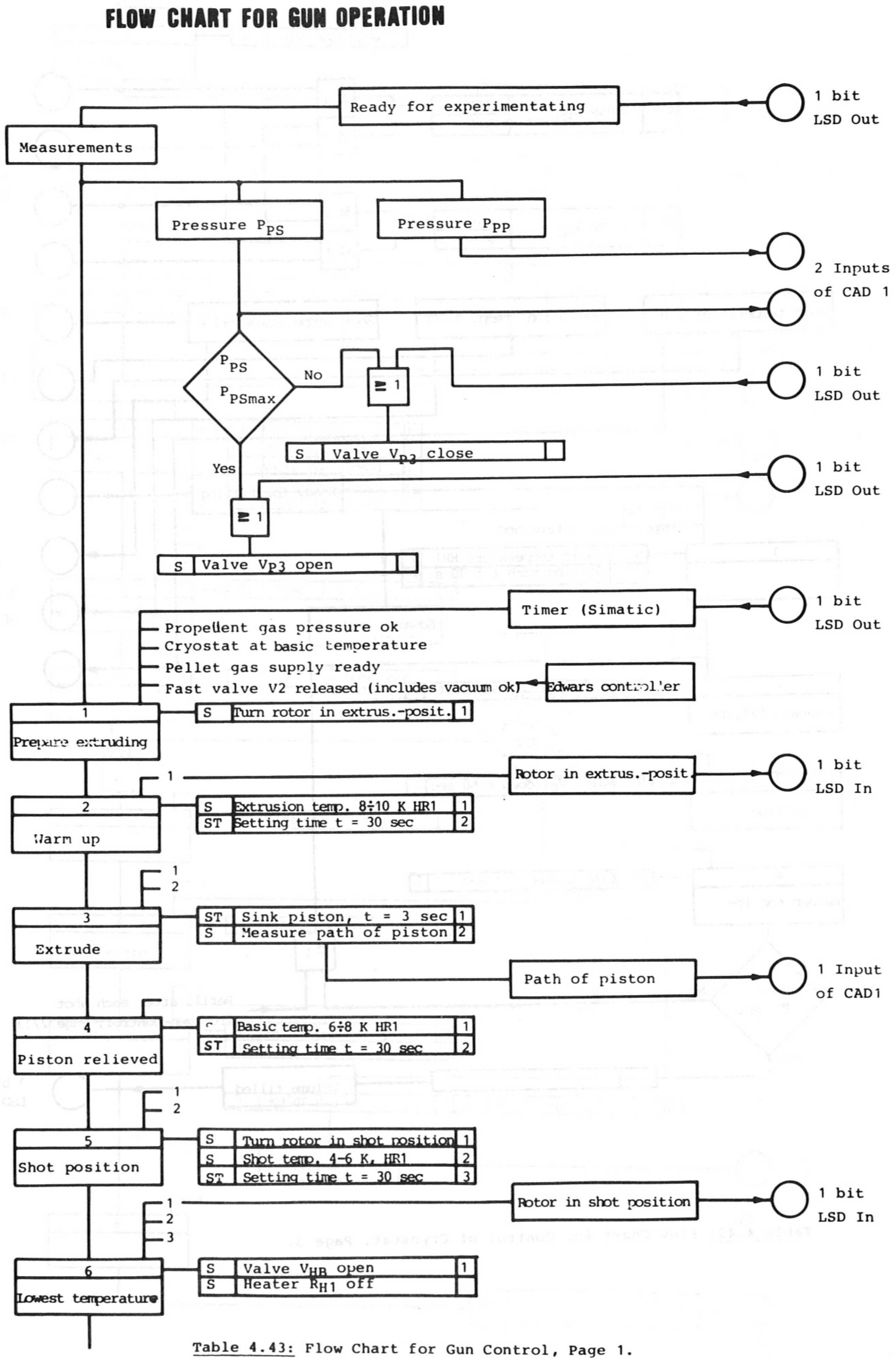

Table 4.43: Flow Chart for Gun Control, Page 1.

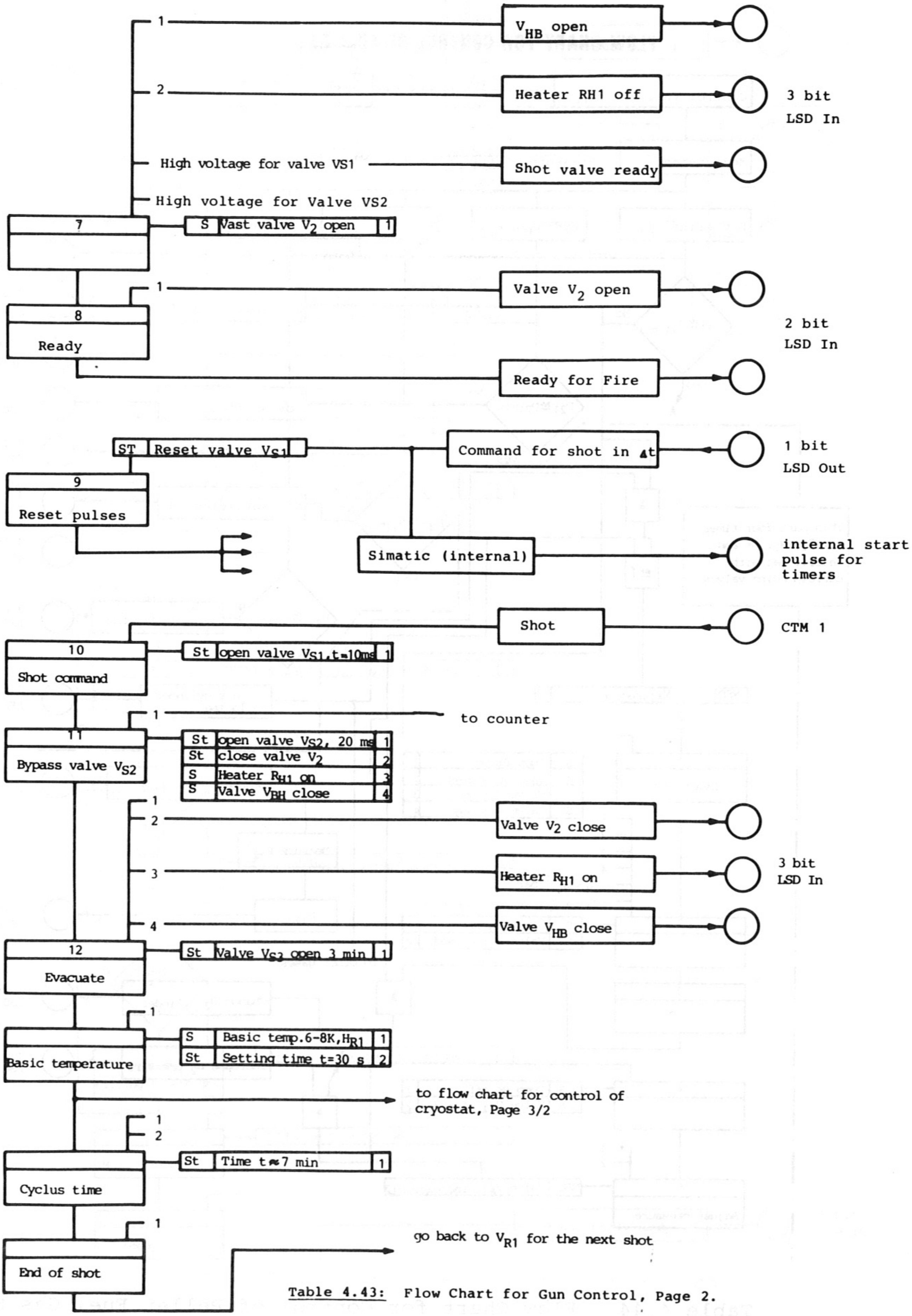

Table 4.43: Flow Chart for Gun Control, Page 2.

FLOW CHART FOR CONTROL OF FUEL GAS

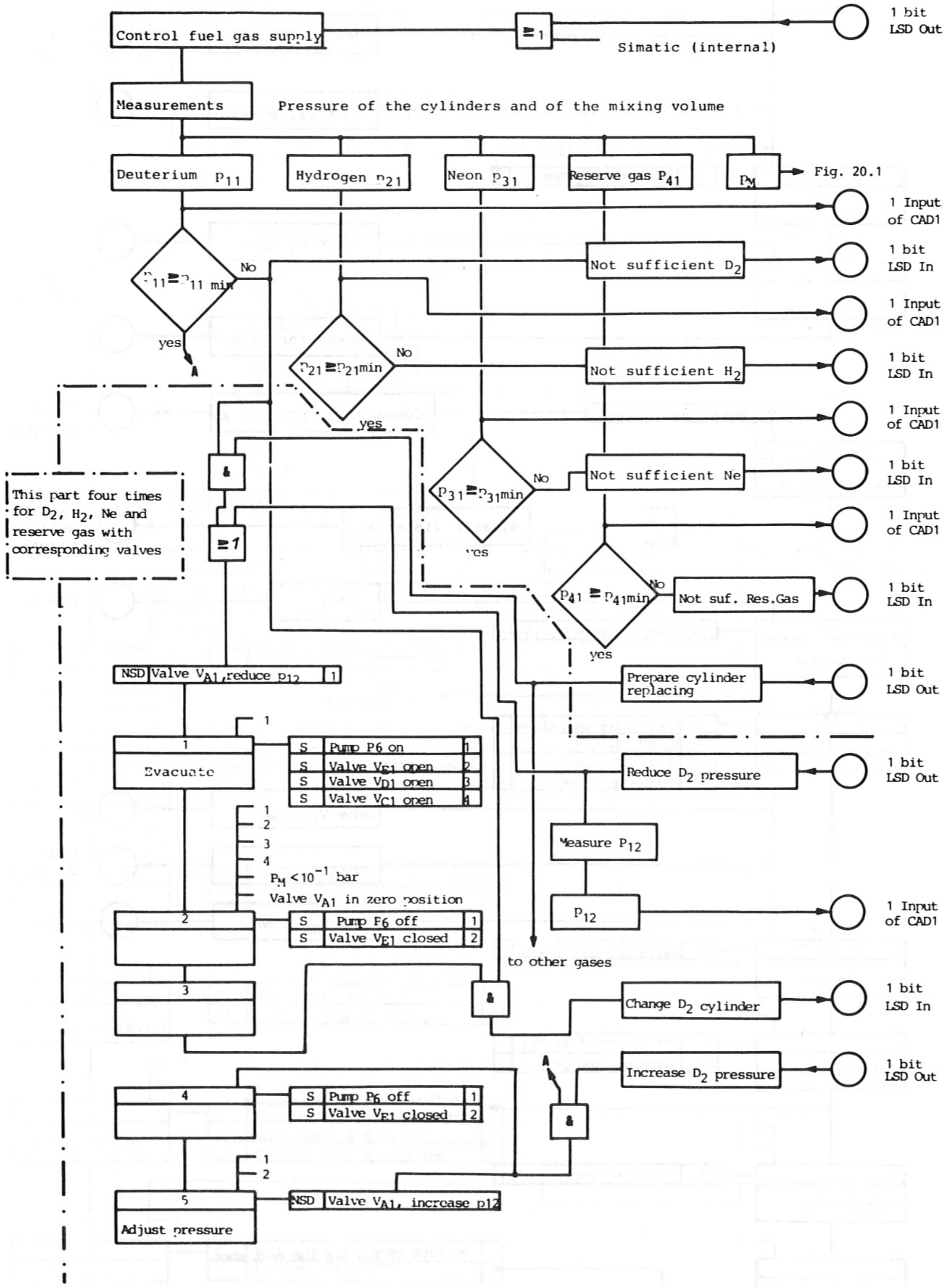

Table 4.44 Flow Chart for Control of Pellet Fuel Gas Supply

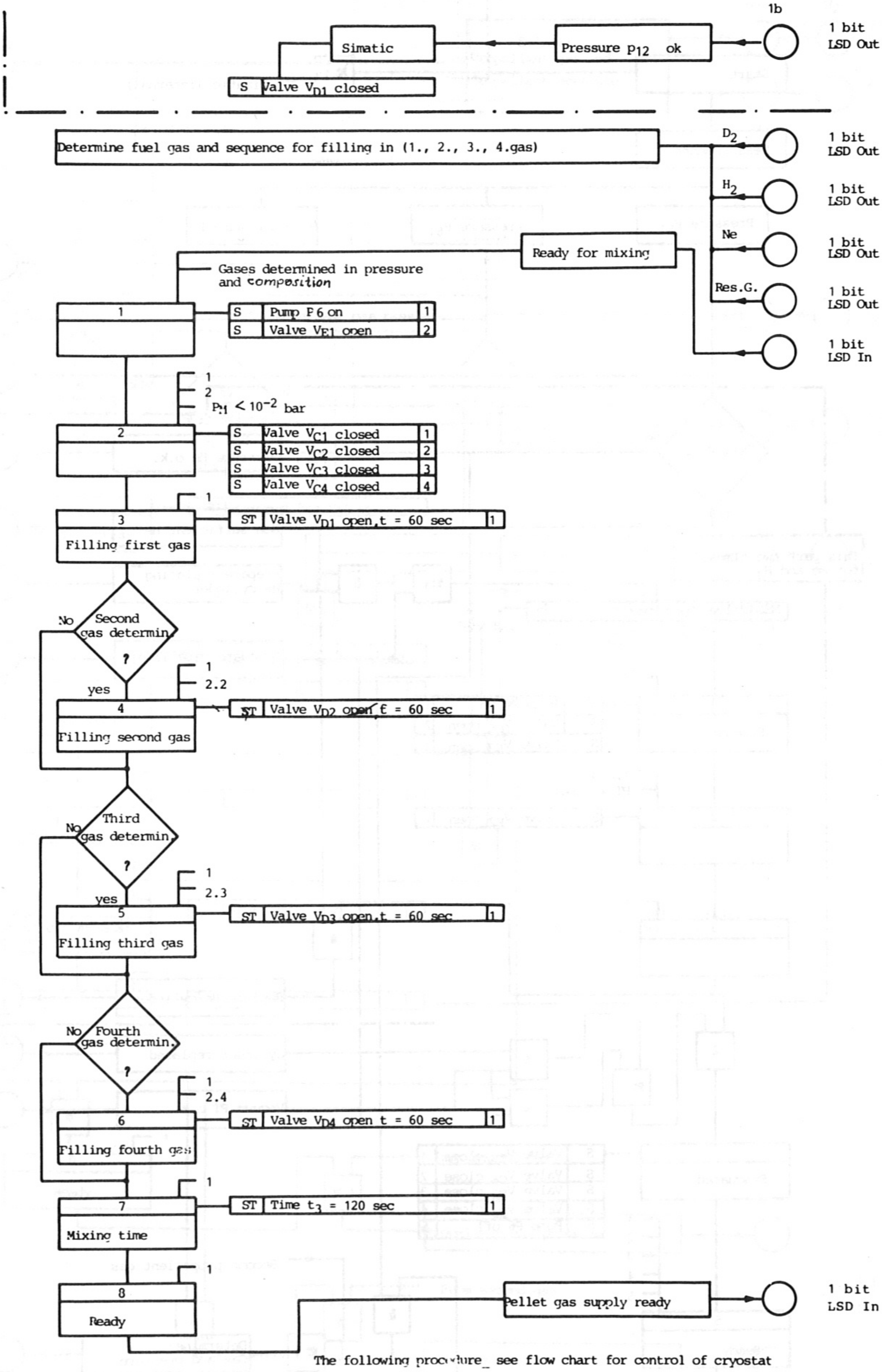

Table 4.44 Flow Chart for Control of Pellet Fuel Gas Supply

FLOW CHART FOR CONTROL OF PROPELLENT GAS

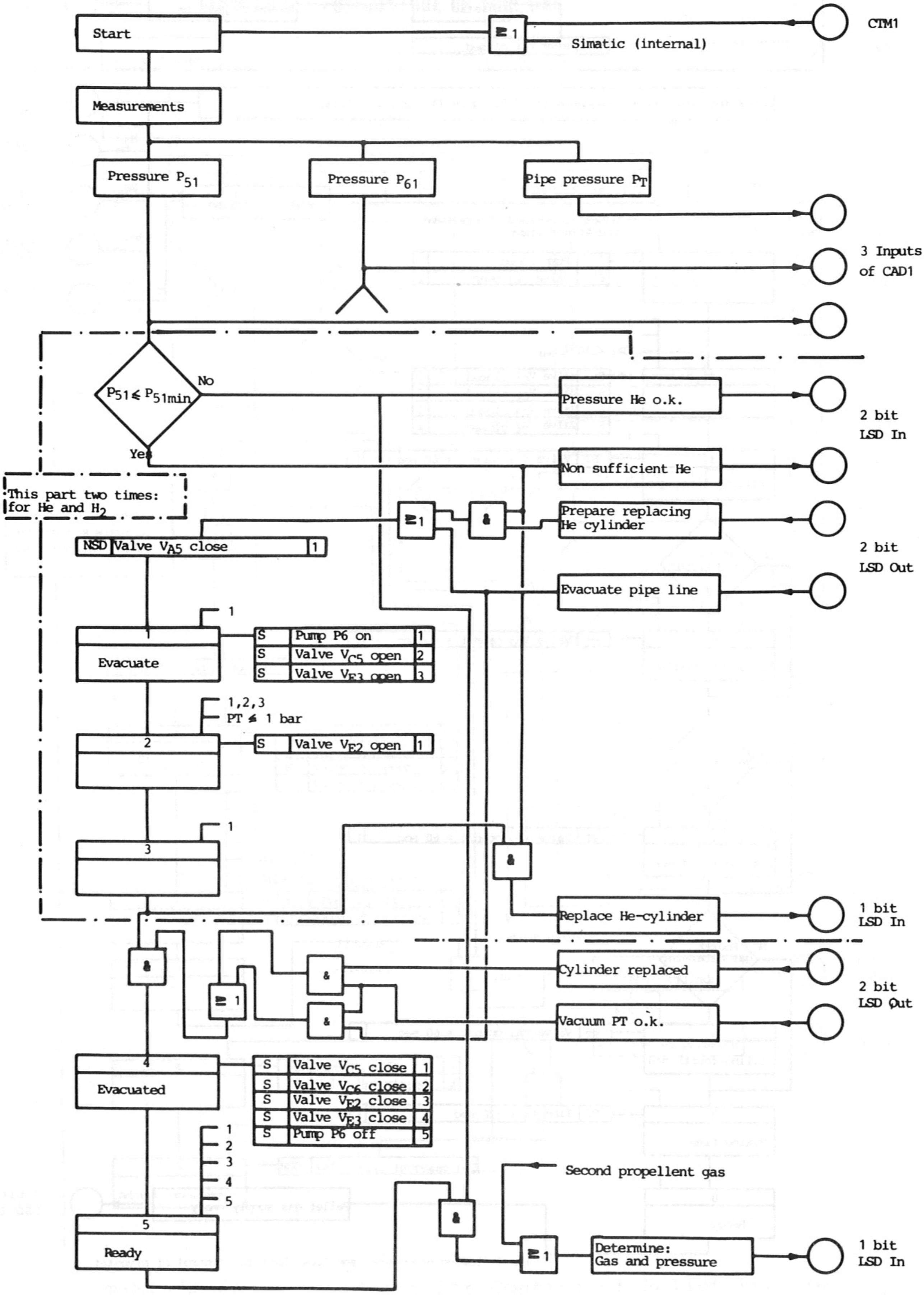

Table 4.45: Flow Chart for Control of Propellent Gas Supply, Page 1.

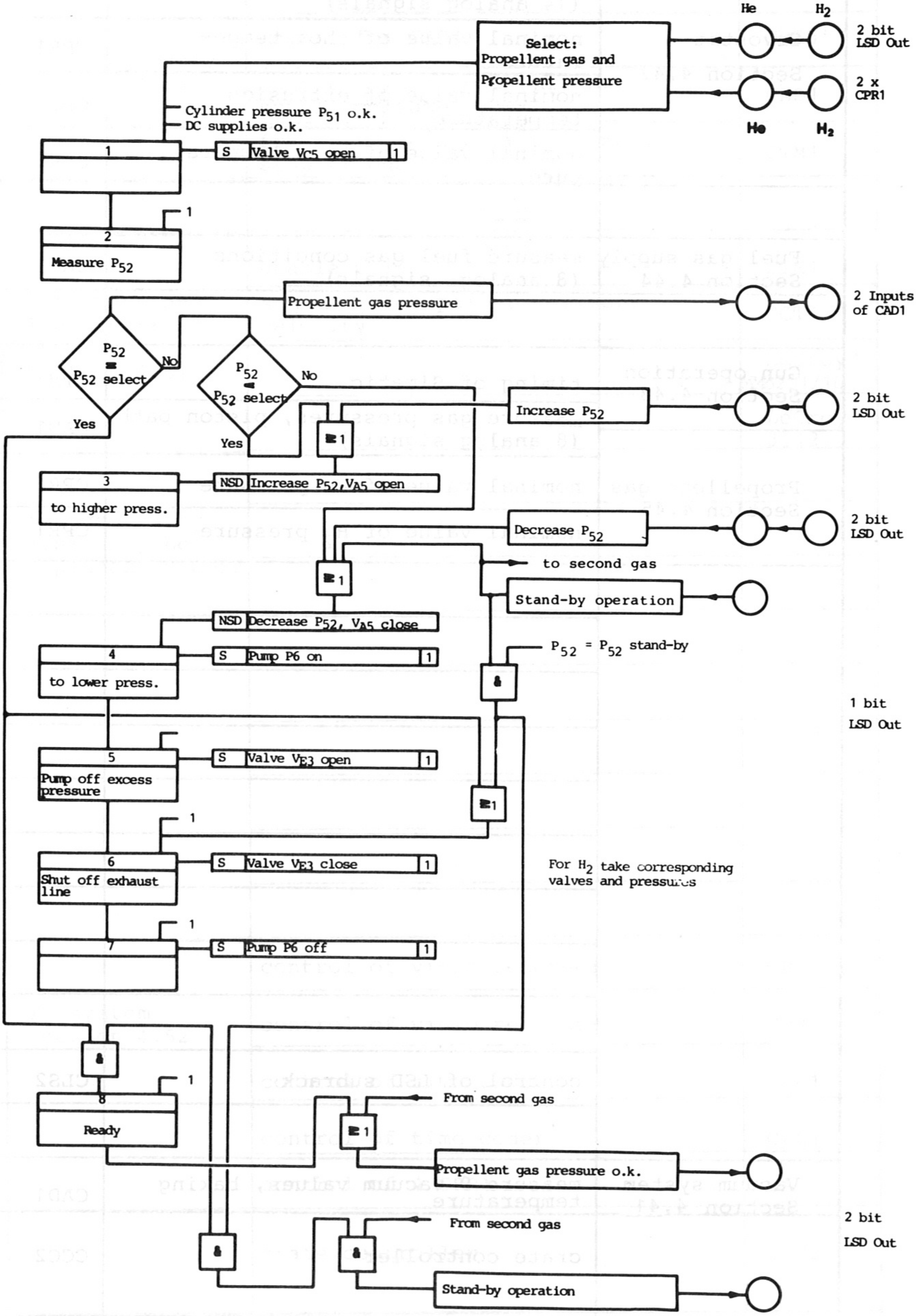

Table 4.45: Flow Chart for Control of Propellent Gas Supply, Page 2.

Cryostat Section 4.42	measure cryostat conditions (14 analog signals)	CAD1
	nominal value of shot temperature	CPR1
	nominal value of extrusion temperature	CPR1
	nominal value of base temperature	CPR1
Fuel gas supply Section 4.44	measure fuel gas conditions (8 analog signals)	CAD1
Gun operation Section 4.43	timing of Simatic	CTM1
Propellent gas Section 4.45	measure gas pressures, piston path (8 analog signals)	CAD1
	nominal value of He pressure	CPR1
	nominal value of H_2 pressure	CPR1
	control of LSD subrack	CLS2
Vacuum system Section 4.41	measure 9 vacuum values, baking temperature	CAD1
	crate controller	CCC2

Table 4.6.1: Complement of CAMAC crate 1

CAMAC crate CCB1

Dα diagnostic Section 4.53	measure Dα signal	CAD4
	memory for CAD4	CME4
	measure diode leak current, supply voltages	CAD1
	freeze in leak current comp., stop trigger for CAD4	CTM1
Microwave and light barrier system Section 4.51	enable CCT4	CTM1
	stopwatch for pellet delivery, velocity	CCT4
		LeCroy* MM8201/16
		LeCroy 3512
*suggested by Risø, may be replaced by CME5		
TV system Section 4.52	control of video recorder	CPR1
	control of video recorder	CPR1
	control of time coder	CPR1
	control of time coder	CPR1
	control of 4 CPR1	CAC
	crate controller	CCC2

Table 4.6.2: Complement of CAMAC crate 2

CAMAC crate CCB1

Cryostat Section 4.42	ULD2
	ULS1
Fuel gas supply Section 4.44	ULS1
	ULD2
Gun operation Section 4.43	ULD2
	ULS1
Propellent gas Section 4.43	ULS1
	ULD2
Vaccum system Section 4.41	ULD2
	ULS1
	ULS1
Dα-diagnostic Section 4.53 and TV-system Section 4.52	ULD2
	ULS1
Connector card	ULC1
Power supply	UPS1

LSD subrack ULB1

Table 4.6.3: Complement of LSD subrack

Table 4.8.1 JET SERVICES/TORUS HALL

Supply	Purpose	Interface	Remarks	Figure
Liquid Helium	Cooling of pellet cryostat	JET-Johnson type coupling	controlled by JET Cryogenic Division, about 50 l/ exp. day, refilling of 100 l helium dewar	14 15
Helium Recycling Line	Helium gas from the cryostat	Rafix	during gun operation about 3000 l/h gas of about 200 - 300 K	14 15
Helium Gas	Ventilation of vacuum system	Rafix	Controlled by Simatic of pellet injector, 5 - 10 bar permanent	22
Pressurized Air	Actuation of valves and pistons	Rafix	(5-) 10 bar permanent	-
Water	Cooling of TPU 510 and TPU 220	Rafix	About 100 l/h controlled by Simatic	-
Electric Power	Vacuum pumps, heater		About 10 KW	-
Vacuum Backing Line	forevacuum of TPU	JET remote handling flange	Pumping speed 60 - 100 m^3/h Controlled by Simatic	22
Vacuum Roughing Line	forvacuum of roots pump	JET remote handling flange	Pumping speed 100 - 200 m^3/h for 10 minutes during the injection, Controlled by Simatic	22

Table 4.8.2 JET SERVICES/BASEMENT

Supply	Purpose	Interface	Remarks	Figure
Hydrogen Exhaust Line	Ventilation of gas systems	Rafix	Controlled by Simatic	16 20
Pressurized Air	Actuation of valves	Rafix	(5-) 10 bar permanent	-
Electric Power	Pumps, electric units	-	about 20 KW	-

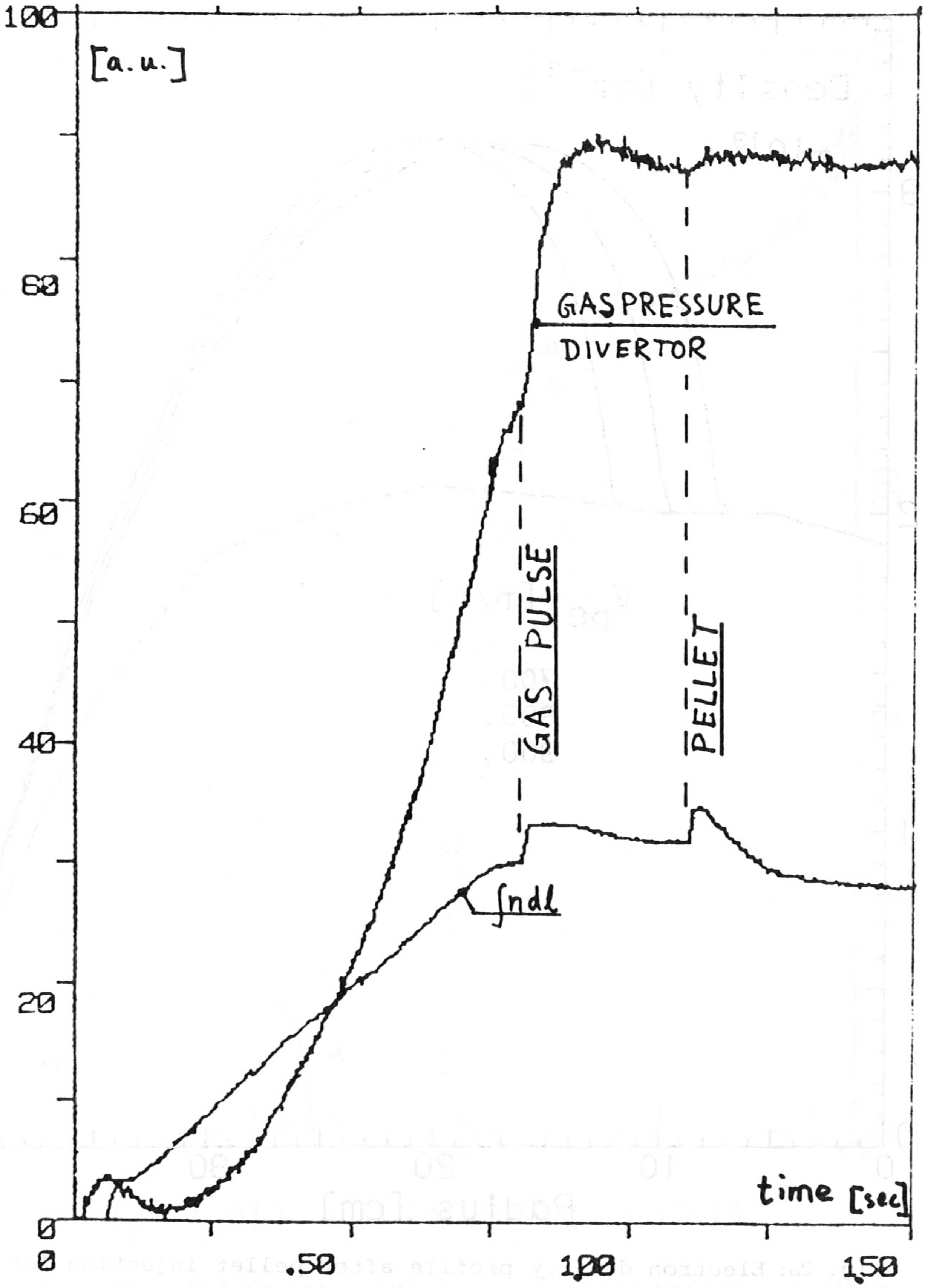

Fig. 1: Comparison between gas pulse and pellet injection in ASDEX. Electron line density measured with HCN-Laser interferometer. Gas pressure measured in the upper divertor chamber /9/.

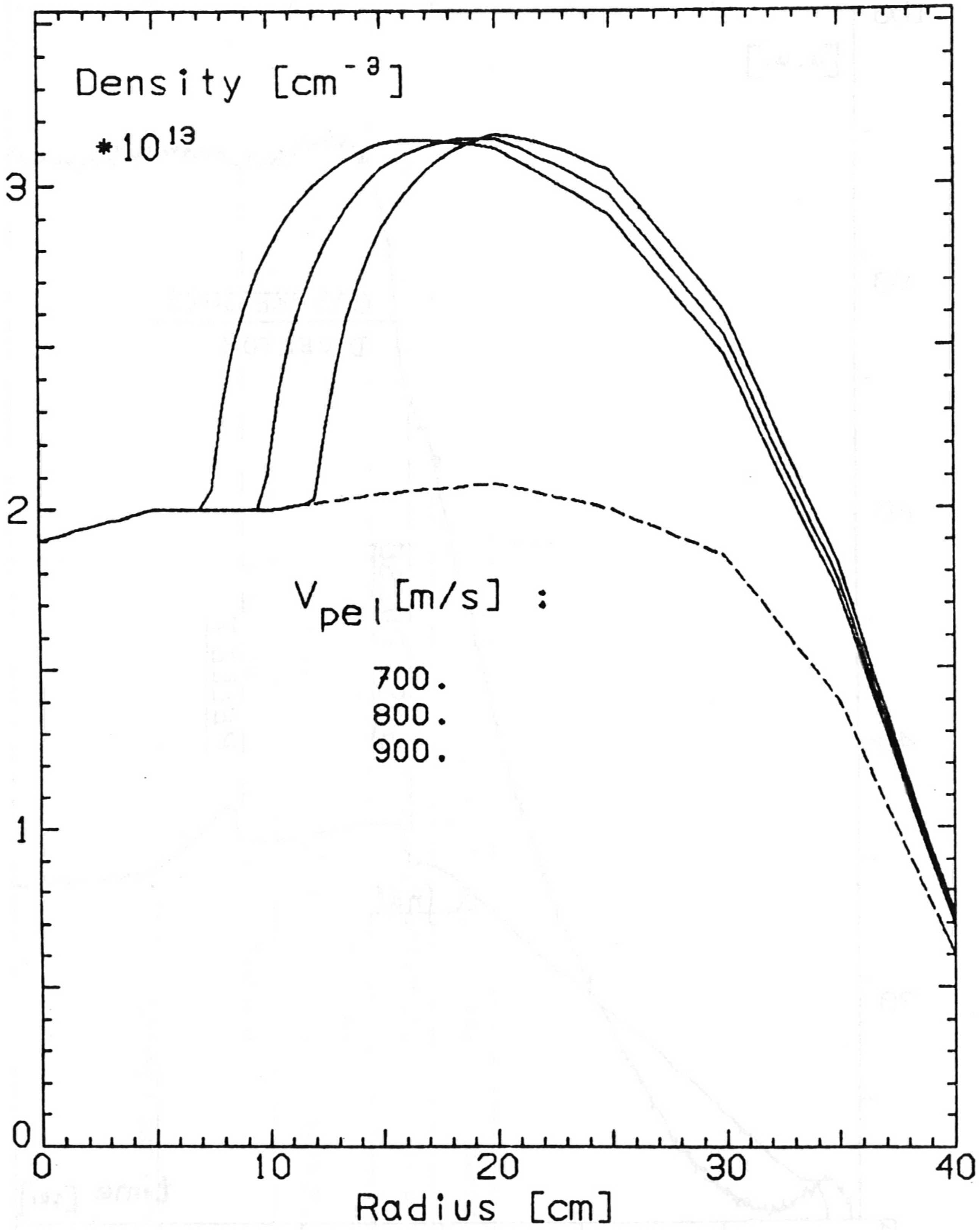

Fig. 2a: Electron density profile after pellet injection for three pellet velocities calculated with neutral gas shielding model. The undisturbed density profile (dashed curve) is fitted to the measured profile of fig. 2b. Pellet diameter 1.0 mm. $T_e(0)$ = 800 eV.

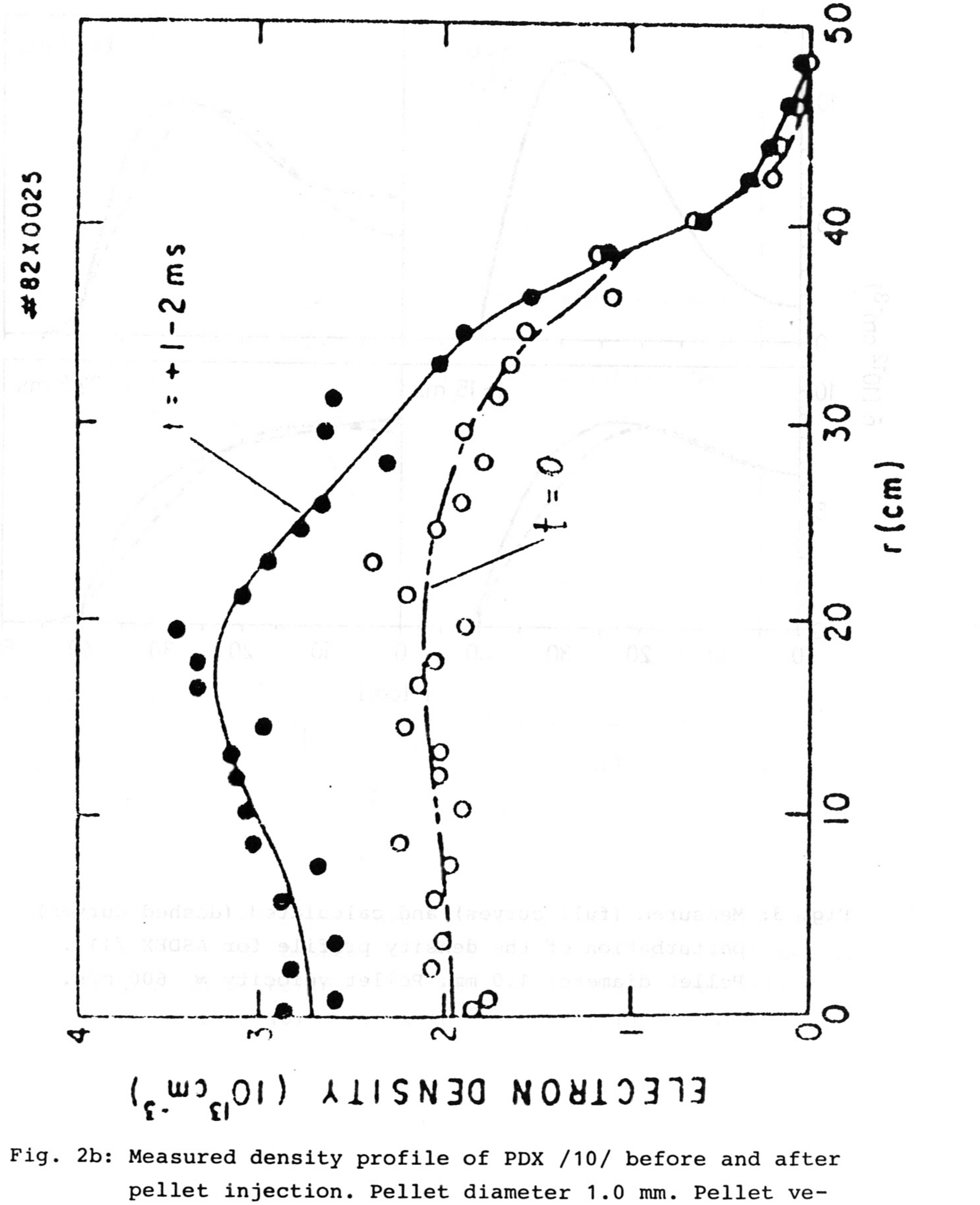

Fig. 2b: Measured density profile of PDX /10/ before and after pellet injection. Pellet diameter 1.0 mm. Pellet velocity 825 m/s. Plasma: $n_e(0) \approx 2 \times 10^{13}$ cm^{-3}; $T_e(0) \approx$ 800 eV.

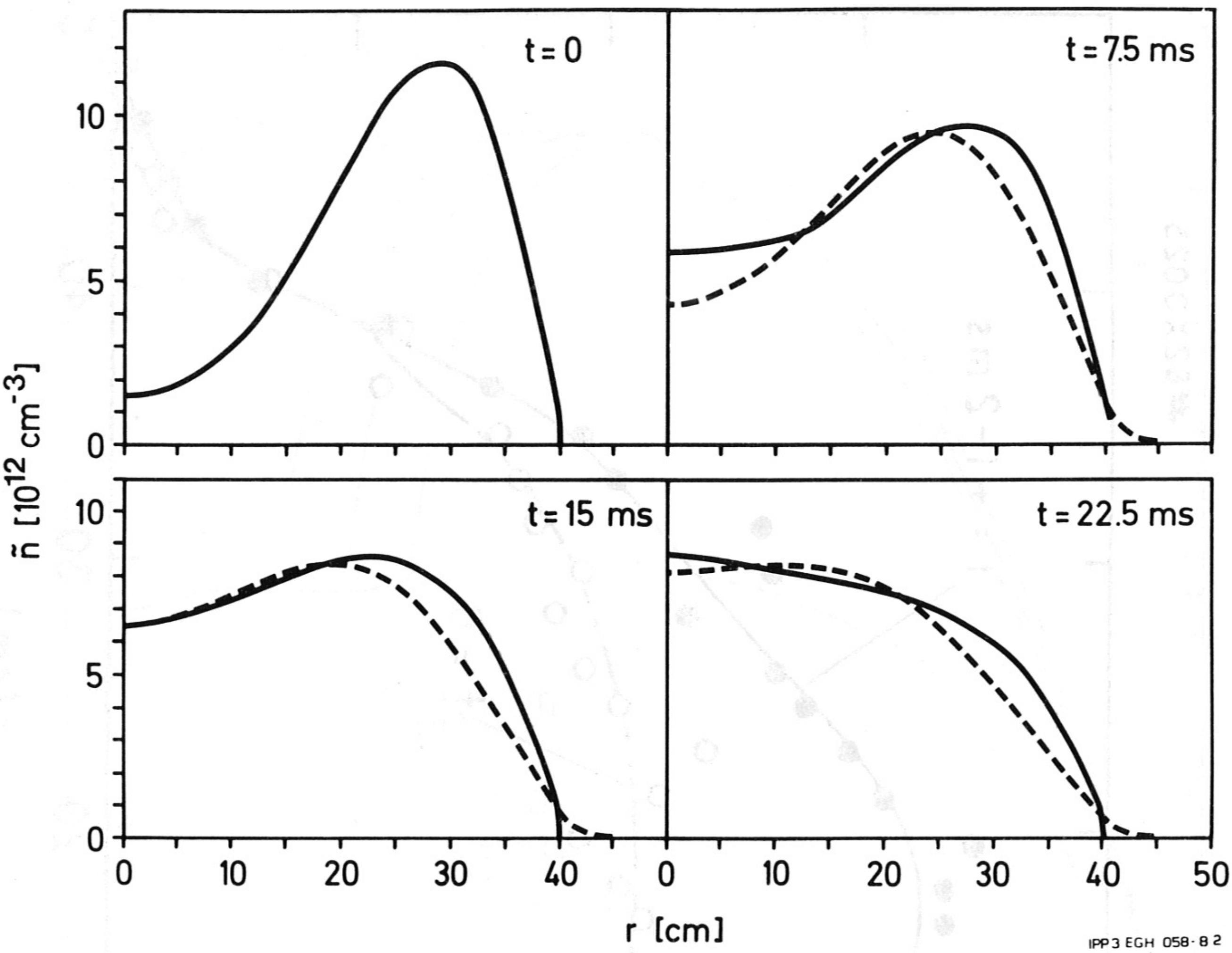

Fig. 3: Measured (full curves) and calculated (dashed curves) perturbation of the density profile for ASDEX /11/. Pellet diameter 1.0 mm. Pellet velocity ≈ 600 m/s.

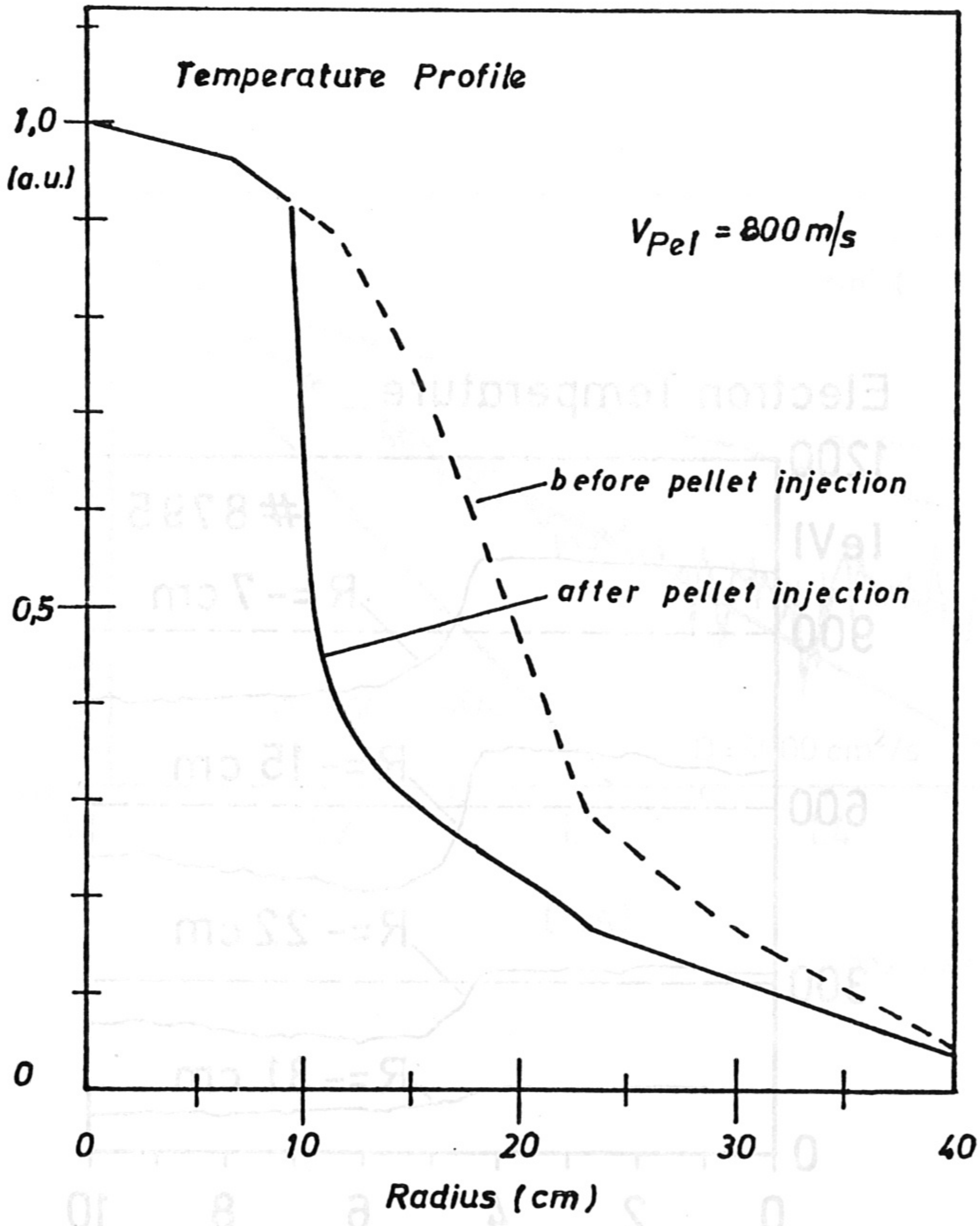

Fig. 4: Calculated temperature profile after pellet injection into ASDEX. Dashed curve is the measured profile before injection. Pellet diameter 1.0 mm. Pellet velocity = 800 m/s; $n_e(0)$ = 1.7 x 10^{13} cm^{-3}; $T_e(0)$ = 1640 eV.

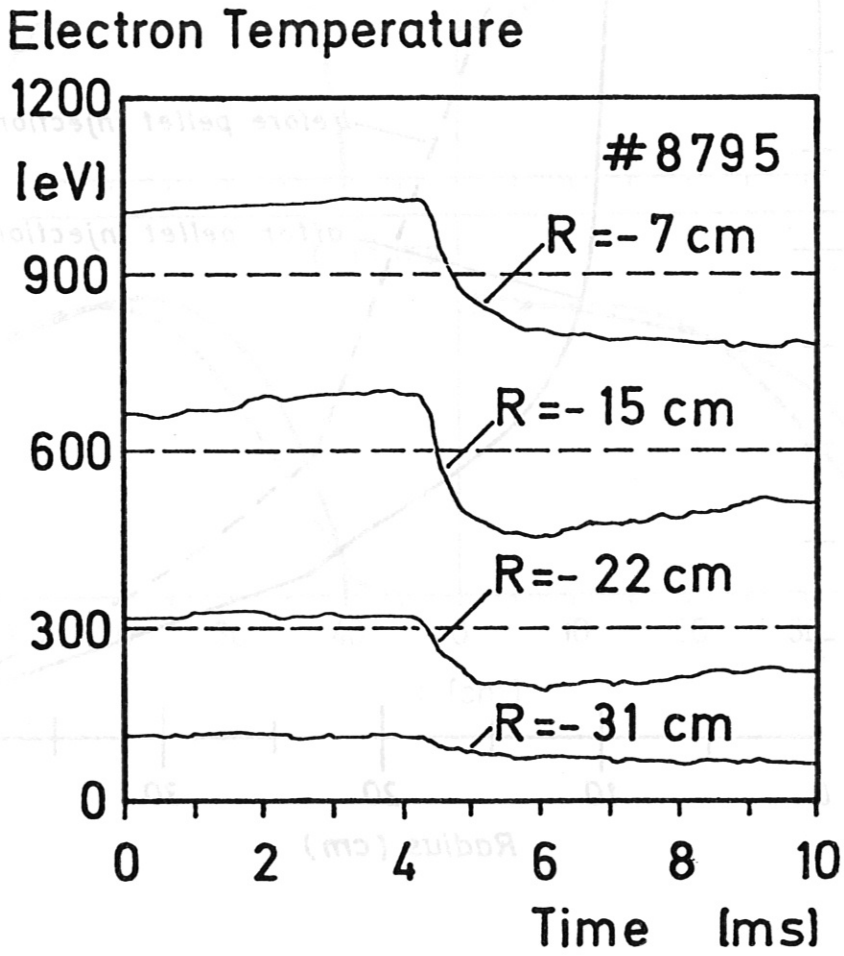

Fig. 5: Electron temperature measured by ECE at four radii during pellet injection /12/. Penetration radius of the pellet (1.0 mm ∅, V_{Pel} = 750 m/s) is about $R_{Pel} \approx$ 15 cm. (origin of time scale is arbitrary)

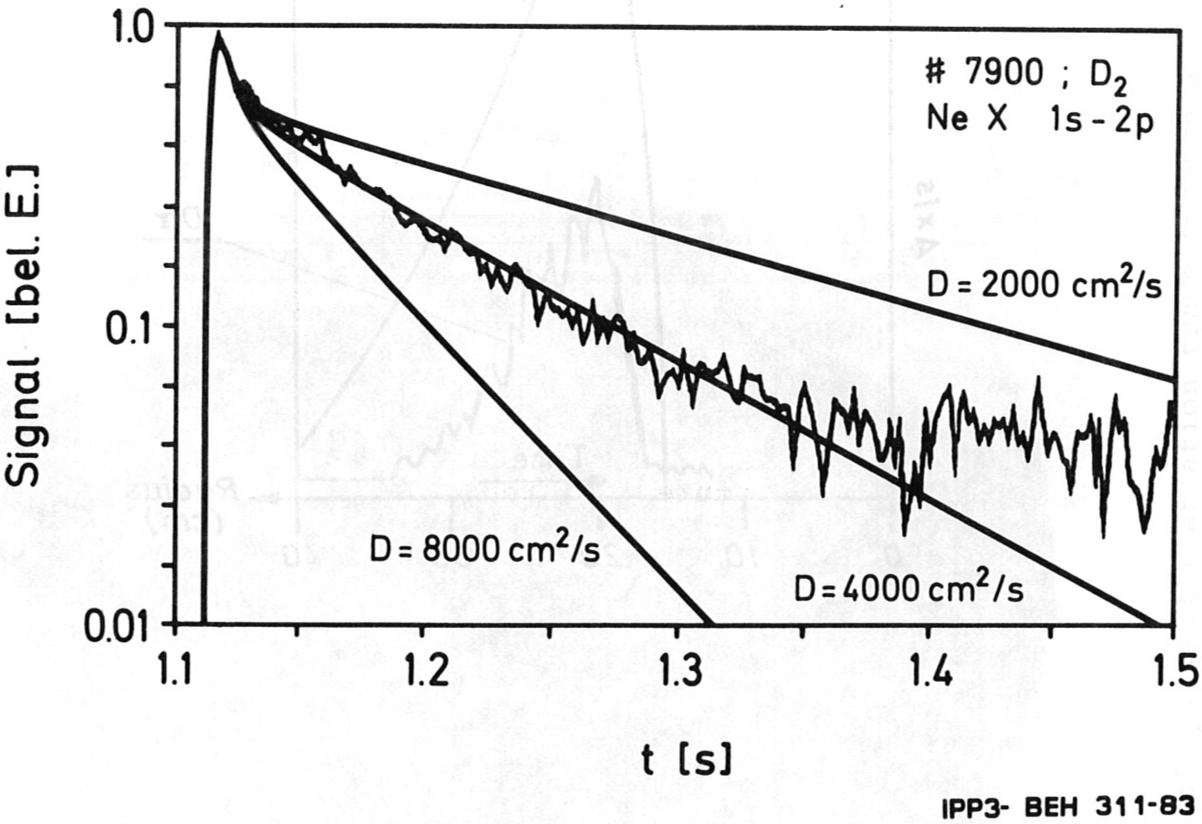

Fig. 6: NeX-Signal after injection of a neon-doped deuterium pellet (1.0 mm ø, V_{Pel} = 900 m/s) in ASDEX compared with simulations for different diffusion coefficients /3/. Plasma: $\bar{n}_e = 4.4 \times 10^{13}$ cm^{-3}; $T_e(0)$ = 620 eV.

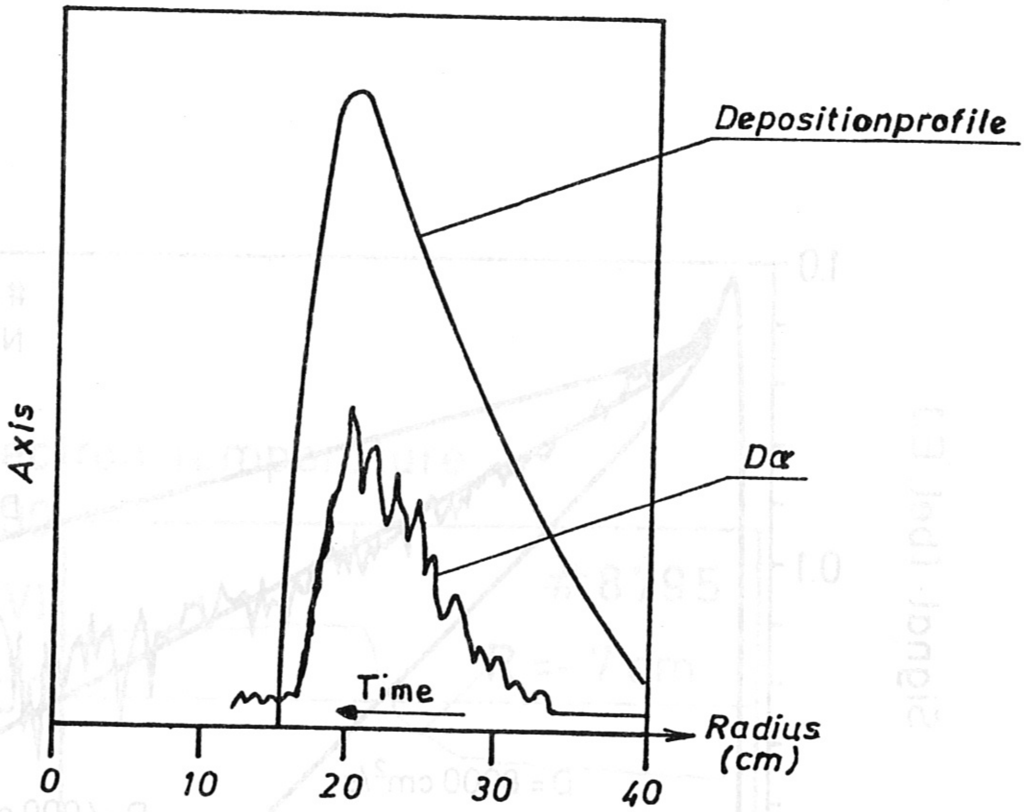

Fig. 7: Measured D_{α}-emission during pellet ablation in ASDEX (Pellet: 1.0 mm ø, V_{Pel} = 725 m/s; $T_e(0)$ = 1640 eV; $n_e(0) = 1.7 \times 10^{13}$ cm^{-3}; penetration radius = 17 cm, # 8837). Calculated deposition profile (0.8 mm ø, V_{Pel} = 700 m/s; $T_e(0)$ = 1640 eV; $n_e(0) = 1.7 \times 10^{13}$ cm^{-3}).

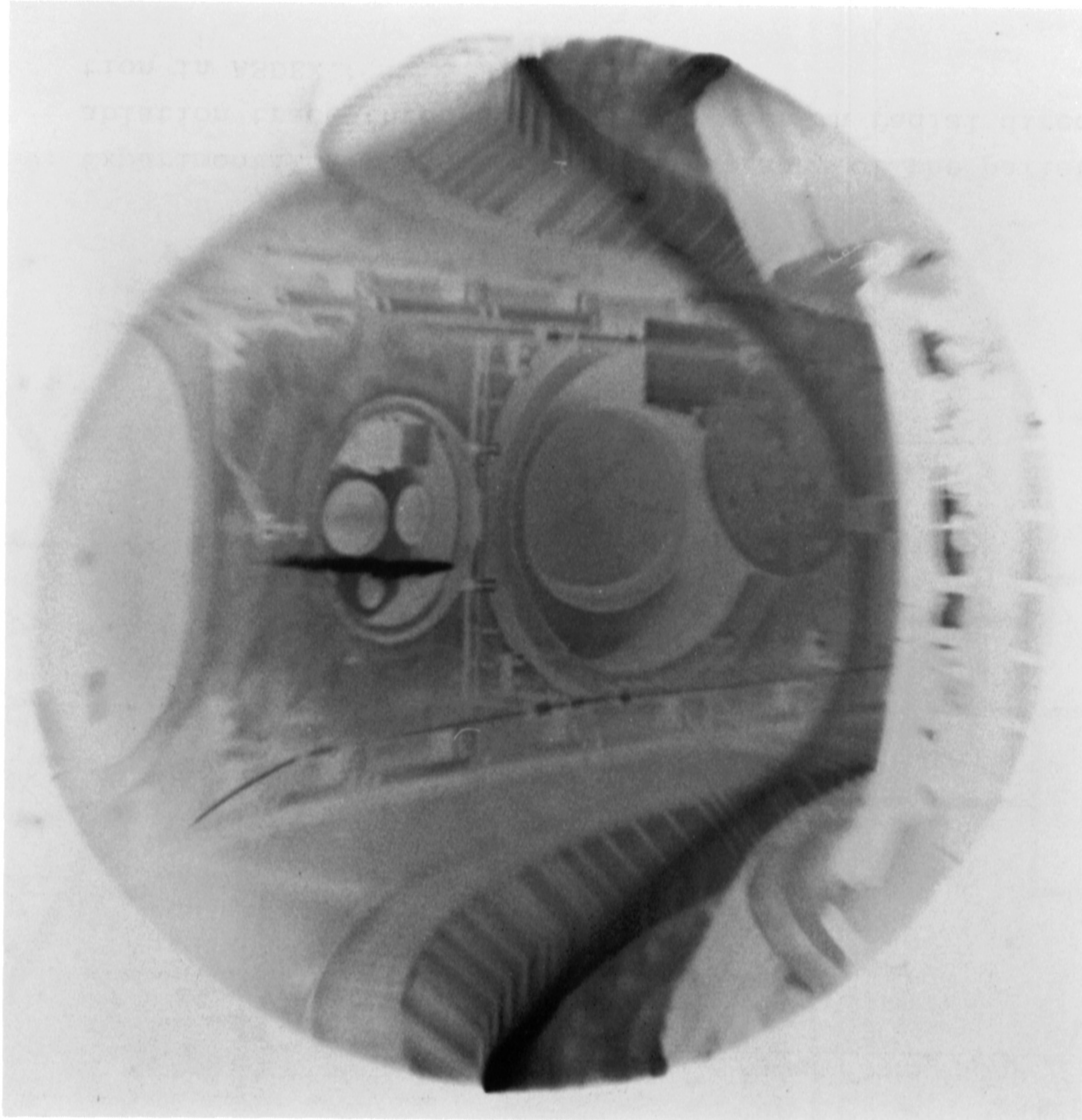

Fig. 8: Photography of the pellet ablation trace through a tangential port in ASDEX. Pellet 1.0 mm ∅, V_{Pel} = 900 m/s; penetration radius R ≈ 10 cm; Plasma: $\bar{n}_e = 4.4 \times 10^{13}$ cm^{-3}; $T_e(0)$ = 620 eV, # 7900.

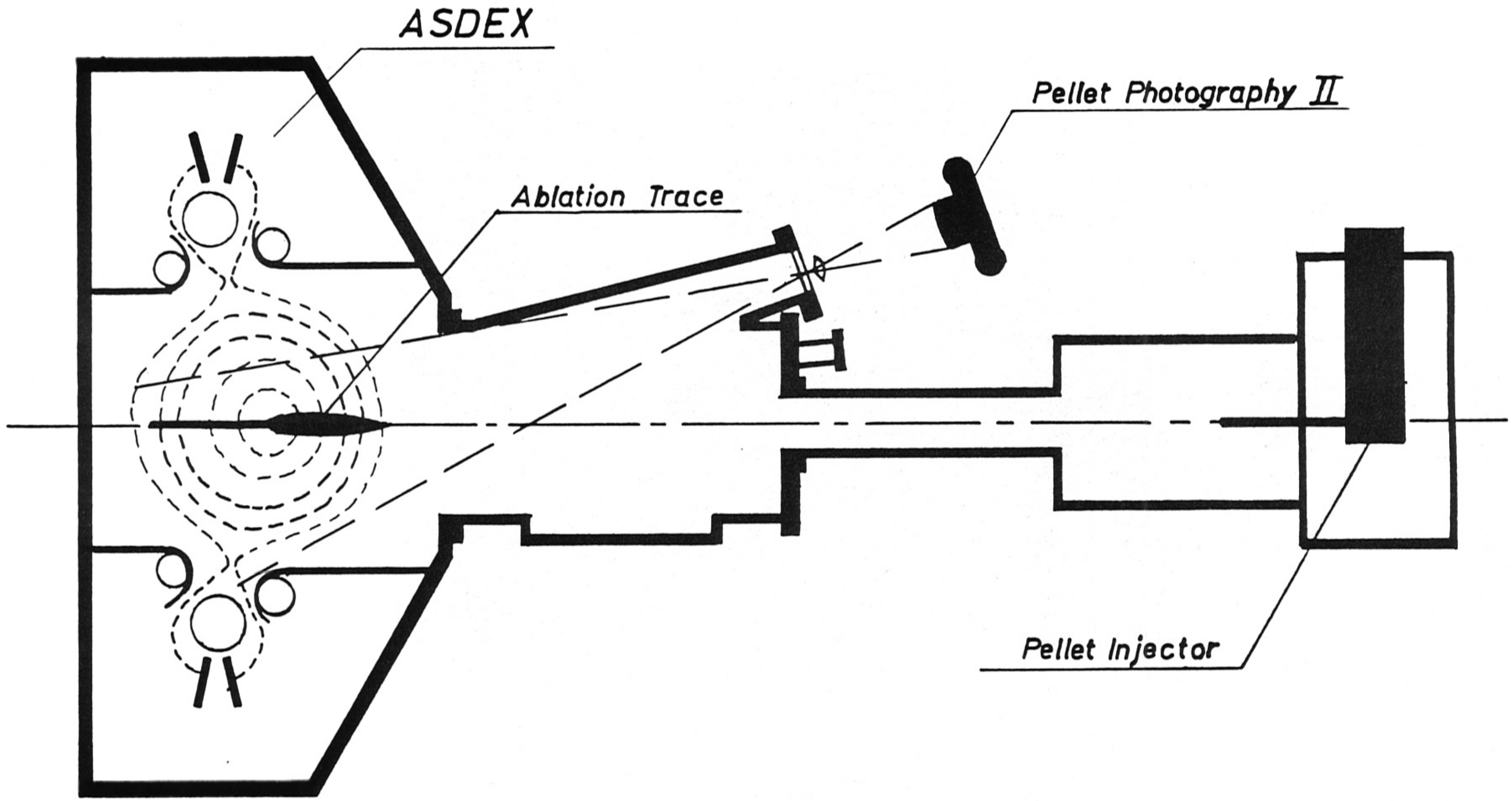

Fig. 9: Experimental arrangement for photography of the pellet ablation trace through an oblique port in radial direction in ASDEX.

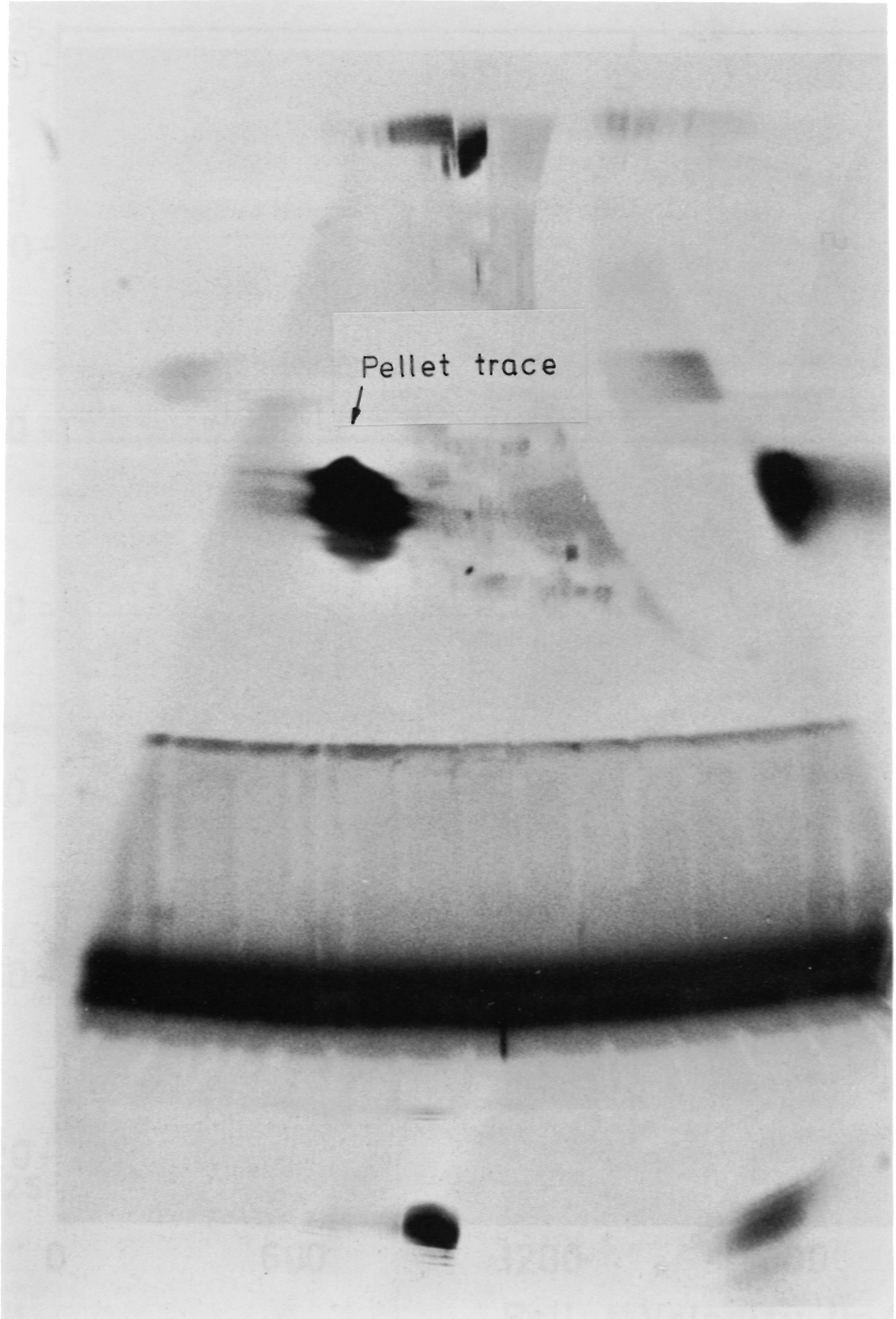

Fig. 10: Photography of the pellet ablation trace in radial direction using set-up of fig. 9. Shot # 7900 of fig. 8.

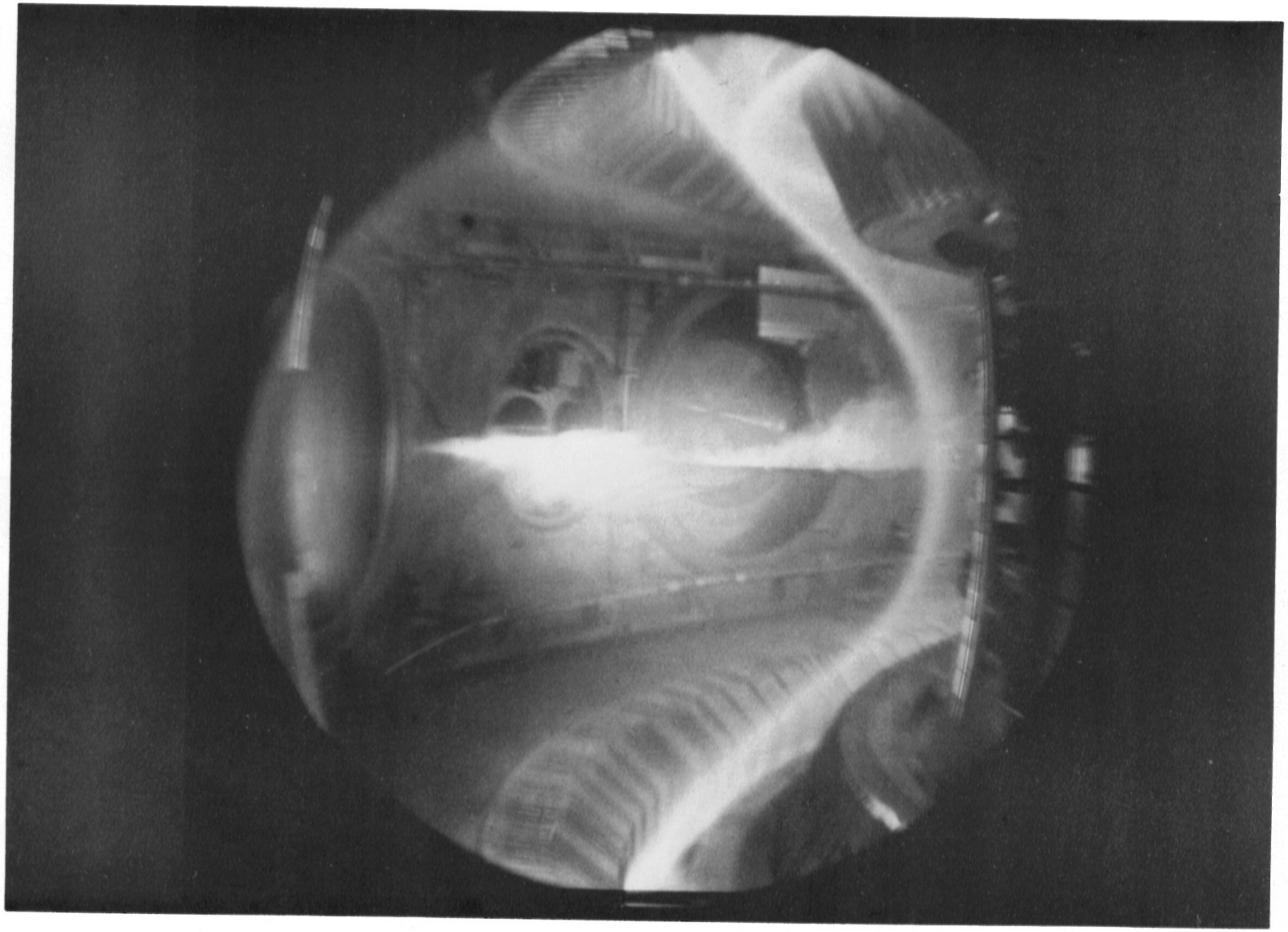

Fig. 11: Photography of the pellet ablation trace through a tangential port in ASDEX. Pellet: 1.8 mm ⌀, V_{Pel} = 625 m/s; Discharge: $\bar{n}_e = 1.1 \times 10^{13}\ cm^{-3}$; $T_e(0) \approx 1000$ eV; # 5938.

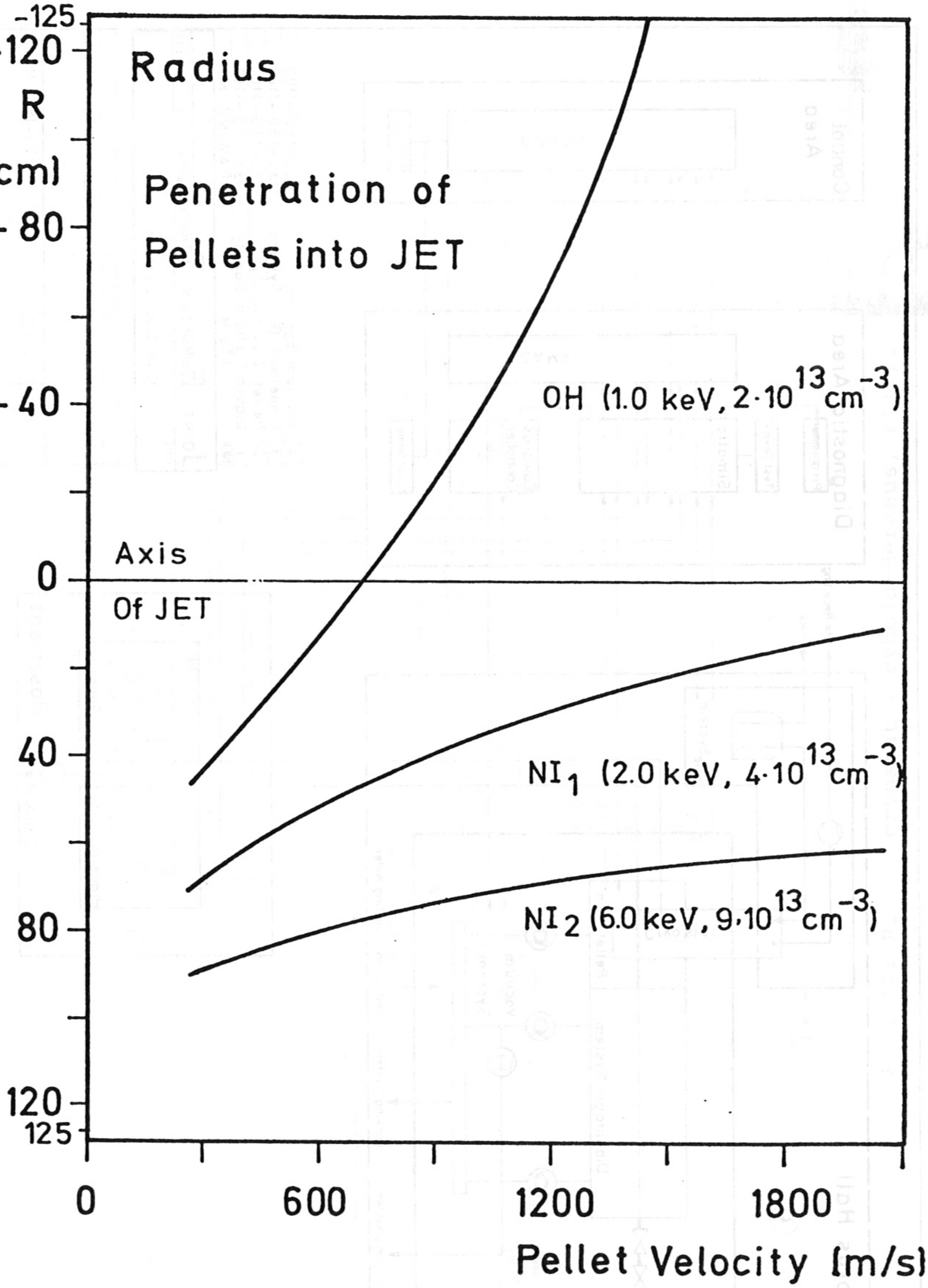

Fig. 12: Calculated penetration depths into JET for 3.0 mm ø D_2-Pellets and different plasmas.

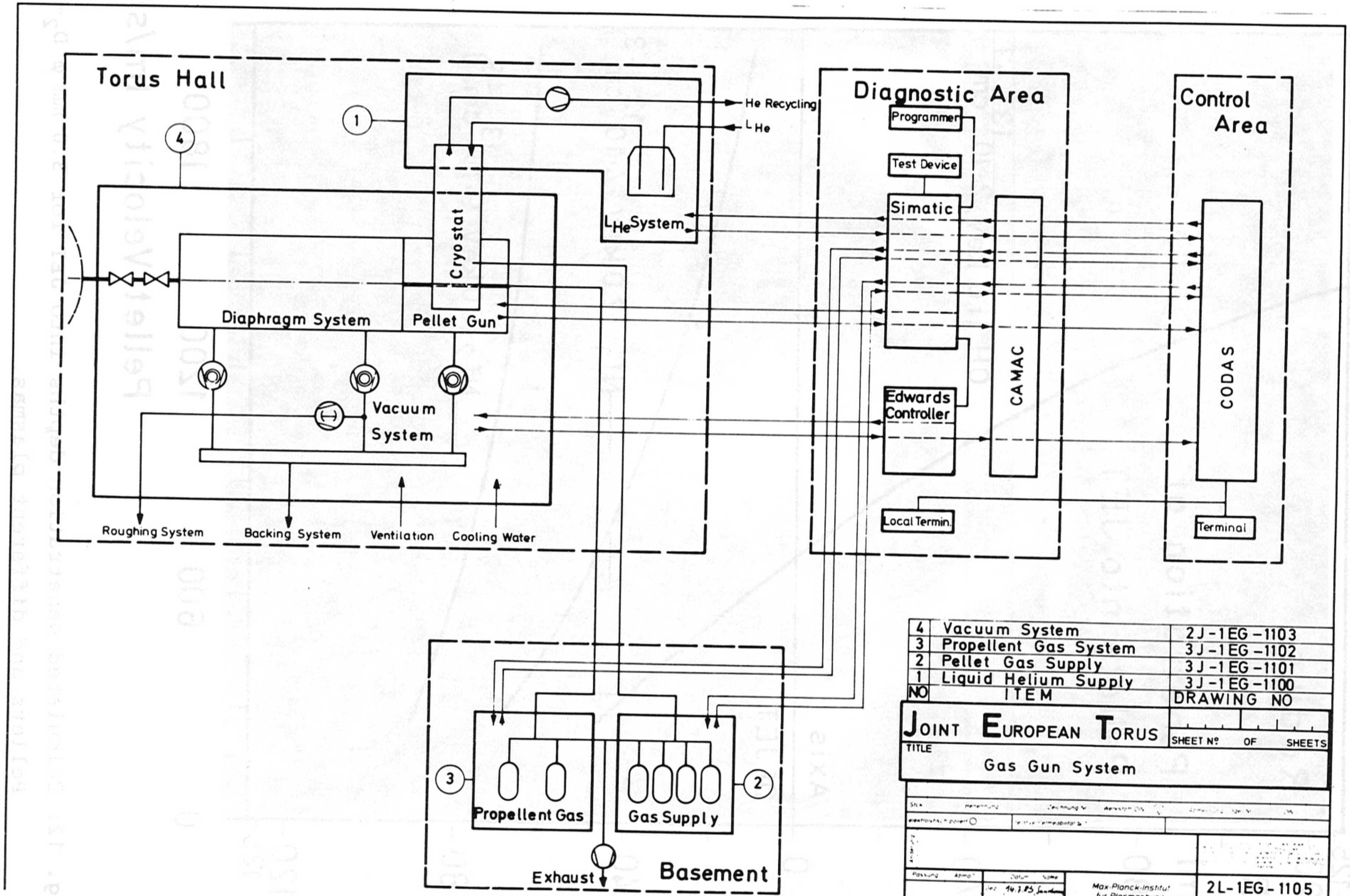

Fig. 13: Block diagram of pellet gas gun system including supply and control devices.

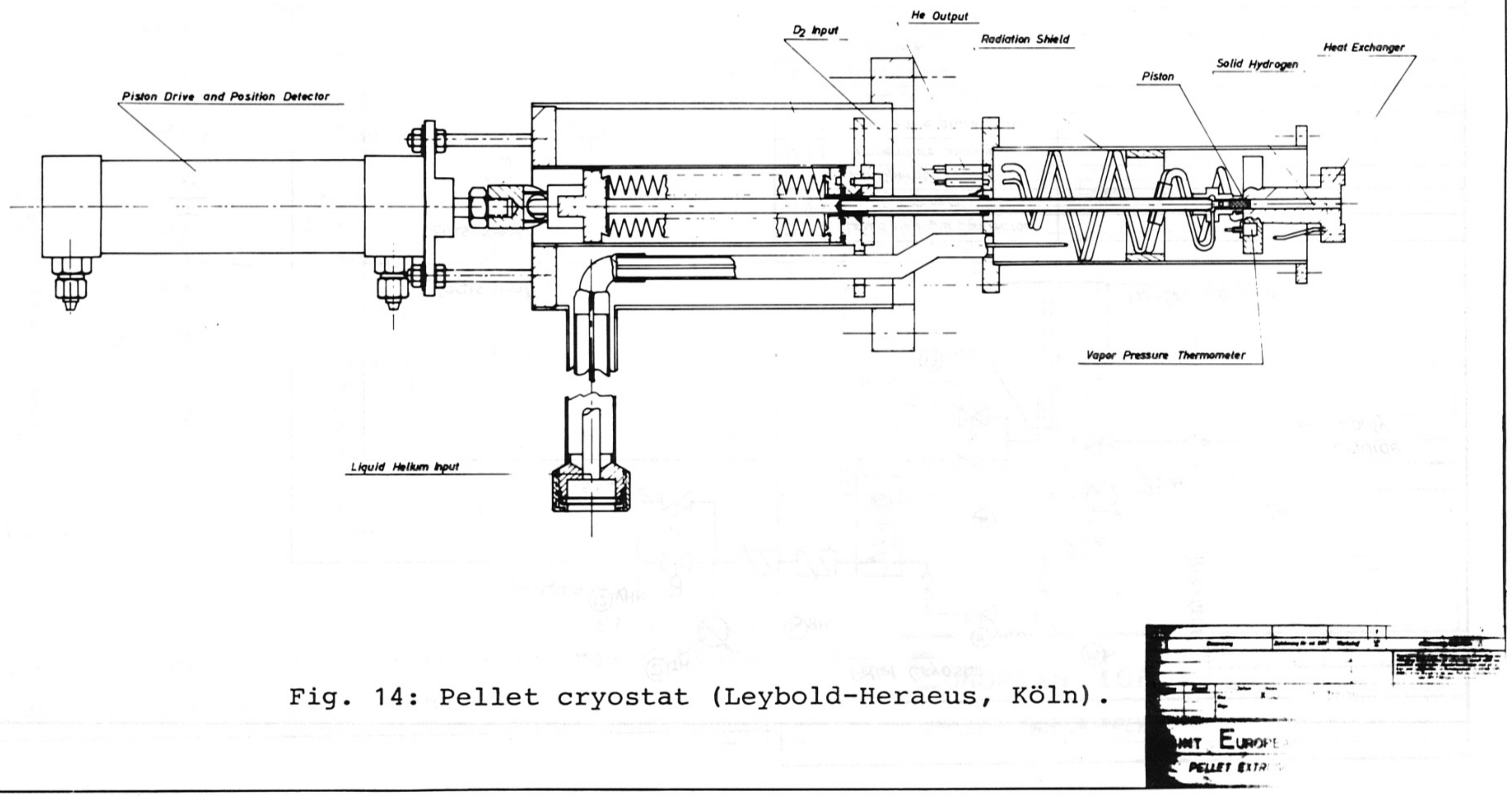

Fig. 14: Pellet cryostat (Leybold-Heraeus, Köln).

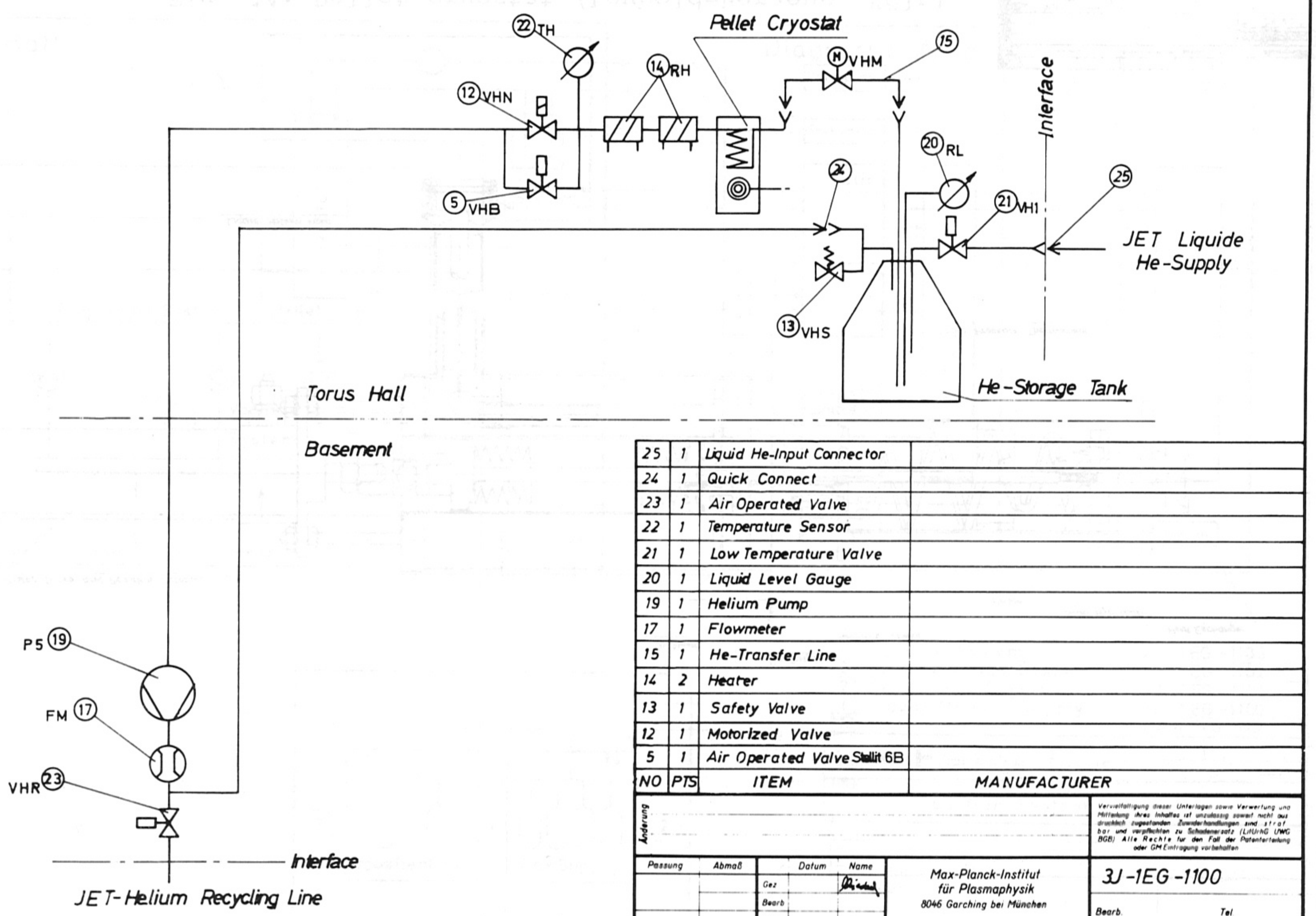

NO	PTS	ITEM	MANUFACTURER
25	1	Liquid He-Input Connector	
24	1	Quick Connect	
23	1	Air Operated Valve	
22	1	Temperature Sensor	
21	1	Low Temperature Valve	
20	1	Liquid Level Gauge	
19	1	Helium Pump	
17	1	Flowmeter	
15	1	He-Transfer Line	
14	2	Heater	
13	1	Safety Valve	
12	1	Motorized Valve	
5	1	Air Operated Valve Stellit 6B	

Änderung

Verveilfältigung dieser Unterlagen sowie Verwertung und Mitteilung ihres Inhaltes ist unzulässig soweit nicht ausdrücklich zugestanden. Zuwiderhandlungen sind strafbar und verpflichten zu Schadenersatz (LitUrhG UWG BGB). Alle Rechte für den Fall der Patenterteilung oder GM Eintragung vorbehalten

Passung	Abmaß		Datum	Name
		Gez		
		Bearb		
		Gepr		

Max-Planck-Institut für Plasmaphysik
8046 Garching bei München

3J-1EG-1100

Bearb. Tel

JOINT EUROPEAN TORUS

SHEET Nº OF SHEETS

TITLE

LIQUID HELIUM SUPPLY

Fig. 15: Liquid helium supply of pellet cryostat.

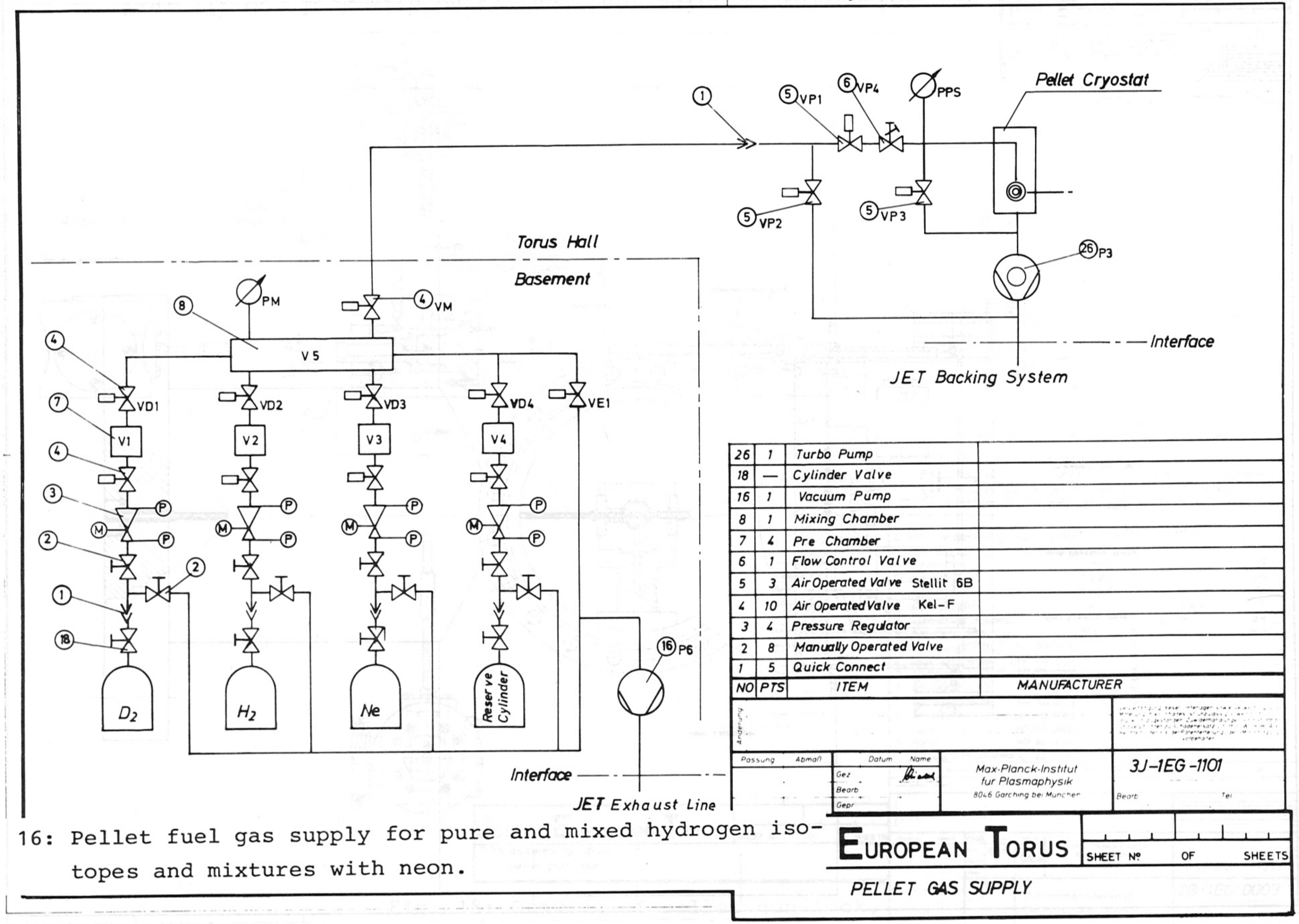

Fig. 16: Pellet fuel gas supply for pure and mixed hydrogen isotopes and mixtures with neon.

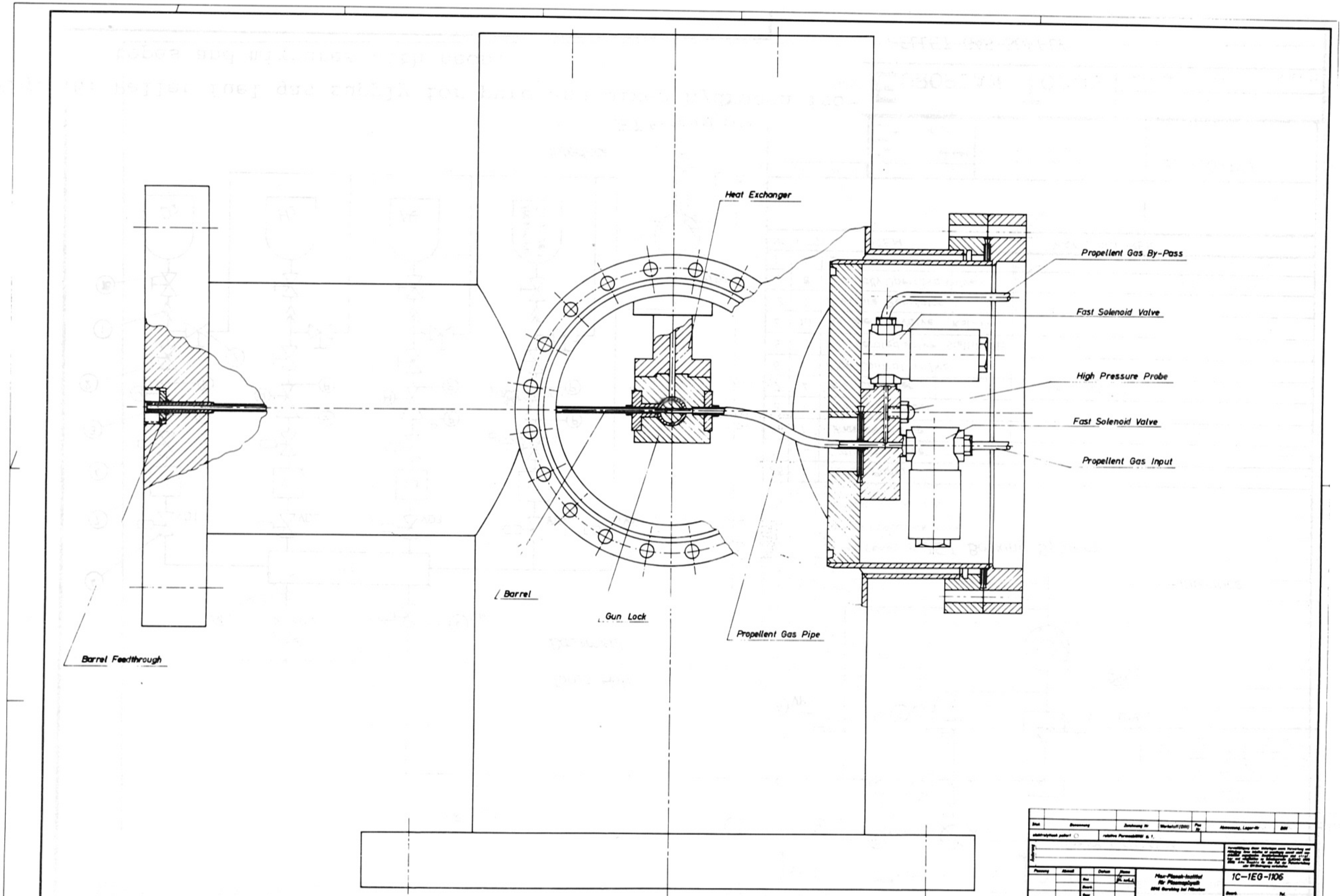

Fig. 17: Gun lock with barrel and fast solenoid valves for propellent gas.

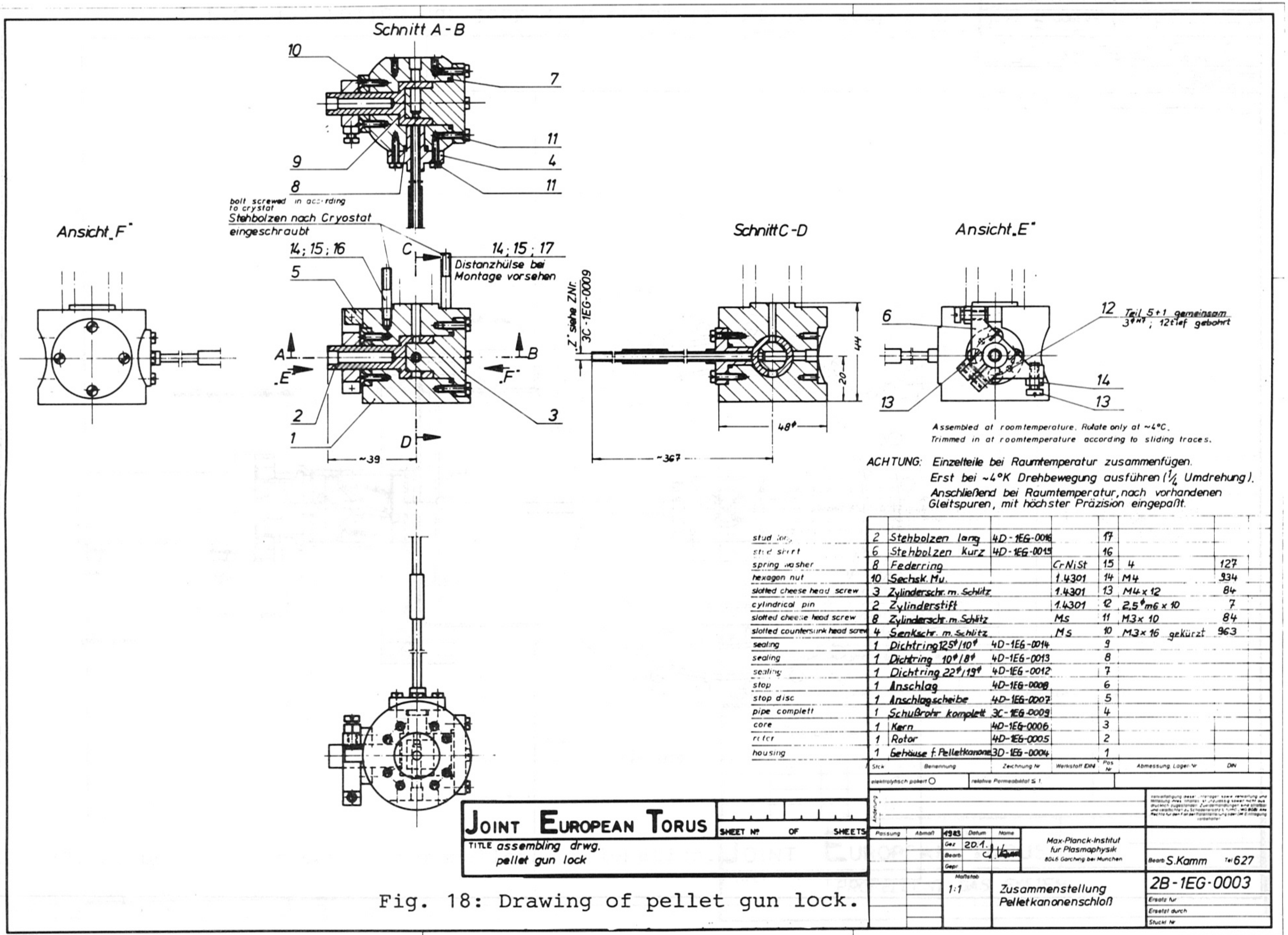

Fig. 18: Drawing of pellet gun lock.

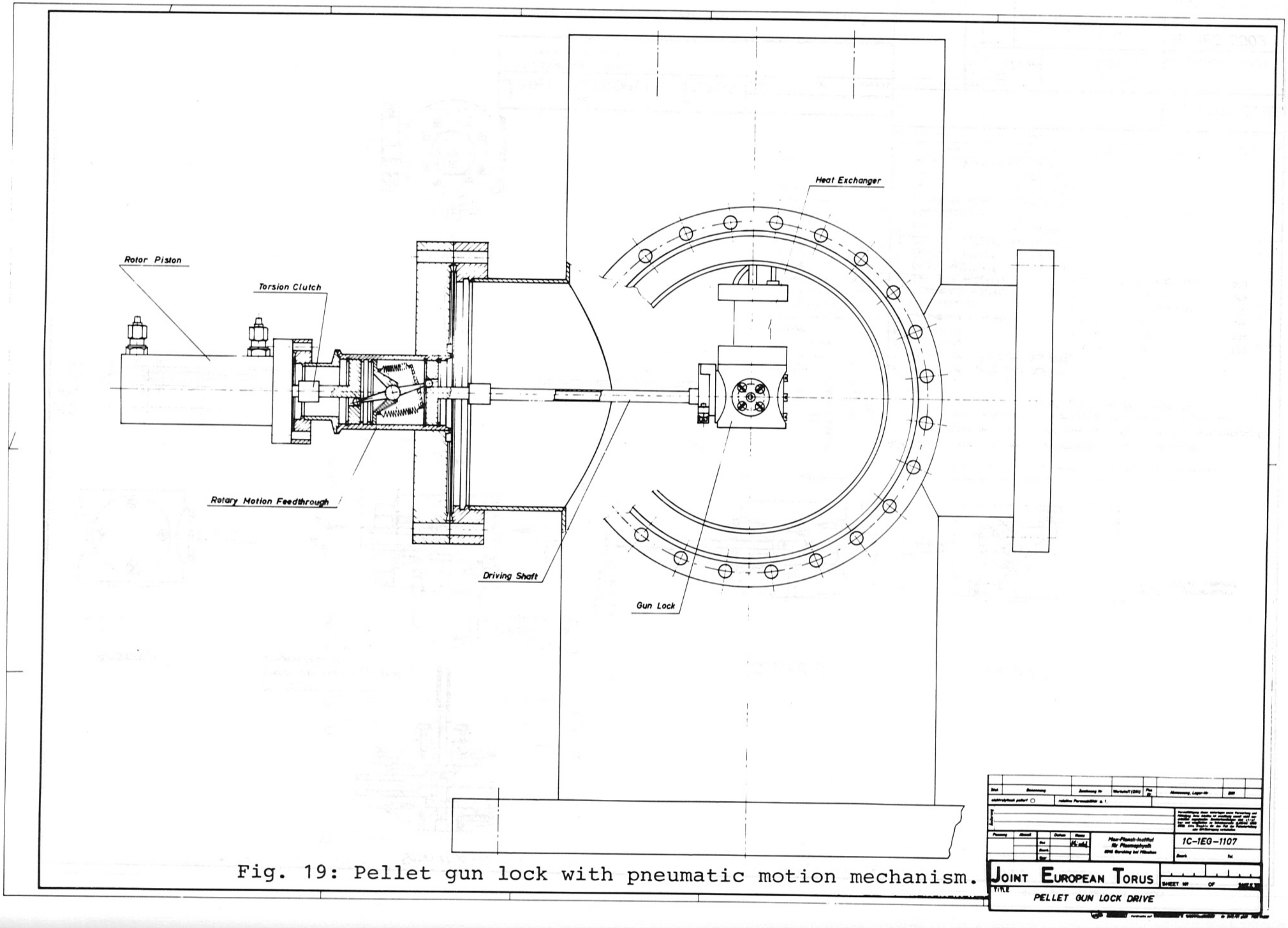

Fig. 19: Pellet gun lock with pneumatic motion mechanism.

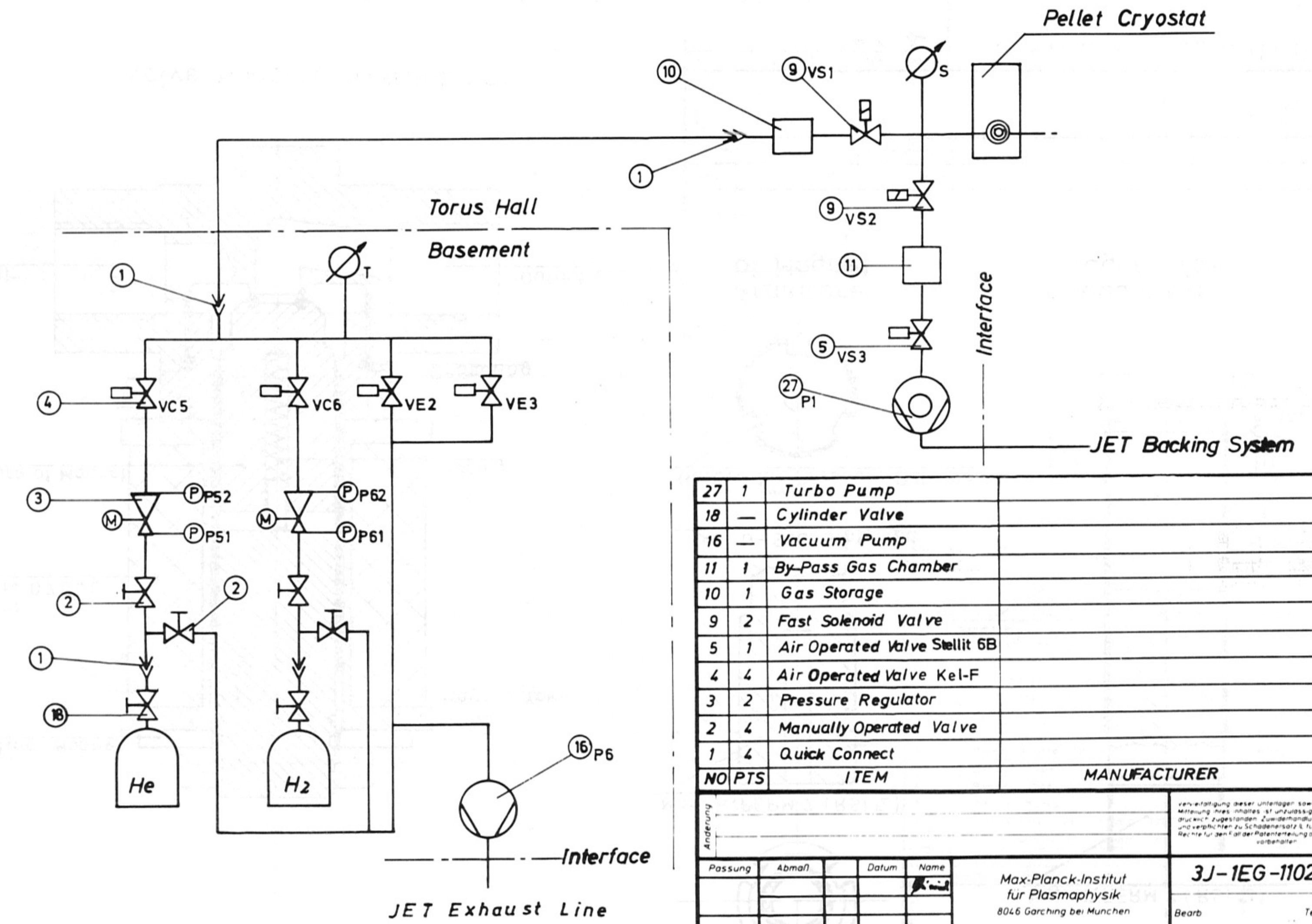

NO	PTS	ITEM	MANUFACTURER
27	1	Turbo Pump	
18	—	Cylinder Valve	
16	—	Vacuum Pump	
11	1	By-Pass Gas Chamber	
10	1	Gas Storage	
9	2	Fast Solenoid Valve	
5	1	Air Operated Valve Stellit 6B	
4	4	Air Operated Valve Kel-F	
3	2	Pressure Regulator	
2	4	Manually Operated Valve	
1	4	Quick Connect	

Änderung

Passung | Abmaß | Datum | Name

Max-Planck-Institut für Plasmaphysik
8046 Garching bei München

3J-1EG-1102

Bearb | Tel

JOINT EUROPEAN TORUS

SHEET Nº OF SHEETS

TITLE PROPELLENT GAS SYSTEM

Fig. 20: Propellent gas supply for pellet acceleration.

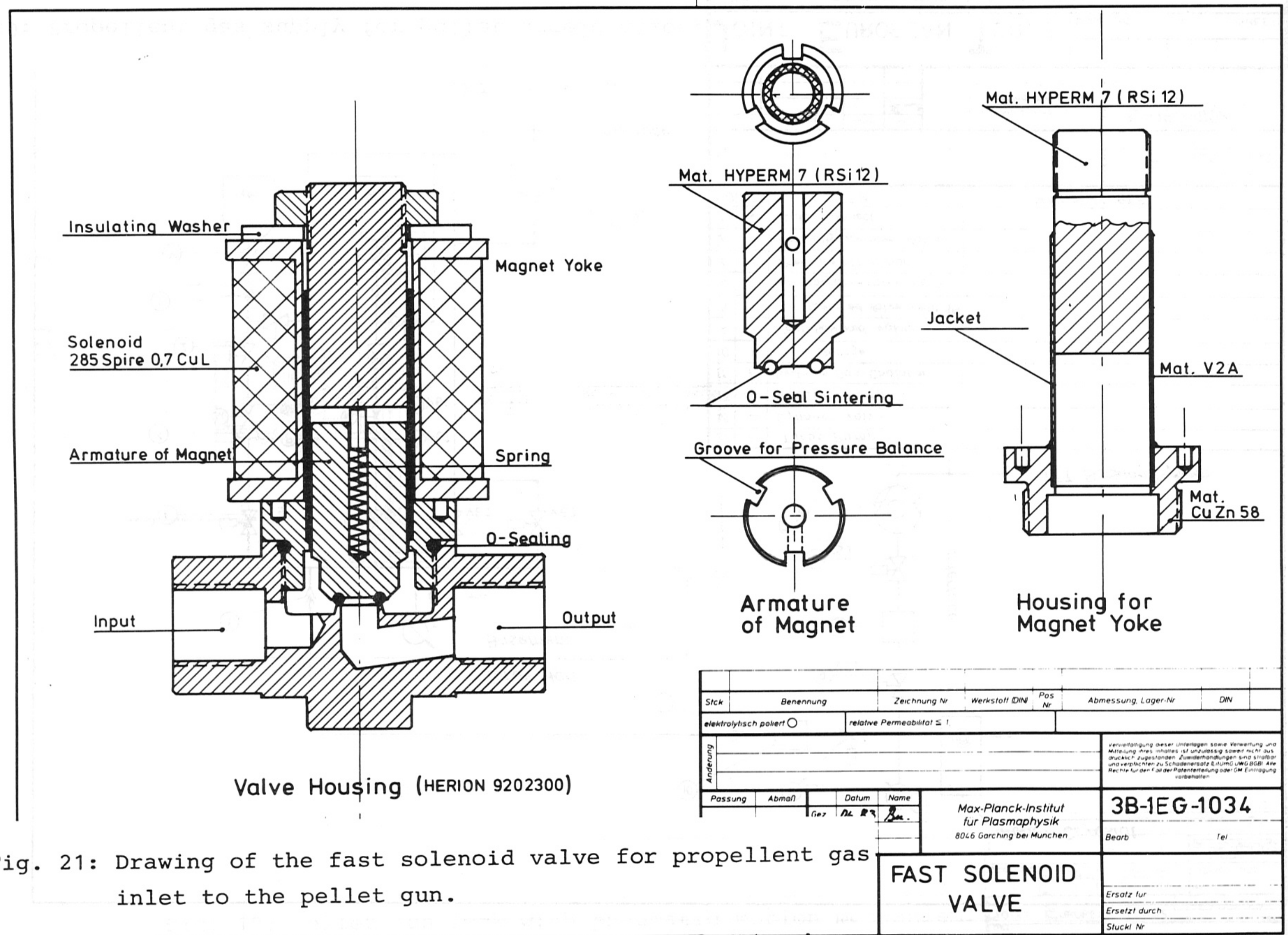

Fig. 21: Drawing of the fast solenoid valve for propellent gas inlet to the pellet gun.

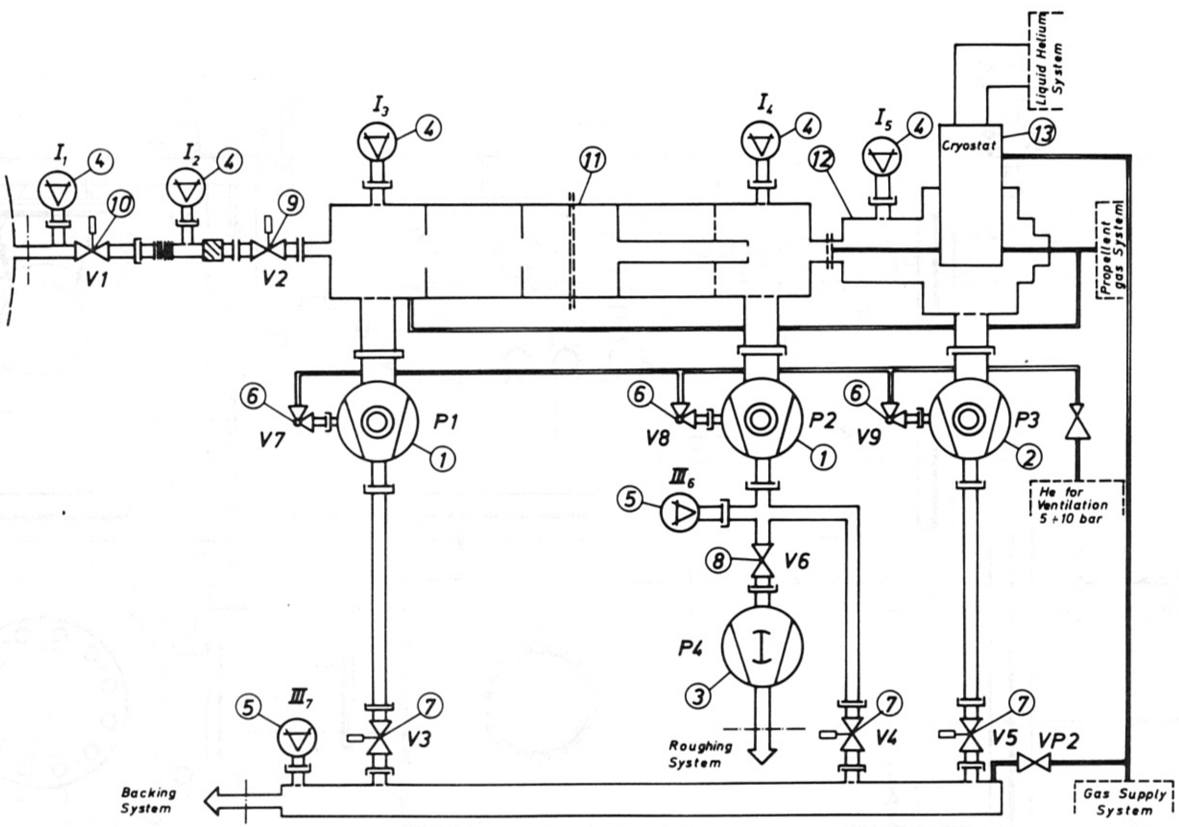

JOINT EUROPEAN TORUS

TITLE: Vacuum System

SHEET Nº OF SHEETS

No	PTS	ITEM	
13	1	Cryostat	LH
12	1	Cryostat Vessel	
11	1	Diaphragm System	
10	1	JET - Valve	JET
9	1	Fast closing Valve	CETEC AG
8	1	Valve	DN 35 Series 40 VAT
7	3	Valve	DN 35 Series 40 VAT
6	3	Right Angle Valve	DN 10 Series 40 VAT
5	2	Branch Pipe Unit	LH
4	5	Branch Pipe Unit	LH
3	1	Roots Pump	
2	1	Turbomolecular Pump 2200	
1	2	Turbomolecular Pump 510	TPU 510 Pfeiffer

Max-Planck-Institut für Plasmaphysik, 8046 Garching bei München

Vacuum System

2J-1EG-1103

2J-1EG-1103

Fig. 22: Vacuum system of the pneumatic pellet injector.

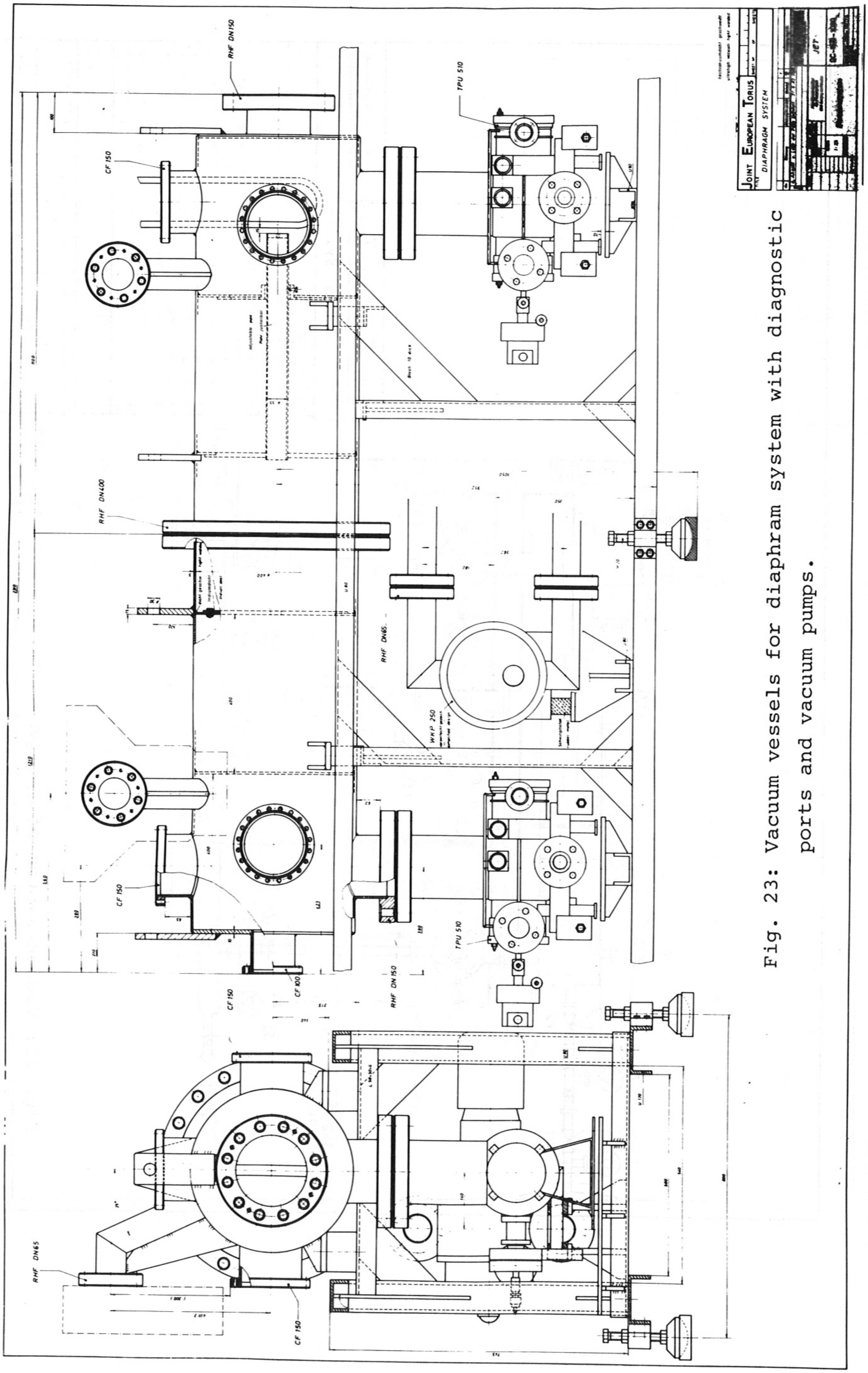

Fig. 23: Vacuum vessels for diaphram system with diagnostic ports and vacuum pumps.

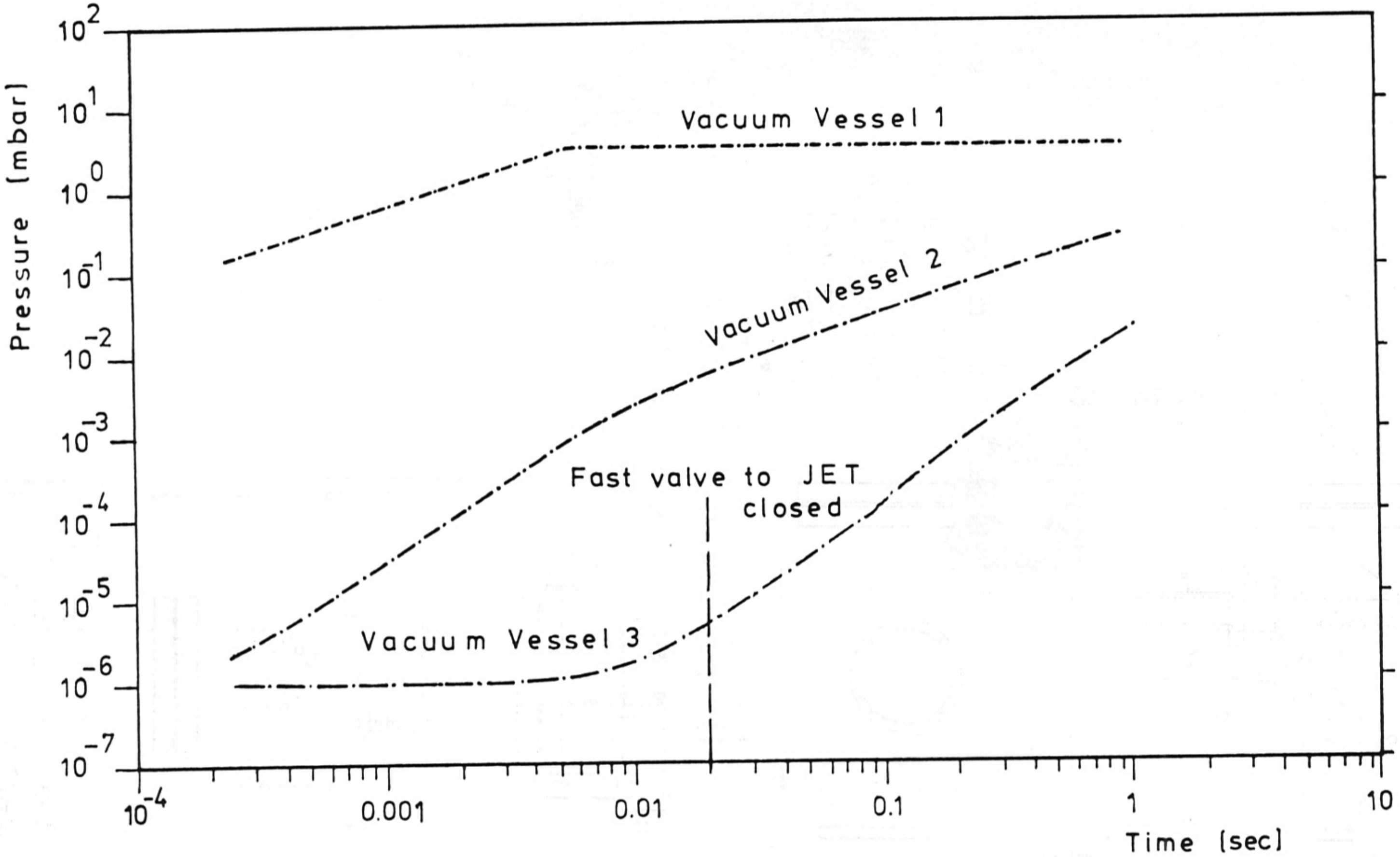

Fig. 24: Pressure rise in the vacuum system during pellet injection due to propellent gas flow. Vacuum vessel 1 at the barrel end, the others are following. Diameter of diaphragms 3 and 5 mm. Propellent gas pressure 20 bar.

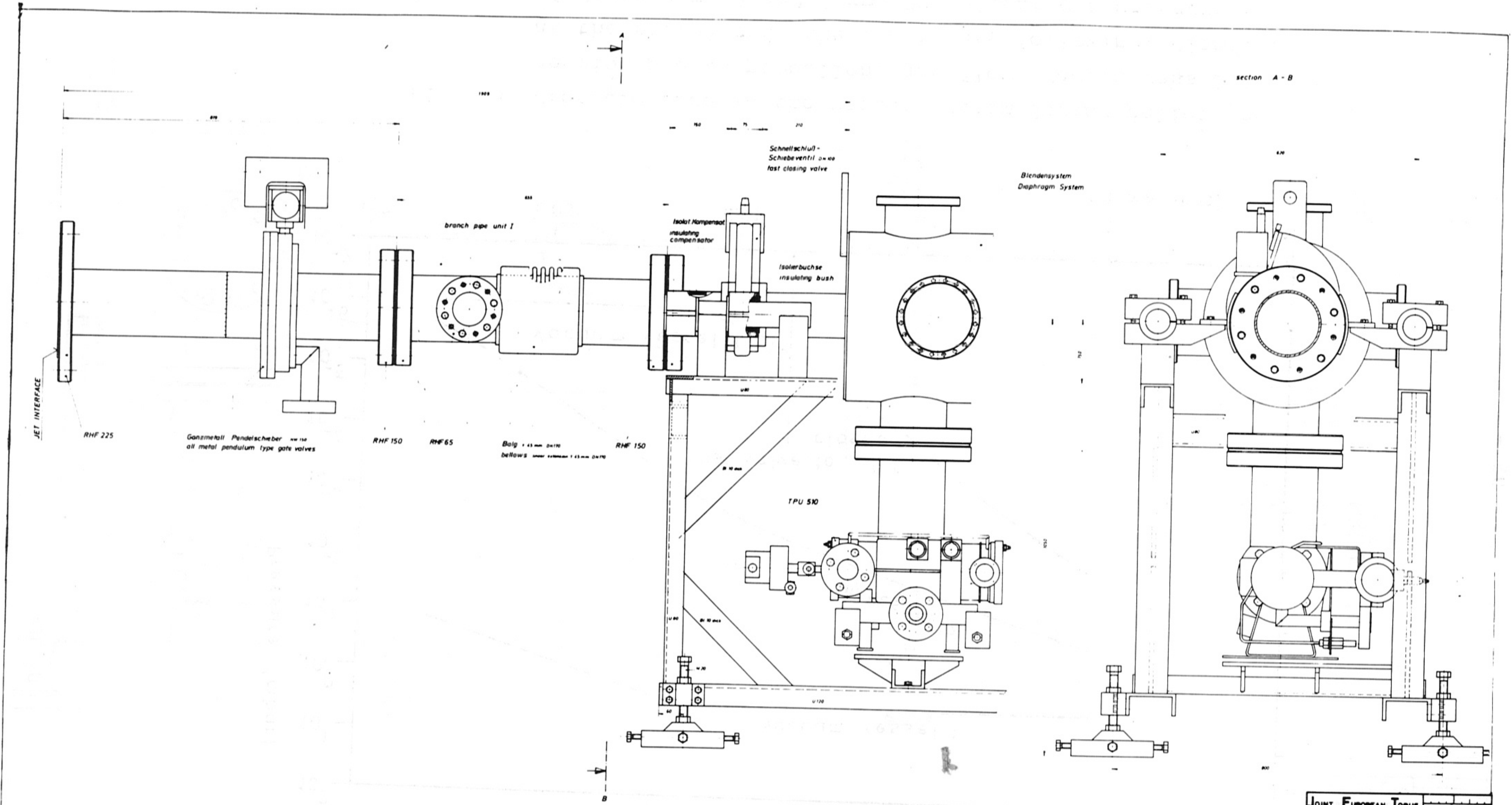

Fig. 25: Pellet beam line with interface to JET including valves, bellows and a ceramic break.

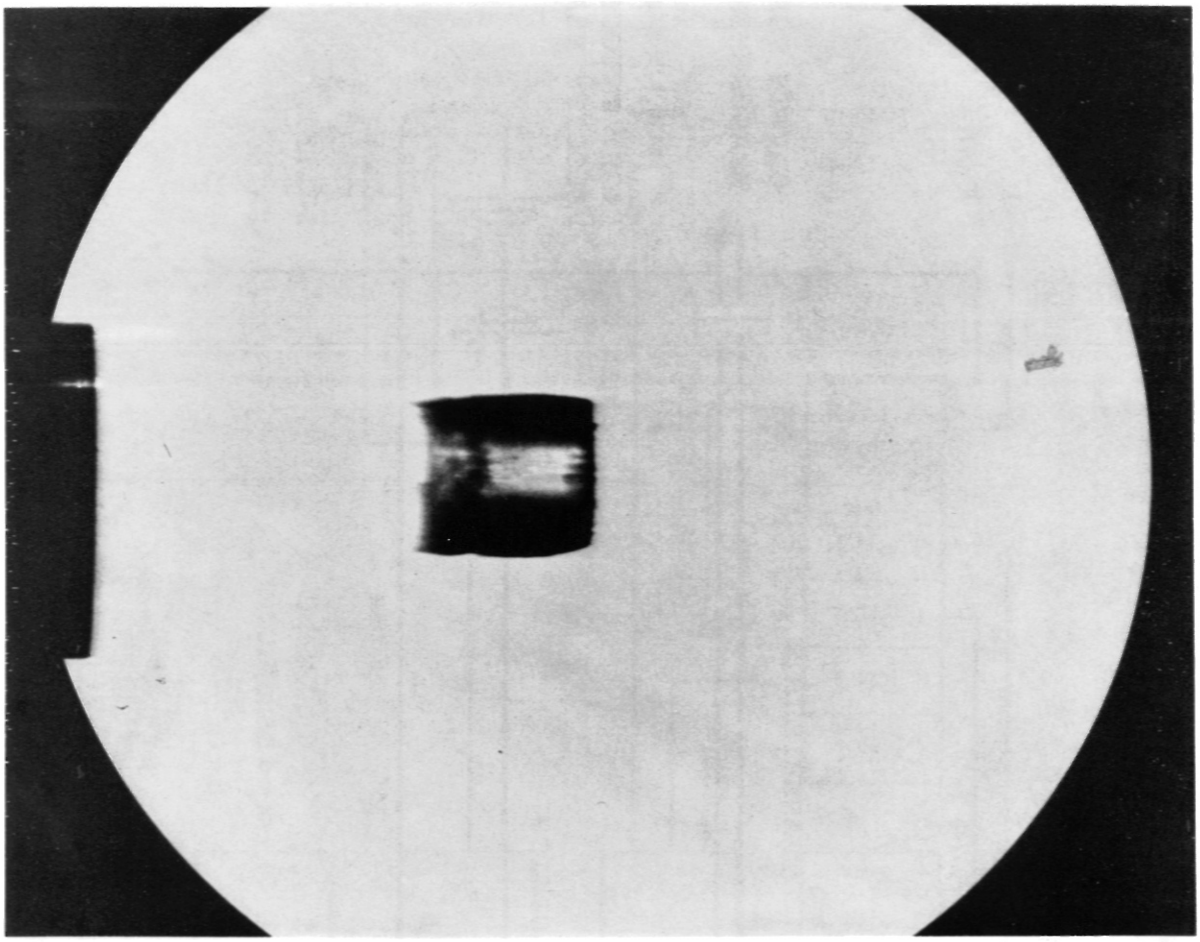

Fig. 26: Photography of a 2.6 mm D_2-pellet in flight (velocity $\approx$ 1200 m/s).

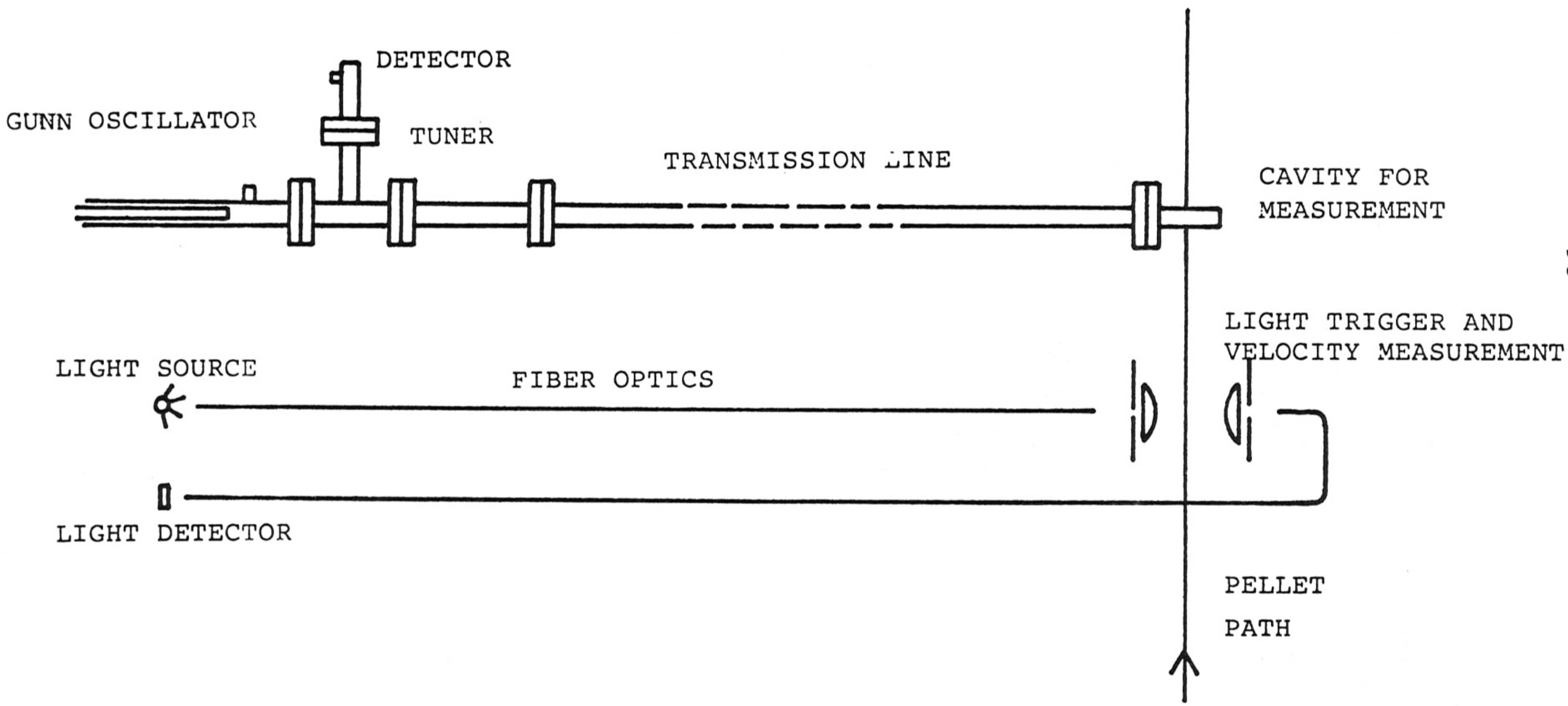

Fig. 27: Light barrier and microwave diagnostics for determination of velocity and mass of the pellet /7/.

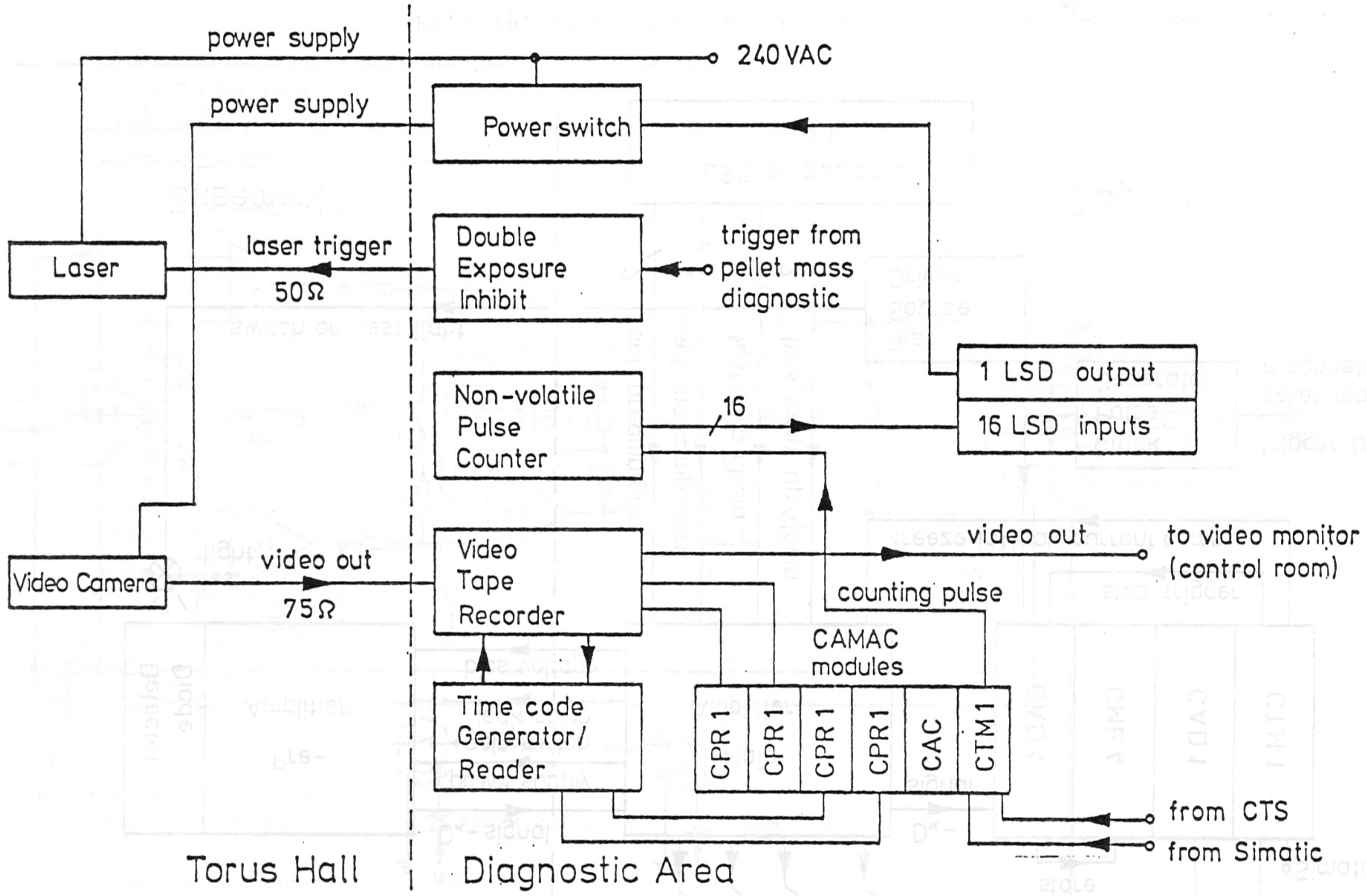

Fig. 28: Block diagram of TV pellet observation and recording system.

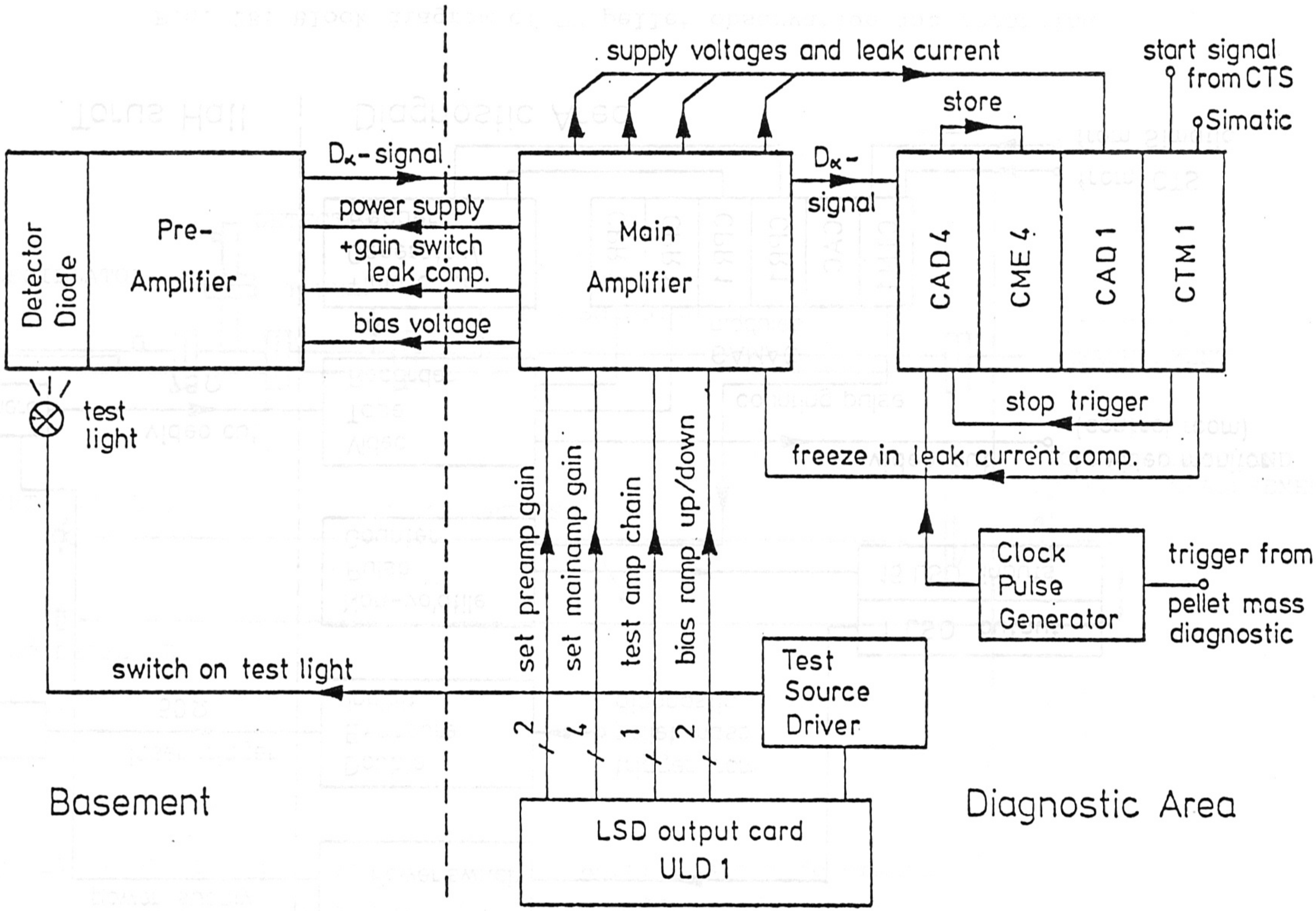

Fig. 29: Block diagram of electronics for D_α-diagnostics.

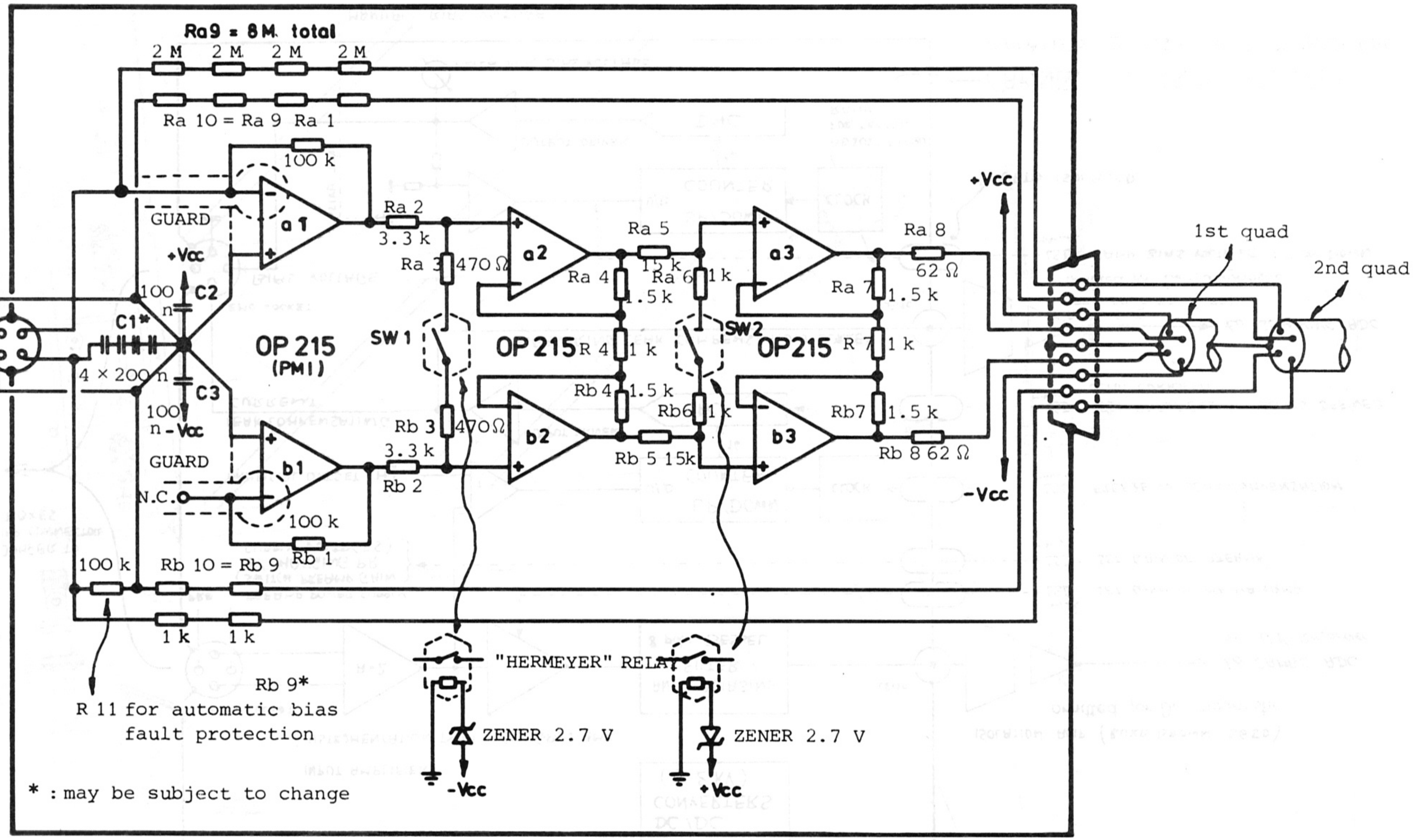

Fig. 30: Preamplifier for D_α-diagnostics.

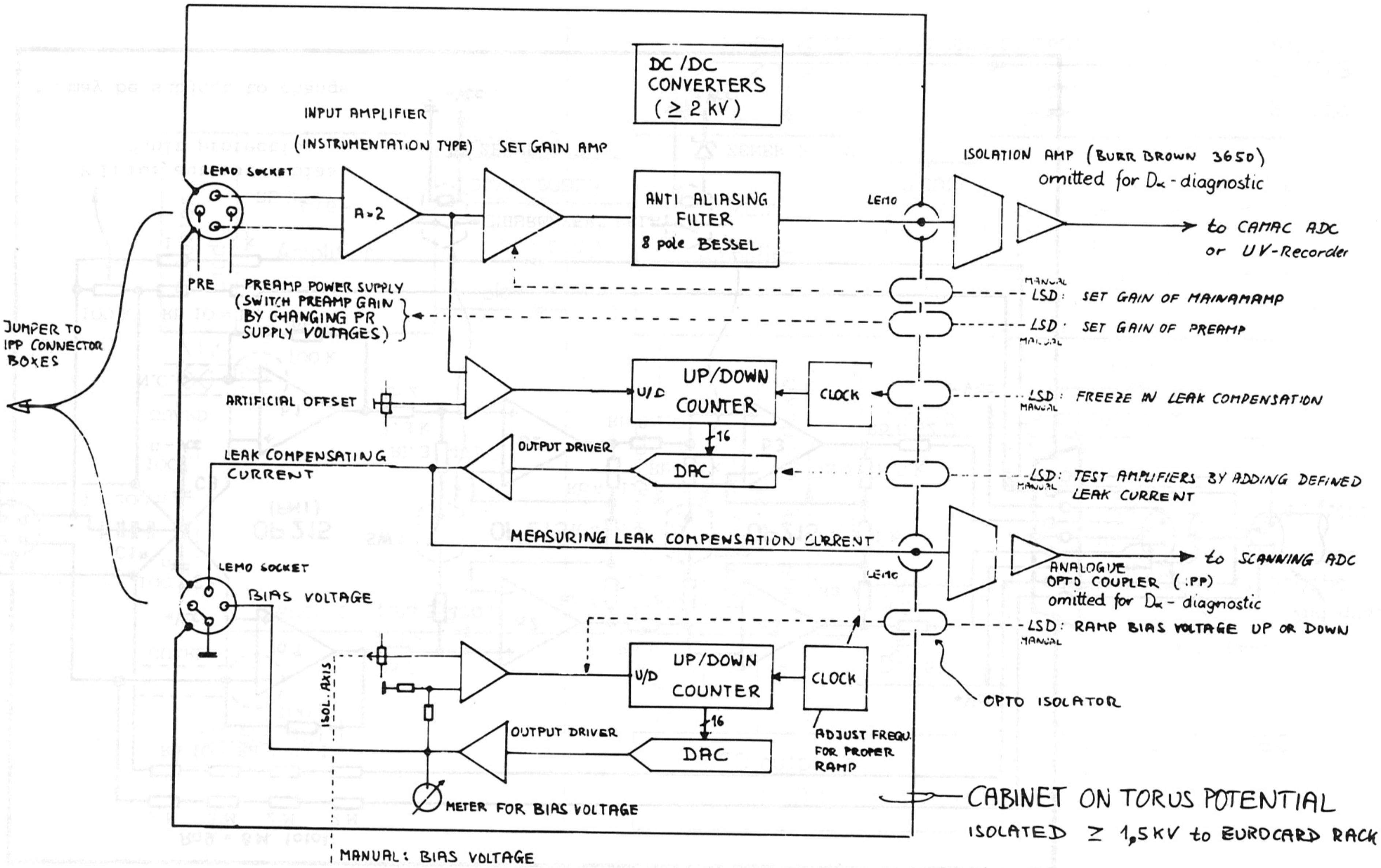

Fig. 31: Main amplifier for D_α-diagnostics.

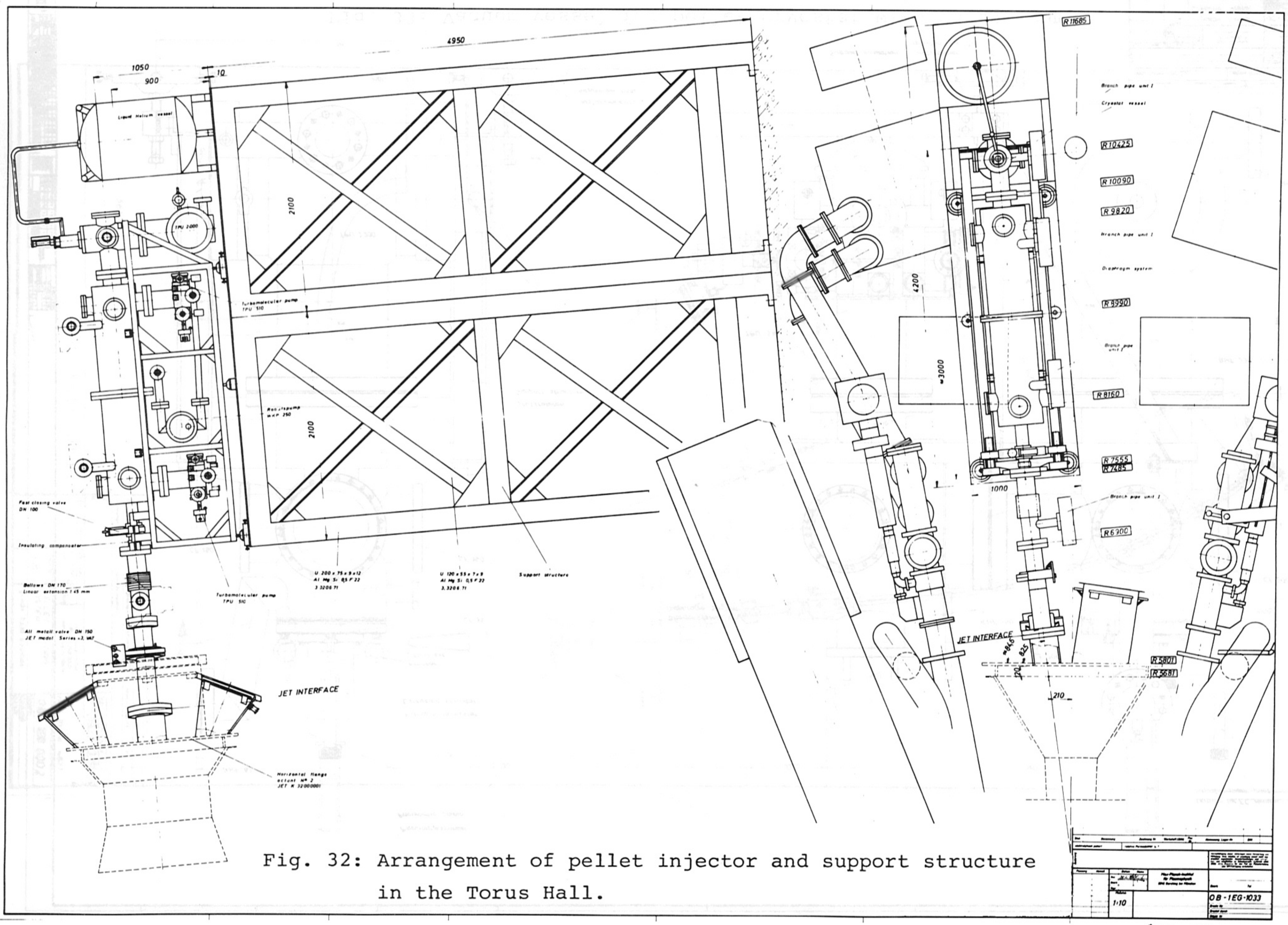

Fig. 32: Arrangement of pellet injector and support structure in the Torus Hall.

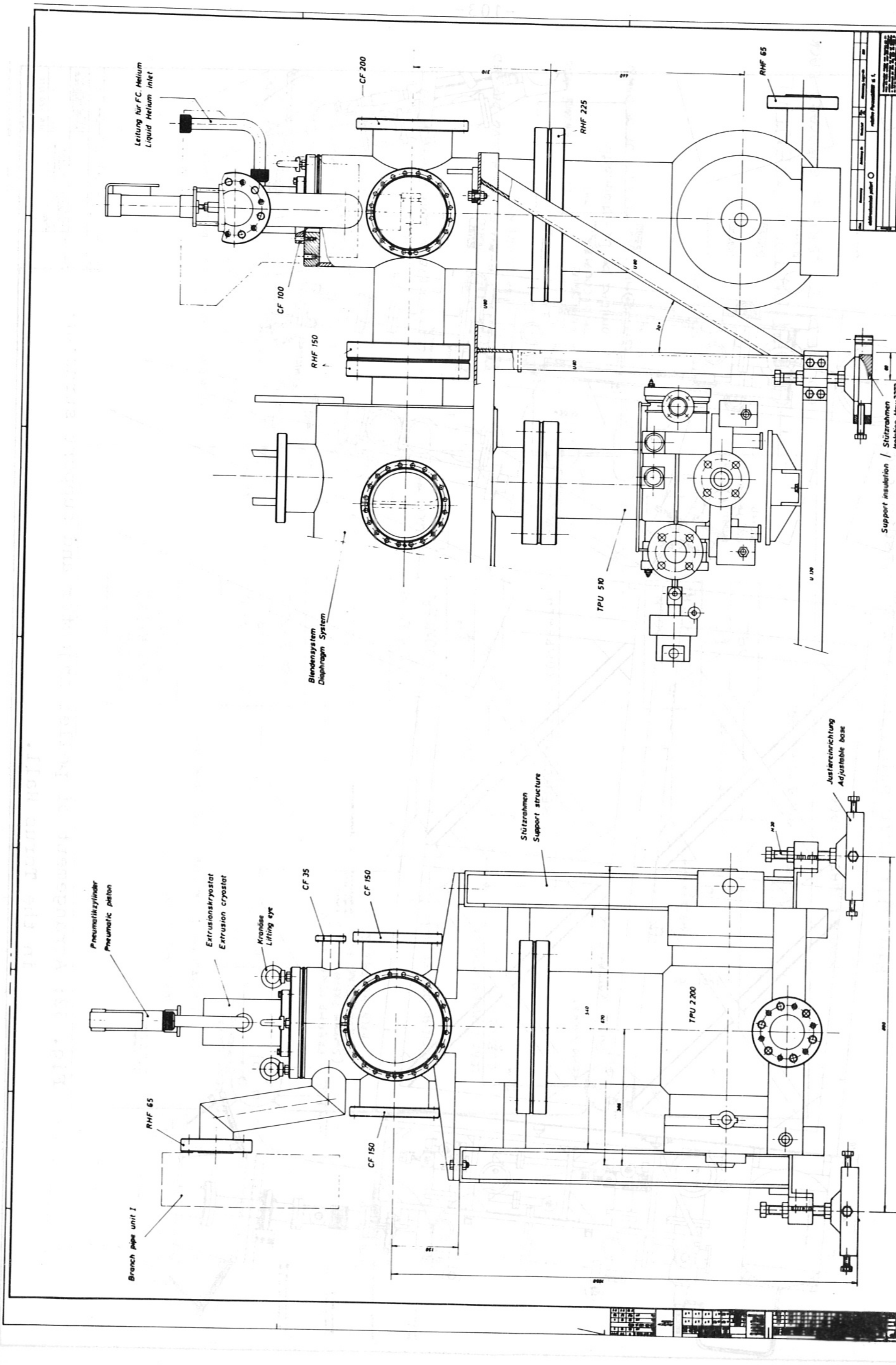

Fig. 33: Vacuum vessel for pellet cryostat with vacuum pump TPU 2200.

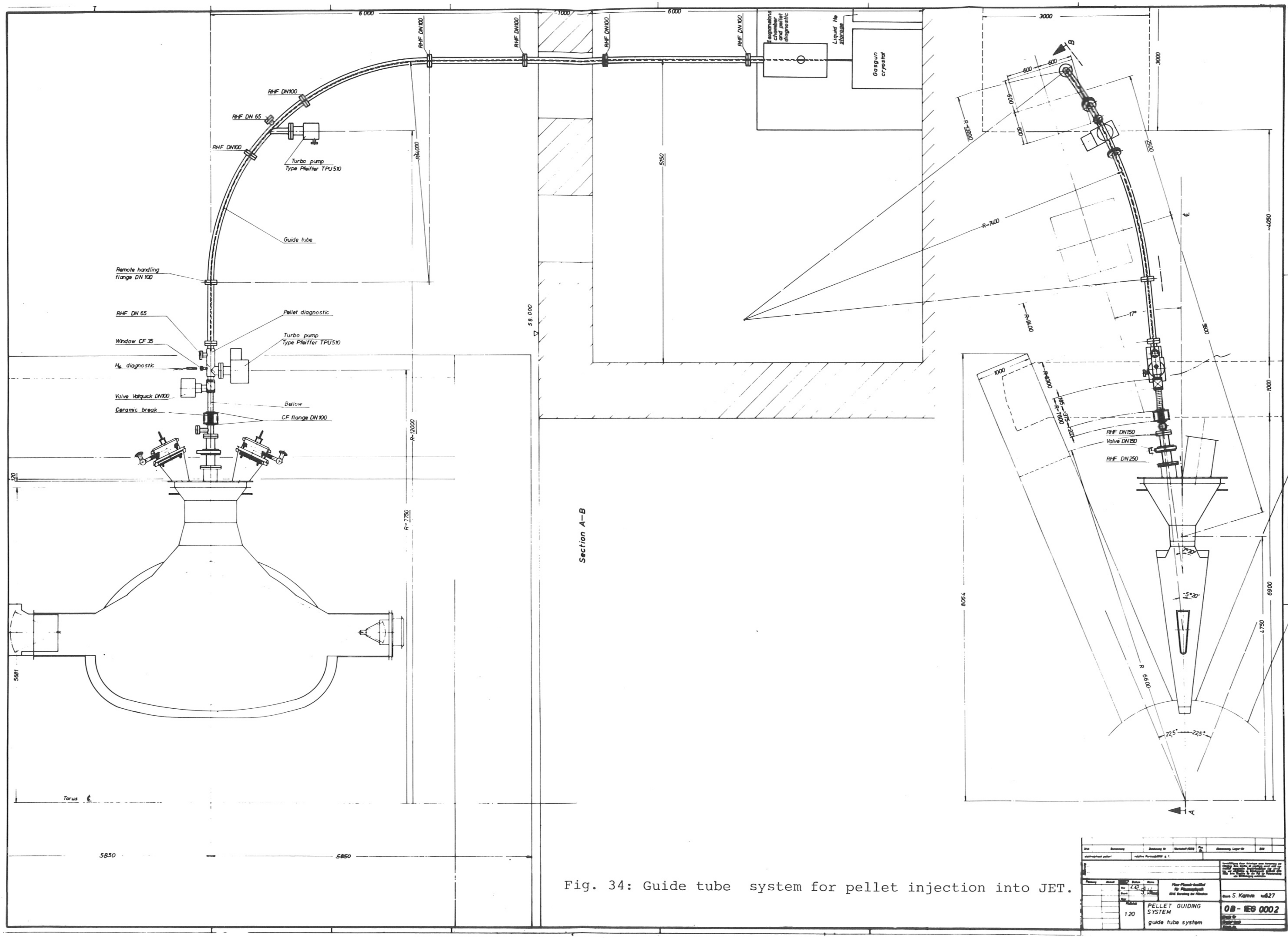

Fig. 34: Guide tube system for pellet injection into JET.

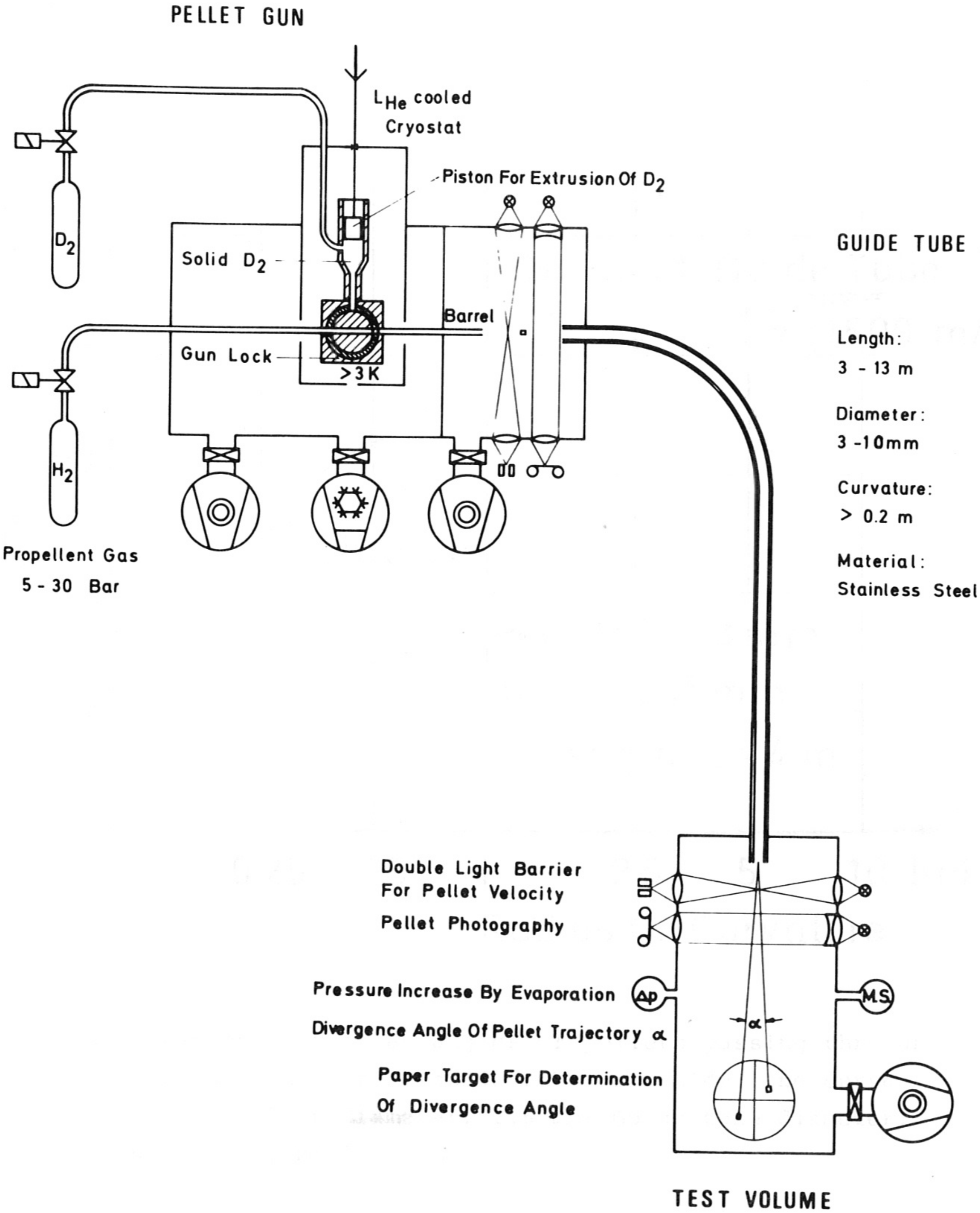

Fig. 35: Experimental arrangement for investigation of pellet propagation through guide tubes.

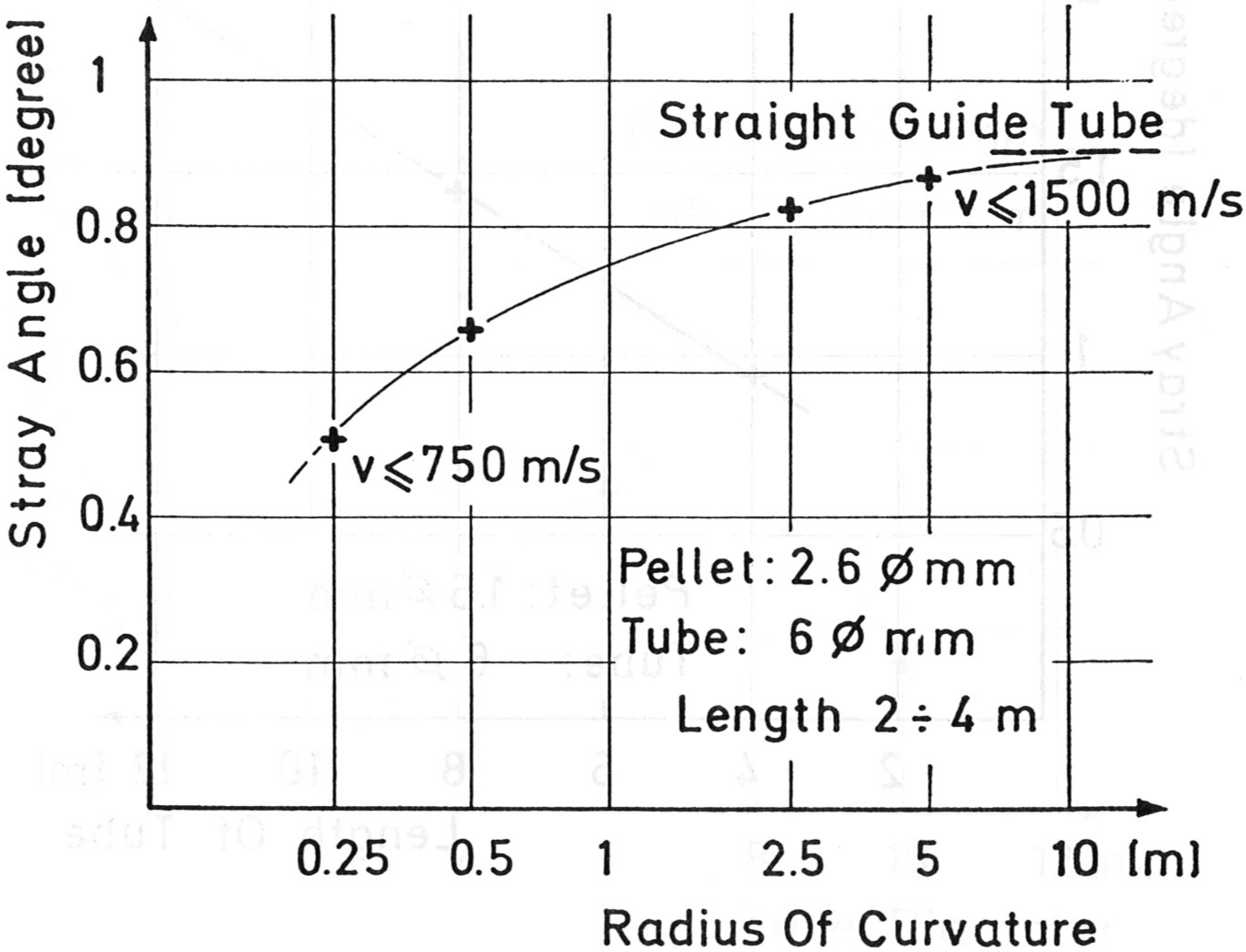

Fig. 36a: Dependence of stray angles of pellets passing through straight and curved guide tubes on guide tube curvatures. Pellet diameter: 2.6 mm; Guide tube diameter: 6 mm; Length: 2 - 4 m.

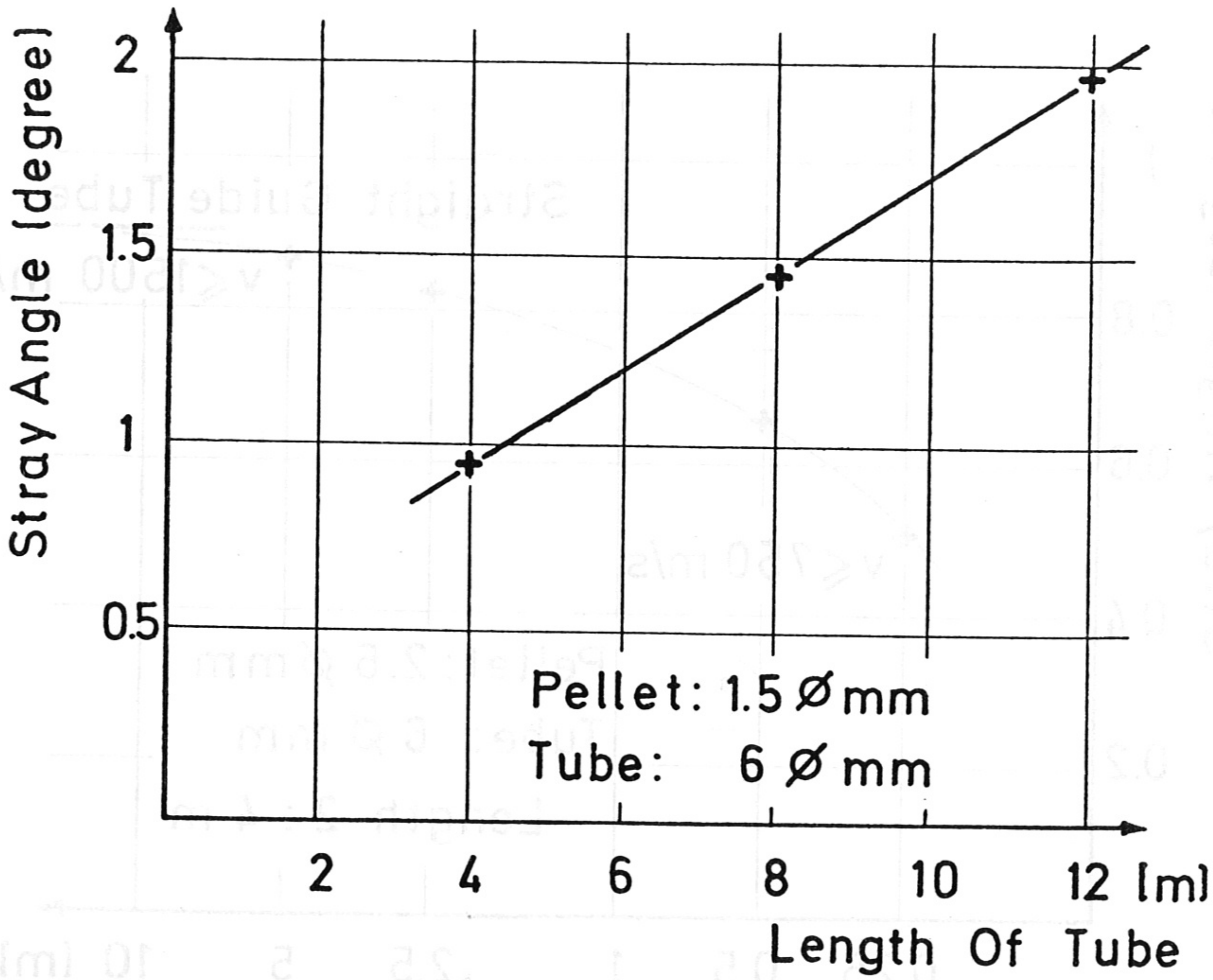

Fig. 36b: Dependence of stray angles of pellets passing through straight guide tubes on guide tube lengths. Pellet diameter: 1.5 mm; Guide tube diameter: 6 mm.

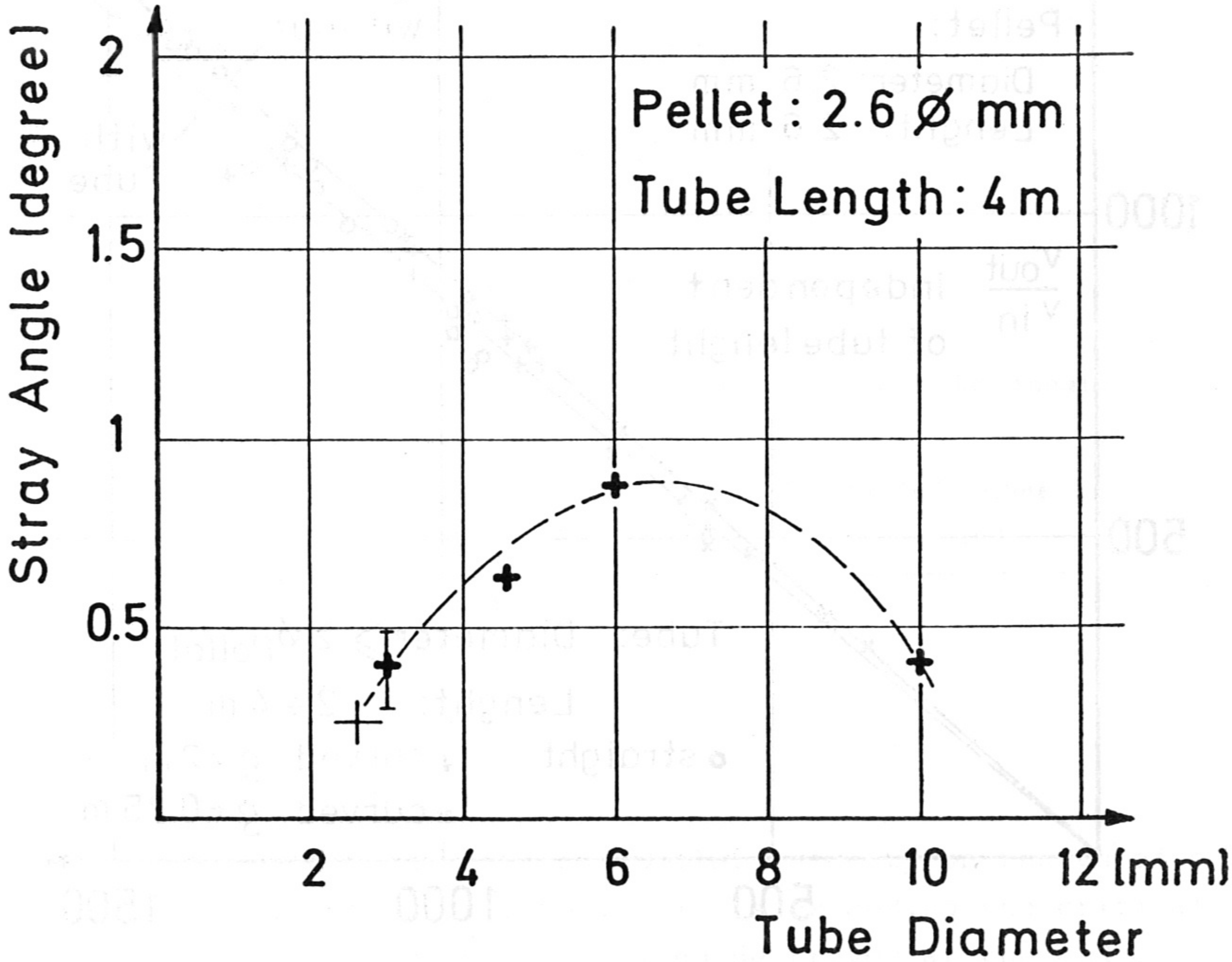

Fig. 36c: Dependence of stray angles of pellets passing through straight guide tubes on guide tube diameters. Pellet diameter: 2.6 mm; Guide tube length: 2.5 - 4 m.

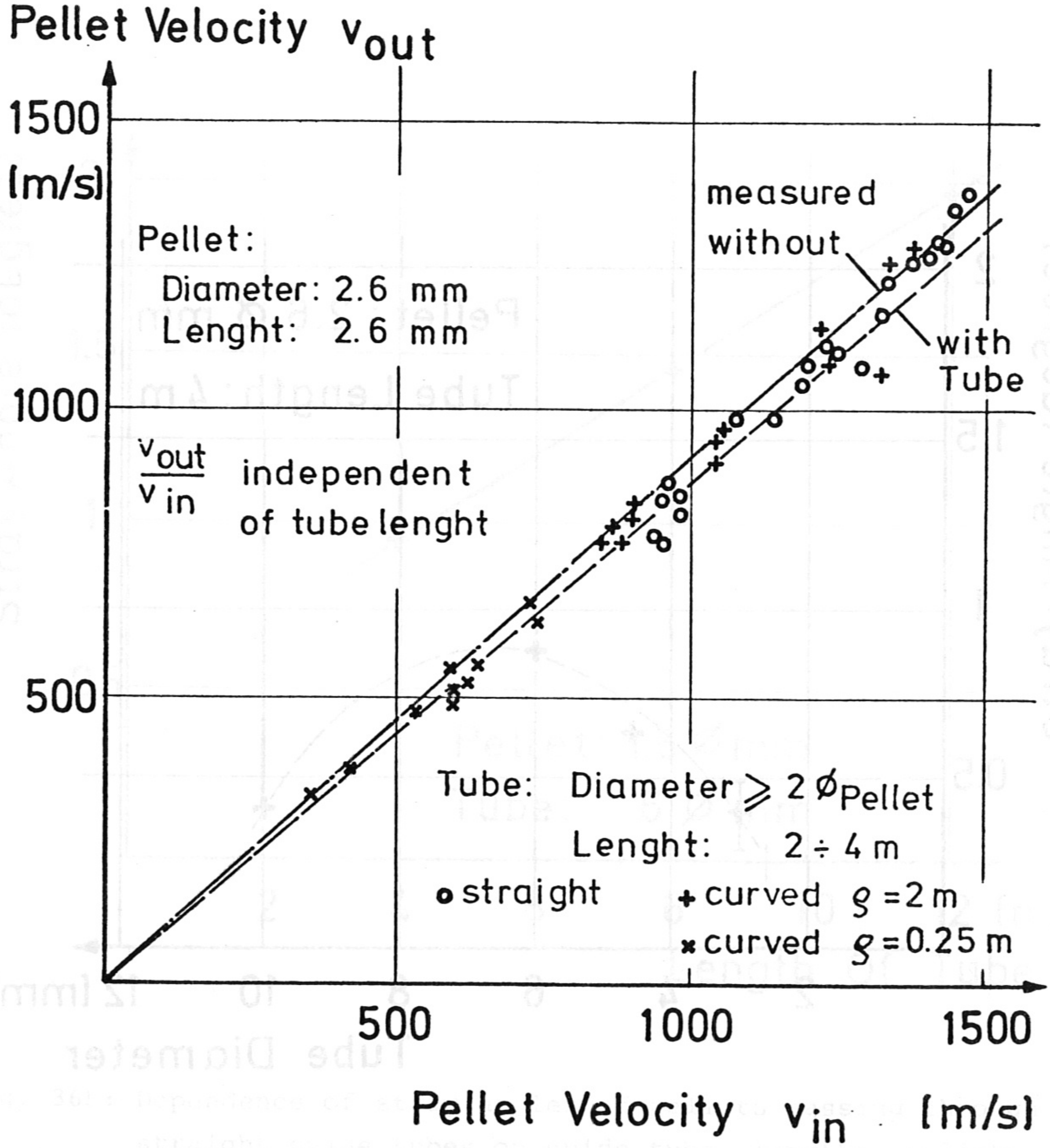

Fig. 37: Loss of velocity of pellets in straight and curved guide tubes. Pellet diameter: 2.6 mm.

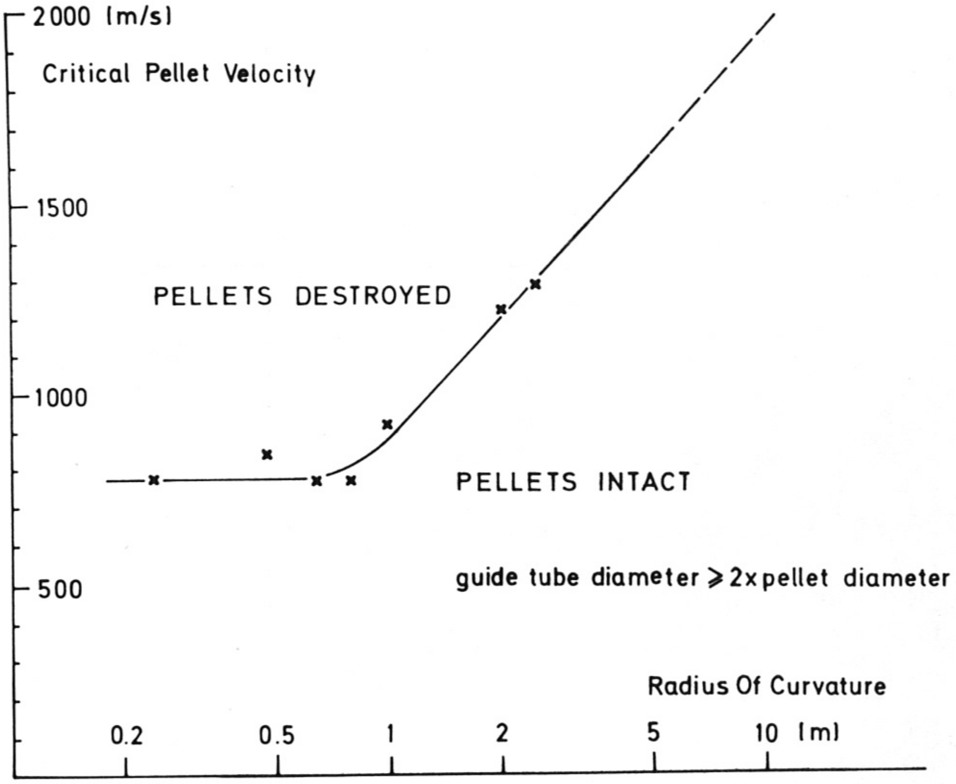

Fig. 38: Dependence of critical pellet velocity on radius of curvature of guide tubes. Pellets exceeding the critical pellet velocity are arriving destroyed at the end of the guide tube. Guide tube length: 3.5 - 4 m; Pellet diameter: 2.6 mm.